Fault Tolerant Control of Autonomous Underwater Vehicles

by

Douglas Edward Perrault
B. Eng., Technical University of Nova Scotia (TUNS), 1996

A Dissertation Submitted in Partial Fulfillment of the
Requirements for the Degree of

MASTER OF APPLIED SCIENCE

in the Department of Mechanical Engineering.

We accept this thesis as conforming
to the required standard

[redacted]

Dr. M. Nahon, Supervisor (Dept. of Mechanical Engineering)

[redacted]

Dr. P. Agathoklis, Supervisor, Outside Member (Dept. of Electrical and Computer Engineering)

[redacted]

Dr. R. Podhorodeski, (Dept. of Mechanical Engineering)

[redacted]

Dr. J. Collins, External Examiner (Dept. of Electrical and Computer Engineering)

Supervisor: Dr. M. Nahon and Dr. P. Agathoklis

Abstract

Autonomous underwater vehicles (AUV's) are used for ocean exploration and underwater research. For practical usage of these vehicles, there must be some form of fault recovery/fault tolerance in the control system. This work explores an adaptation of existing theory for synthesizing controls in the event of partial failure of the nominal control system. This control method will synthesize small motions in a given unactuated direction via open loop control of motions in actuated directions. Our goal is to determine the usefulness of the method for a typical streamlined vehicle in which control forces are generated by control planes rather than directly with thrusters. Using these algorithms in their present form, we find that the righting moment of the vehicle interferes with the achievement of the desired motions. However, motion synthesis can be achieved on a modified model that has no righting moment.

Examiners:

[redacted]

Dr. M. Nahon, Supervisor (Dept. of Mechanical Engineering)

[redacted]

Dr. P. Agathoklis, Supervisor, Outside Member (Dept. of Electrical and Computer Engineering)

[redacted]

Dr. R. Podhorodeski, (Dept. of Mechanical Engineering)

[redacted]

Dr. J. Collins, External Examiner (Dept. of Electrical and Computer Engineering)

Table of Contents

List of Figures

List of Tables

Dedication

To my Lord Jesus Christ, the Master Engineer - Gen. 1:1; John 1:3; Col. 1:16; Heb.11:3 – to Him be the glory in all things.

To my wife Marina, who encouraged me to come back to school, who has stuck with me in graduate work, and who continues to be my cheerleader and a very suitable helper.

To Dr. Meyer Nahon, whose patience, grace, and good sense have much to do with the completion of this work.

Acknowledgements

I was supported by a scholarship from the Natural Sciences and Engineering Research Council of Canada. I also received awards from the British Columbia Advanced Systems Institute, and from the University of Victoria.

I would also like to thank Cristina Stoica for her invaluable assistance with the theory of differential geometry.

Last, but by no means least, I would like to thank my fellow students for their suggestions and comments. In particular, Juan Carretero was consistently helpful throughout my research and writing.

Chapter 1

Introduction

The surface of the earth is two thirds water... yet we know so little about what is there. In fact, we know more about objects in space millions of kilometers away than we do about the ocean that is only 11 kilometers deep at its deepest point. There are huge expanses of water that we know virtually nothing about. For example, the South Pacific is largely unexplored because there are no landfalls between the coast of South America and the Fiji Islands and, therefore, few shipping lanes. Yet the ocean may hold a wealth of resources we may need in the future. Undersea exploration is the key to tapping these resources. We also know that these huge masses of water play a major role in the earth's weather patterns, but more information must be obtained in order to understand and model their role in the earth's ecosystems. In addition, knowledge of what is happening under the waves is a major concern for defense of any country with a coastline.

To accomplish the necessary exploration, manned submarines have been the tool of choice since they allow humans to get down there and have a look for themselves. They are, however, expensive and involve risk for the occupants.

Remotely operated vehicles (ROV's) are unmanned submersibles that are remotely controlled from a ship via a tether through which power and communications are available to the vehicle. They are less expensive and remove the risk to the operators by allowing them to sit in relative comfort on the surface ship. The major drawback is the tether. There is a high risk of the vehicle getting tangled up in it. Also, at greater depths, these systems tend to run into problems with snap loading, during which large tensions are generated in the tether. It is not uncommon to lose an ROV when the tether breaks.

Autonomous underwater vehicles (AUV's) have no cable and are free swimming devices. In principle they further reduce the operating costs since it should not be necessary to have a surface ship constantly monitoring them – once launched they are left to carry out their mission and return to a pre-arranged pick-up site. The onboard power supply limits this type of vehicle in terms of the duration of mission achievable. They require a compact, lightweight, long-lasting power source.

Hybrid vehicles and systems exist, such as the ROVER, an untethered ROV (called an AROV) controlled by acoustic signals; as well as mother-daughter systems where an ROV is sent out from a submarine (ALVIN-Jason), a cage, or another ROV.

The focus of the present work is the fully autonomous undersea vehicle. Autonomous underwater vehicles are poised to become an indispensable tool for ocean exploration, underwater research and development, and military activities. One of the key elements for practical usage of these vehicles is dependable controllability. We must have confidence that the vehicle can deal with unexpected events, such as actuator failures, in a predictable manner. If possible, we would prefer that the AUV continue its mission, and if not, we at least want the vehicle to make itself recoverable. In either event, there must be some form of fault recovery/fault tolerance in

the control system.

1.1 Literature Survey

The problem of nominal control of Autonomous Underwater Vehicles (AUV's) has been well stated by Yuh [37]. The dynamics of AUV's are fundamentally multivariable and nonlinear due to rigid body coupling and the hydrodynamic forces on the vehicle. This nonlinear behaviour is similar to that of aircraft except that the high density of water increases the significance of the forces and moments due to fluid motion. The dense fluid also leads to significant effects as a result of accelerating the fluid surrounding the vehicle ("added mass"). In fact, hydrodynamic characteristics of the vehicle are often poorly known and change with operating conditions. Even when tests are conducted to find the parameters, the values obtained are only valid for conditions near those of the test. In addition, the operating environment is unstructured and it is subject to stratification and currents. These effects result in disturbances which are difficult to measure.

Controlling a highly nonlinear system such as an AUV, that has significant uncertainty in the parameters, and is operating in an unpredictable, nonhomogeneous environment, in such a way as to be able to maintain control even in the event of component failure has typically been addressed as three separate problems. First – a robust nominal controller that will handle the nonlinearities and parameter uncertainties. Second – detection and isolation of component failures (before they become debilitating, if possible). Third – reconfiguring the controller to accomplish the task.

Most nominal control systems found in literature which are applied to underwater vehicles, are model based. When assumptions are made to linearize the model, some

well-established techniques for linear systems can be employed. Jalving and Storkersen [18] linearized and decoupled an AUV model then applied PID controllers. Tacconi and Tiano [34] and Healy [14] used the Linear Quadratic Gaussian (LQG) method because it is robust with respect to parameter uncertainties and small disturbances to the vehicle system. Chellabi and Nahon [3] used feedback linearization with an LQG approach to develop a controller. Adaptive control (Fossen and Fjellstad [10], Fossen and Sagatan [12], Goheen and Jefferys [13], and Yuh [40] [37] [39]) has been used to attempt to account for uncertainty of the parameters, but still relies on a linear model. Others have focused on sliding mode control (see e.g., Fossen and Foss [11], Dougherty, et al. [7], and Yoerger and Slotine [36]). Crist, et al. [5] have combined sliding mode control with adaptive control. Yuh, et al. [38] have also used neural networks as a vehicle controller. Sordalen [32], et al. use differential geometry to derive a control law based only on a kinematic model. Nakamura and Savant [28] [29] use a Liapunov-like function for a control law. Fjellstad and Fossen [8] also use a Liapunov-like function in conjunction with quaternions.

There is much less information in the literature on fault detection in AUV control systems. Determining when a fault has occurred or will occur is dependent on the values of system parameters. Alekseev et al. [1] use an observer-based approach to identify parameters. Healy proposed methods for identifying parameters using Kalman filters and neural networks [15] and using Kalman filters, batched least squares, and exponentially weighted least squares [16].

There is also relatively little in the literature on fault handling in AUV control systems. Rodríguez and Dobeck [31] use an expert systems approach to keep the vehicle safe. Barnett et. al. [2] also use a rule based method for handling faults, but their application is more sophisticated and allows completion of the mission where

possible. Payton et al. [30] have a novel approach that uses what is known to be possible rather than trying to determine the problem. Leonard [21] [22] [23] synthesizes controls using differential geometry, and averaging theory.

1.2 Goals

This work is principally concerned with the last of the three stages just described – fault tolerant control. The methodology used in our work is an adaptation of the theory developed by Leonard [21] for synthesizing controls. She implemented the theory on a symmetrical vehicle controlled exclusively by thrusters. The approach entails the use of differential geometry and averaging theory (see Appendix B) to develop equations that describe the motion of an AUV. These equations are then used to develop control algorithms. The theory is based on a kinematic model of the vehicle, a rigid body with six degrees of freedom. The control algorithms involve synthesis of small motions in a given unactuated direction via open loop control of motions in actuated directions.

Leonard [21] [23] provides an example of a synthesized yaw motion performed with SCAMP (Supplemental Camera and Maneuvering Platform), a 26-sided box which is normally fully actuated via thrusters, i.e. all six DOF are directly controllable by sets of thrusters acting together or differentially. SCAMP is a testbed for zero gravity experiments at the University of Maryland's Space Systems Laboratory (SSL); it is not a production vehicle. Leonard's example takes advantage of the symmetry of the SCAMP and does not point out the effects of the vehicle's inherent stability.

The focus of our work is to implement the control algorithms proposed in [21] and [23] on a model of a streamlined vehicle in which control forces are generated indirectly

using control planes, rather than directly with thrusters. As a particular test case, we use a modified model of the ARCS (Autonomous Remote Controlled Submersible). This vehicle is designed and built by International Submarine Engineering of Port Coquitlam, B. C., Canada. The ARCS is a streamlined, propeller-driven vehicle with one plane of symmetry and six control planes to direct its motion through the water. It is, by design, underactuated, i.e. the forward motion (surge) is controllable via the propeller; the roll, pitch, and yaw rates are controllable via the foreplanes, tailplanes, and rudder planes, but there is no direct control of sideways motion (sway), or up and down motion (heave). There is no real need to have direct control of sway and heave for the missions which the ARCS was designed to carry out. Since forward motion is fundamental to the purpose of the vehicle, this surge, when combined with yaw or pitch, will result in a sway or heave displacement respectively over a finite distance. In addition to being underactuated, the control of roll, pitch, and yaw is coupled to the surge velocity, because the motion resulting from control plane deflections is a function of the reaction forces (lift and drag) from water passing over the planes. ARCS represents a class of typical underwater vehicles.

The model of the ARCS we use was developed by Nahon [27]. It was written in Matlab, and is a fully nonlinear, dynamic model. The modifications we have made to this model allow us to separate the effects of the rigid body coupling from the effects of the righting moment of the vehicle. The modified model is called SYMARCS.

In this work, we will go beyond the example presented by Leonard [21] to deal with the effects of the control actuators being control planes rather than thrusters and of the stability of the vehicle interfering with the control outcomes.

First, we interpret the theory in light of the particular type of vehicle being considered. Then the algorithms for control synthesis are implemented and the results

analyzed. The end result is the determination of the usefulness of the fault tolerant control method for a typical streamlined vehicle.

The code to implement the algorithms was written in Matlab, as were the models of ARCS and SYMARCS. As a first step, single small steps were performed to gauge the success of the technique on a vehicle of this type. Next, a sequence of these small steps were performed to accomplish a larger motion.

In chapter two the details of the three vehicle models - SCAMP, ARCS, and SYMARCS are discussed. In chapter three the kinematics necessary to generate the control model are reviewed. Chapter four will present the control concept and the important considerations in applying the control algorithms. Chapter five will detail the determination of controller parameters and present some typical results. In chapter six the structure of the implementation on the SYMARCS model are described. Finally, in chapter seven conclusions and suggestions for future work are made.

Chapter 2

Vehicles

The control algorithms we use were developed and evaluated by Leonard [21] on an AUV which was controllable in all 6 degrees of freedom (DOF) via thrusters. Thrusters directly cause changes in translational or angular velocities of a vehicle, while lift and drag forces on control surfaces generate moments about the center of gravity, and the moments cause changes to the angular rates of the vehicle. We were interested in applying the methodology to a streamlined AUV controlled mainly with control surfaces. We chose the ARCS because it is typical of this type of vehicle. To isolate the effects of rigid body coupling and inherent dynamics from those caused by the righting moment (see sections 2.2 and 2.3), we modified ARCS to create a second vehicle we call SYMARCS.

SCAMP

Leonard [21] developed the control algorithms, then tested them at the University of Maryland's Space Systems Laboratory (SSL) on the Supplemental Camera and Maneuvering Platform (SCAMP). This underwater vehicle (see Figure 2.1) is a neutrally buoyant icosahexahedron (26-sided). It has a pair of ducted fan propellers

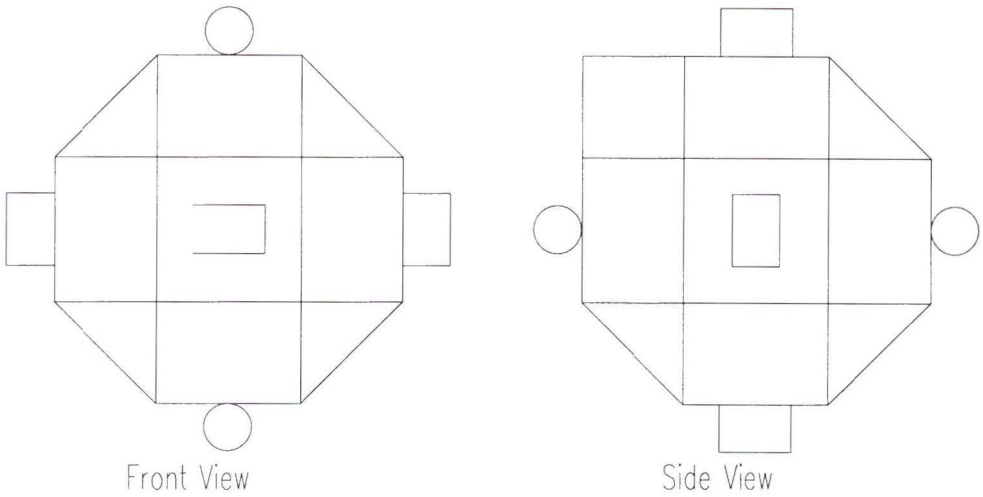

Figure 2.1: University of Maryland's SCAMP

about each of its three principle axis so that any pair of propellers running in the same direction causes translation along their associated axis, while rotation is the result of running a pair in opposing directions. It also has a 7-lb lead weight pendulum hung internally below its geometric center along the yaw axis. This pendulum remains fixed with respect to the body frame unless it is used for active pitch control. She used this vehicle to test her algorithm for a yaw manoeuver.

Leonard took advantage of the fact that constant propeller speed corresponds to constant vehicle speed, as the drag of the water on the vehicle dynamically balances the propulsive force of the thruster. She also noted that there was a time delay for the vehicle to follow the command, and that this time delay was related to the natural frequency of the vehicle. Because of the symmetry of the SCAMP, she was able to

assume that the time delay was the same for roll and pitch (the motions required to synthesize a yawing motion). SCAMP is a test bed. We wanted to test the control method on a typical autonomous undersea vehicle.

2.1 ARCS

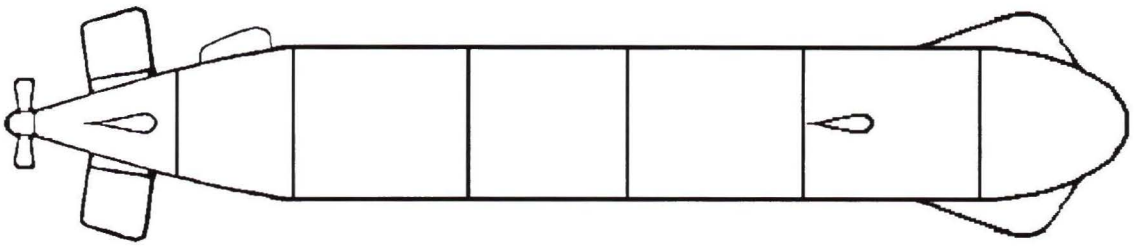

Figure 2.2: ISE ARCS

We used the ARCS vehicle (built by International Submarine Engineering of Coquitlam, B. C.) because it is a typical steamlined, propeller-driven, control-plane-actuated AUV. ARCS (see Figure 2.2) is a torpedo-shaped vehicle with one plane of symmetry and with six control planes; two horizontal foreplanes, two horizontal tailplanes, and two vertical tailplanes. Each of the six planes is capable of independent motion, but are used most often in pairs. The motive force is supplied by a propeller at the rear of the vehicle. In addition there are two nodules at the front of the vehicle; one on top and one on the bottom of the nose. These are for sonar and other instruments that may be required for the particular mission undertaken.

The ARCS can be described as a vehicle that is underactuated by design. It is not designed with sideways or vertical motions in mind, since there is no reason to

have pure sway or pure heave in the type of mission the vehicle is meant to perform. Any change in horizontal track or change in depth is accomplished by use of yaw and pitch respectively over a finite forward displacement. For example, if the vehicle is to go deeper, it is commanded to pitch downward, move "forward" (in the direction of surge for the vehicle), and then return to horizontal running at the desired depth. The rate of change of depth can be controlled by the amount of pitch angle and the forward speed of the AUV.

Changes in roll, pitch, and yaw are achieved by deflecting the control planes. At the rear of the vehicle, the vertical planes act as a rudder when they are actuated together in the same direction. They can also effect roll when actuated differentially. The horizontal tail planes at the rear are used for pitch control when moved together and roll when moved differentially. The horizontal foreplanes can also be used for pitch and/or roll. The foreplanes, because of their position forward of the center of mass (cm), will destabilize the vehicle, while the tail planes, being aft of the cm will stabilize ARCS.

The built-in redundancy of the vehicle allows full or partial control even in the event of a failure of a plane [25]. Roll can be accomplished as long as one of the six planes is functional and is fully available if one of the three sets of planes is operating. Pitch is possible using either the foreplanes or the horizontal tailplanes, or even just one of the four. To get a yawing motion at least one of the vertical surfaces must be working. The synthesis of controls we are implementing allows further redundancy of motions, e.g., if the yawing motion is not directly controllable, it can be synthesized by alternating roll and pitch motions.

Lift and drag forces are generated by the flow of water over the control planes. It is these forces that effect the change of orientation of the vehicle by generating

moments about the center of mass of the vehicle. The flow of water is mainly the result of the vehicle's forward motion through the water, so the controllability of the ARCS is a function of the forward speed. Because lift and drag are proportional to the square of the velocity, the control planes are more effective as the vehicle speed increases, but are useless when the ARCS is not moving.

Changes in orientation involve rotations about the center of mass of the vehicle. As is typical of ocean vessels of all kinds, the center of mass of the vehicle is located directly below the center of buoyancy, such that there is a finite distance between them. The distance between them directly influences the stability the vehicle. The force of gravity acts downward through the center of mass, and would cause the vehicle to sink, except that it is balanced by the buoyant force which acts upward through the center of buoyancy. The equivalence in magnitude of the gravitational force and the buoyant force is a design criterion and is referred to as *neutral buoyancy.* When the center of mass is directly below the center of buoyancy, the associated forces act along a common line and merely balance one another, but when the vehicle rolls or pitches, the lines of action of each force are separated by some moment arm, (see Figure 2.3 for the case of a roll angle). This distance between the lines of action is a function of the angle of roll or pitch and the distance between the two centers. The moment arm of the couple of forces (buoyancy and gravity) that will cause the vehicle angle of orientation to return to zero roll angle or zero pitch angle. The force couple and the associated moment arm is called the *righting moment.*

The center of buoyancy is fixed by the geometry of the vehicle, while the center of mass is established by the distribution of components in the vehicle. In the ARCS the center of buoyancy lies above the plane passing through the foreplanes and horizontal tailplanes, and the center of mass is below the plane.

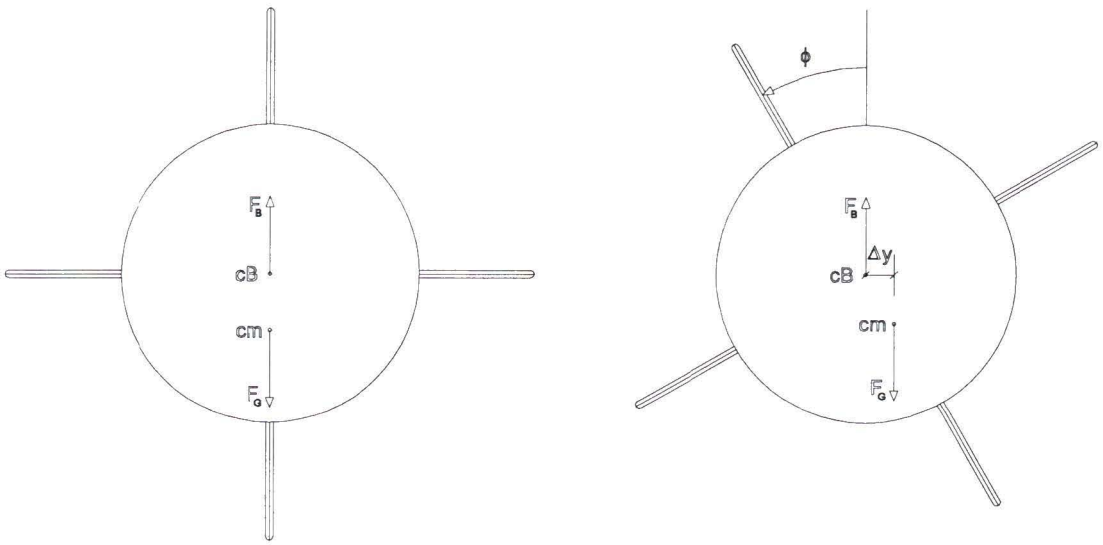

Figure 2.3: Stability of an AUV

When the vertical distance between the center of mass and the center of buoyancy is present in the model, the response to various inputs of control plane deflection is significantly different than when the vertical distance is not included (see Appendix A for details of the responses of the unmodified ARCS). In particular, for a direct control input, where we desire the vehicle to take up a new angle of orientation, the righting moment returns the roll angle to zero and the pitch angle to near zero. Only the yaw motion remains at the commanded angle. Due to the righting moment, the ARCS can only sustain a pitch or roll angle if the control planes remain at some given angle of attack. Since the control method used here depends on sinusoidal signals (i.e. the control planes are not held at a set angle of attack while a particular vehicle orientation is required), the righting moment is detrimental to the control method. The inability to get proper response to direct control suggests that synthesizing controls for the ARCS is not possible using the present methods. It may be possible and advantageous

to have an onboard system that will redistribute the weight in the vehicle to cause the center of mass to be coincident with the center of buoyancy negating the righting moment.

2.2 SYMARCS

To isolate the effects of the vehicle's righting moment, a second model was created by modifying the ARCS code. The second model, SYMARCS, has the vehicle center of mass in the same location as the center of buoyancy, so that both centers are in the plane passing through the horizontal tailplanes and foreplanes. This removes the righting moment. The SYMARCS model allows us to study the effects of the control algorithms due to the rigid body coupling and inherent nonlinearities of the vehicle independent from the effects of the righting moment.

2.3 Implementation

ARCS and SYMARCS are dynamic models based on the nonlinear equations of motion [27]. Typically with this type of vehicle,we are interested in speed control, heading control, and depth control. By depth control, we do not mean pure heave motions, but change of depth over a distance caused by pitching the vehicle to make it dive or ascend to the desired depth. With the control mode we use for the ARCS (see Table 2.1), the forward motion is controlled by propeller speed, the roll controlled via the foreplanes, the pitch controlled using the tailplanes, and the heading controlled with the rudders. There is no way to synthesize the forward velocity, so we can exclude it from the fault tolerance scheme. Heading and depth changes are accomplished by

changes of orientation, so if speed control is handled as a separate issue, all that remains is to control the orientation via the control planes. Thus we need only concern ourselves with the orientation of the vehicle when applying the control method.

Actuator(s)	DOF
Foreplanes	Roll
(Horizontal) Tailplanes	Pitch
Rudders (Vertical Tailplanes)	Yaw
Propeller	Fwd. Vel.

Table 2.1: Actuator Control of DOF Assignment

The top speed of the ARCS is about 4 m/s. In this work analysis was carried out using vehicle speeds between 0.5 m/s and 4.0 m/s.

Chapter 3

Kinematics

Typically we are interested in the position and orientation of the vehicle at any given instant of time. As stated in the last chapter, however, only the orientation is necessary for the implementation of the fault tolerant control method on the vehicles being considered, the kinematics discussion is limited to rotations and angular rates.

3.1 Reference Frames

An autonomous underwater vehicle can be modelled as a rigid body in space, having six possible degrees of freedom (DOF). All movements of the vehicle can be described in terms of these DOF. These descriptions of the vehicle motions, as well as descriptions of the orientation and position of the vehicle, are facilitated by the use of two orthogonal reference frames (see Figure 3.1). The first frame is "fixed" to the earth; it is designated the inertial reference frame and denoted by the subscript I, e.g. $[\mathbf{r}]_I$

denotes an arbitrary vector, $\mathbf{r}$, described (or "decomposed") in the inertial frame[1]. We will define the inertial frame as follows: The z_I-axis is directed downward towards the center of the earth (i.e. in the direction of the pull of gravity). The direction of the x_I-axis is arbitrary as long as it is in the horizontal plane (orthogonal to the z_I-axis). Once the direction of the x_I-axis has been chosen, the direction of the y_I-axis is defined in accordance with the right hand rule for right orthogonal frames. The second frame is fixed to the vehicle with its origin at the center of mass. It moves with the vehicle, and is designated the body-fixed reference frame. This frame is denoted by the subscript B, e.g. $[\mathbf{r}]_B$ denotes the vector, $\mathbf{r}$, described in the body frame. It is to be noted that $[\mathbf{r}]_I$ and $[\mathbf{r}]_B$ describe the same vector with respect to the two different reference frames. The x_B-axis of the body frame is pointed towards the nose of the vehicle, the y_B-axis points directly starboard (out the right-hand side of the vehicle), and the z_B-axis is directed toward the bottom of the vehicle. The six basic motions are: translation along the x_B-axis (called surge), translation along the y_B-axis (sway), translation along the z_B-axis (heave), rotation about the x_B-axis (roll), rotation about the y_B-axis (pitch), and rotation about the z_B-axis (yaw).

3.2 Orientation Kinematics

The orientation of the vehicle can be described in the inertial frame by three angles: ϕ (roll angle), θ (pitch angle), and ψ (yaw angle). At any instant of time, knowledge of the value of these three angles allows us to relate the description of any vector, in the

[1]Technically the earth-fixed frame is not an inertial reference, since the earth moves relative to the stars, however the motion of the vehicle is not significantly affected by the accelerations of a point on the earth.

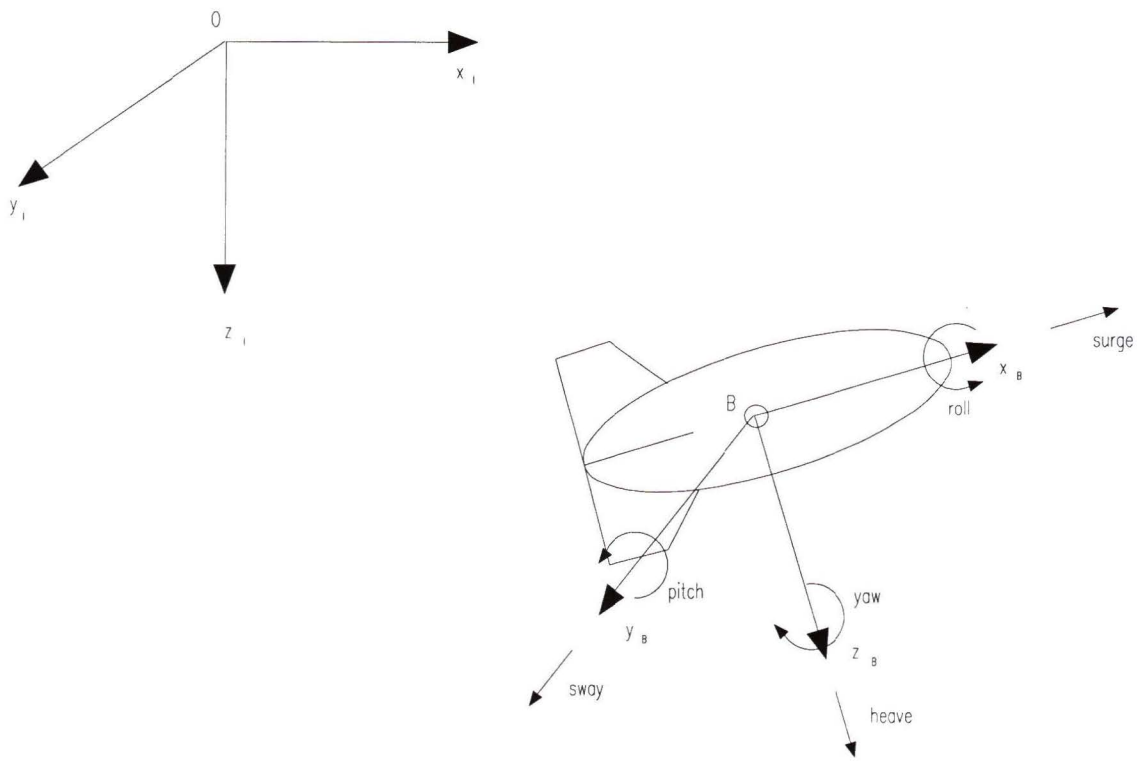

Figure 3.1: Inertial and Body-fixed Reference Frames

body-fixed frame, to its description in the inertial frame via an orthogonal rotation matrix, **R**.

A rotation matrix may be determined using Euler's Theorem on rotation [9]

> *Every change in the relative orientation of a frame B with respect to another frame A can be produced by means of a simple rotation of B in A.*

Consider two frames, A and B, which are initially coincident. Consider also an arbitrary vector, **r**, which can be described in either frame and initially

$$[\mathbf{r}]_A = [\mathbf{r}]_B$$

Finally, consider a unit vector, **k**, representing the axis about which frame B is rotated

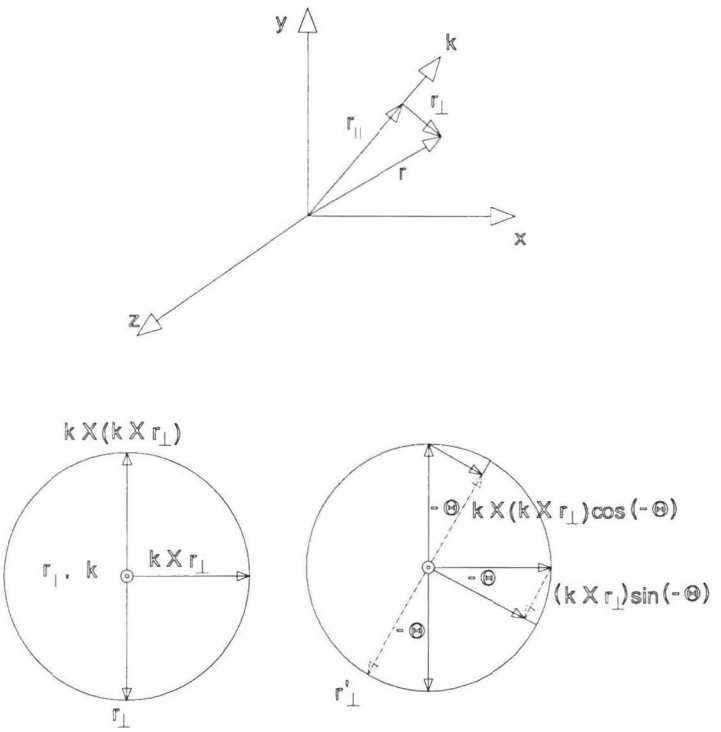

Figure 3.2: Rotation About Equivalent Axis

by an arbitrary angle of Θ (see Figure 3.2). $\mathbf{k}$ is called the equivalent axis, and is expressed in frame A as

$$\mathbf{k} = \begin{bmatrix} k_x & k_y & k_z \end{bmatrix}^T$$

The rotation matrix, $\mathbf{R}$, is given by [4]:

$$\mathbf{R}_k(\Theta) = \begin{bmatrix} k_x^2(1-c\Theta)+c\Theta & k_xk_y(1-c\Theta)-k_zs\Theta & k_xk_z(1-c\Theta)+k_ys\Theta \\ k_yk_x(1-c\Theta)+k_zs\Theta & k_y^2(1-c\Theta)+c\Theta & k_yk_z(1-c\Theta)-k_xs\Theta \\ k_zk_x(1-c\Theta)-k_ys\Theta & k_zk_y(1-c\Theta)+k_xs\Theta & k_z^2(1-c\Theta)+c\Theta \end{bmatrix} \tag{3.1}$$

$$c = \cos \text{ and } s = \sin$$

After the rotation we can write

$$[\mathbf{r}]_A = \mathbf{R}\,[\mathbf{r}]_B$$

We say that $\mathbf{R}$ maps the decomposition of $\mathbf{r}$ in frame A to a decomposition of $\mathbf{r}$ in frame B. For example, for a pure rotation about the x-axis (roll)

$$\mathbf{k} = \begin{bmatrix} 1 & 0 & 0 \end{bmatrix}^T$$

$$\mathbf{R}_k(\Theta) = \begin{bmatrix} 1 & 0 & 0 \\ 0 & c\Theta & -s\Theta \\ 0 & s\Theta & c\Theta \end{bmatrix}$$

so that

$$\begin{aligned} [r_x]_A &= [r_x]_B \\ [r_y]_A &= [r_y]_B \cos\Theta - [r_z]_B \sin\Theta \\ [r_z]_A &= [r_y]_B \sin\Theta + [r_z]_B \cos\Theta \end{aligned}$$

$\mathbf{R}$ can be used to map the decomposition of a given vector in the body-fixed frame to a decomposition in the inertial frame.

$$[\mathbf{r}]_I = \mathbf{R}\,[\mathbf{r}]_B \tag{3.2}$$

for an arbitrary vector, $\mathbf{r}$. Technically, a rotation matrix may be developed to map any frame into any other frame, and the notation should include indication of which frame is the *from* frame and which is the *to* frame, e.g. ${}^{X}_{Y}\mathbf{R}$ would indicate the mapping from the Y-frame to the X-frame. We will define $\mathbf{R}$ (without indices) as the rotation matrix mapping a vector from the body frame to the inertial frame.

One of the properties of $\mathbf{R}$ is that it is orthonormal

$$\mathbf{R}^T\mathbf{R} = \mathbf{I} \tag{3.3}$$

$\mathbf{R}^T$ is the transpose of $\mathbf{R}$ and maps a vector from the inertial frame to the body frame. Note that $\mathbf{R}$ merely changes the basis of description of a given vector, and the vector itself is unchanged, that is, we are talking about the *same* vector before and after the transformation. The metric of vector length remains unchanged under the transformation by a rotation matrix.

3.3 Velocity Kinematics

Taking the time derivative of equation (3.3) gives

$$\mathbf{R}^T\dot{\mathbf{R}} + \dot{\mathbf{R}}^T\mathbf{R} = \mathbf{0} \tag{3.4}$$

Let

$$\mathbf{S} = \mathbf{R}^T\dot{\mathbf{R}}$$

or,

$$\dot{\mathbf{R}} = \mathbf{RS} \tag{3.5}$$

Equation (3.4) can be written

$$\mathbf{S} + \mathbf{S}^T = \mathbf{0}$$

or

$$\mathbf{S} = -\mathbf{S}^T$$

showing that $\mathbf{S}$ is a skew symmetric matrix, which can be written as [4]:

$$\mathbf{S} = \begin{bmatrix} 0 & -\omega_z & \omega_y \\ \omega_z & 0 & -\omega_x \\ -\omega_y & \omega_x & 0 \end{bmatrix}$$

Note that $\mathbf{S}$ is the matrix form of a cross product operation involving

$$[\boldsymbol{\omega}]_B = \begin{bmatrix} \omega_x & \omega_y & \omega_z \end{bmatrix}$$

the angular velocity of the vehicle expressed in the body frame. For an arbitrary vector, $[\mathbf{r}]_B$, decomposed in the body frame

$$[\boldsymbol{\omega}]_B \times [\mathbf{r}]_B = \mathbf{S}\,[\mathbf{r}]_B$$

Equation (3.5) expresses the rate of change of orientation of the vehicle decomposed in the inertial frame, as a matrix product of the rate of change of orientation of the vehicle decomposed in the body frame and the rotation matrix relating the inertial frame to the body frame. This is very much like equation (3.2), where we have now defined the vector, $\mathbf{r}$, to be the angular rate of the vehicle. The difference between (3.5) and (3.2) is that in (3.5) the angular rates are expressed in matrix form rather than as vectors.

3.4 Mathematical Notes

Rotation matrices belong to the group of *Special Orthogonal* matrices.

$$\mathbf{R} \in SO(3)$$

where

$$SO(3) \triangleq \left\{ \mathbf{R} \in \mathbb{R}^{3\times 3} \mid \mathbf{R}^T\mathbf{R} = \mathbf{I}, \det(\mathbf{R}) = 1 \right\} \tag{3.6}$$

Since $\det(\mathbf{R}) = 1$, $\mathbf{R}$ is, by definition, never singular, and, therefore, always invertible.

The matrix $\mathbf{S}$ belongs to the group of all 3×3 skew symmetric matrices with real elements:

$$\mathbf{S} \in so(3)$$

where

$$so(3) \triangleq \left\{ \mathbf{S}(\boldsymbol{\beta}) \in \mathbb{R}^{3\times 3} \mid \mathbf{S}^T + \mathbf{S} = \mathbf{0}; \boldsymbol{\beta} \in \mathbb{R}^3 \right\} \tag{3.7}$$

In our application $\boldsymbol{\beta} = [\boldsymbol{\omega}]_B$.

Through $\mathbf{R}$ and its derivative, $\dot{\mathbf{R}} = \mathbf{RS}$, we have all the information about the orientation and rate of change of orientation of the vehicle. $\mathbf{R}$ defines the state of the vehicle in terms of orientation. This will be the basis of the controller model.

Chapter 4

Control System Model

In this chapter we will review the development of the control model based on the kinematics discussed in chapter 3. We will then describe the mechanics of achieving the desired vehicle response in DOF's that are directly actuated as well as those that must be synthesized. And finally, we will look at the equations used to generate the input to the control planes of the vehicle.

4.1 Constructive Controllability

We can state the control problem [23] in terms of orientation of the vehicle:

> Given an initial orientation $\mathbf{R}_i \in G$, a final orientation $\mathbf{R}_f \in G$ and a time $t_f > 0$, find controls $\mathbf{u}(t) = (u_1(t), \ldots, u_m(t))$, $t \in [0, t_f]$, such that $\mathbf{R}(0) = \mathbf{R}_i$ and $\mathbf{R}(t_f) = \mathbf{R}_f$.

In simple terms we use the relation

$$\mathbf{R}_i + \dot{\mathbf{R}} t_f = \mathbf{R}_f$$

where we choose $\dot{\mathbf{R}}$. Recall equation (3.5),

$$\dot{\mathbf{R}} = \mathbf{RS}$$

We choose $\dot{\mathbf{R}}$ by specifying $\mathbf{S}$. We specify $\mathbf{S}$ by controlling the angular rate of the vehicle $[\boldsymbol{\omega}]_B$ via control plane deflections. The vehicle's angular rate can be expressed in terms of orthogonal unit vectors (basis vectors [33]), $\widehat{x}$, $\widehat{y}$, and $\widehat{z}$.

$$\begin{aligned}
[\boldsymbol{\omega}]_B &= \begin{bmatrix} \omega_x & \omega_y & \omega_z \end{bmatrix} = \begin{bmatrix} \omega_1 & \omega_2 & \omega_3 \end{bmatrix} \\
&= \omega_1 \begin{bmatrix} 1 & 0 & 0 \end{bmatrix} + \omega_2 \begin{bmatrix} 0 & 1 & 0 \end{bmatrix} + \omega_3 \begin{bmatrix} 0 & 0 & 1 \end{bmatrix}
\end{aligned}$$

Similarly, $\mathbf{S}$ can be expressed in terms of basis matrices where each basis matrix is the skew symmetric representation of a rotation about one of the unit basis vectors.

$$\begin{aligned}
\mathbf{S} &= \omega_1 \begin{bmatrix} 0 & 0 & 0 \\ 0 & 0 & -1 \\ 0 & 1 & 0 \end{bmatrix} + \omega_2 \begin{bmatrix} 0 & 0 & 1 \\ 0 & 0 & 0 \\ -1 & 0 & 0 \end{bmatrix} + \omega_3 \begin{bmatrix} 0 & -1 & 0 \\ 1 & 0 & 0 \\ 0 & 0 & 0 \end{bmatrix} \\
&= \omega_1 \mathbf{B}_1 + \omega_2 \mathbf{B}_2 + \omega_3 \mathbf{B}_3 \\
&= \sum \omega_k \mathbf{B}_k
\end{aligned}$$

So (3.5) becomes

$$\dot{\mathbf{R}} = \mathbf{R} \sum \omega_k \mathbf{B}_k$$

Let our inputs to the control planes be in terms of the desired vehicle angular rates

$$\epsilon \, u_k = \omega_k \tag{4.1}$$

The vehicle changes its angle of orientation at a rate proportional to the angle of attack of the control plane. For a given control input, $\epsilon \, u_k$, the angle of attack of the control plane will follow the input, as will the vehicle angular rate, but the vehicle's

orientation changes by an amount proportional to the area under the input curve. This is not the case when the righting moment is present, because it tends to negate any non-zero pitch or roll angle.

We can express the control vector as a matrix in the form

$$\mathbf{U} = \sum u_k \mathbf{B}_k$$

Then we can write

$$\dot{\mathbf{R}}(t) = \epsilon \mathbf{R}(t)\,\mathrm{U}(t), \qquad \mathbf{U}(t) = \sum_{k=1}^{m} u_k(t)\,\mathbf{B}_k \qquad m \leq n \tag{4.2}$$

where m is the number of directly actuated DOF and n is the number of DOF of the system. (The orientation of the vehicle involves three DOF; $n = 3$.) $\mathbf{R}(t)$ is the state of the vehicle orientation at time, t; $\dot{\mathbf{R}}(t)$ is the rate of change of that state. $\epsilon\mathbf{U}(t)$ is the controllable angular velocity of the vehicle in the body frame. ϵ is a small scaling parameter that comes from the averaging theory (see Appendix B).

This is all fairly simple mathematics, but it sets up the synthesis of motions in DOF that are not directly actuated. A basis matrix that is not available, that is, we cannot directly control the motion in that DOF, can be synthesized via a Lie bracket operation (see Appendix B):

$$\mathbf{AB} - \mathbf{BA} = \mathbf{C}$$

In particular

$$\begin{aligned} \mathbf{B}_2\mathbf{B}_3 - \mathbf{B}_3\mathbf{B}_2 &= \mathbf{B}_1 \\ \mathbf{B}_3\mathbf{B}_1 - \mathbf{B}_1\mathbf{B}_3 &= \mathbf{B}_2 \\ \mathbf{B}_1\mathbf{B}_2 - \mathbf{B}_2\mathbf{B}_1 &= \mathbf{B}_3 \end{aligned}$$

If motion in any two of the three DOF are directly controllable, motion in the third DOF can be synthesized. It is clear that at least two basis matrices are necessary to

synthesize the third, i.e. $m = 2, 3$ are the only possibilities for maintaining control of the vehicle.

Equation (4.2) provides a kinematic model of motion of the AUV by describing the rate of change of $\mathbf{R}$, the orientation of the vehicle, as a function of the vehicle angular velocity, $[\boldsymbol{\omega}]_B$. Clearly if there is no control input matrix, $\mathbf{U}$, there will be no change in orientation of the vehicle. This is termed *drift-free*. In a dynamic model, even if there is no righting moment, the drift free condition may not necessarily be true, and the mathematics behind this approach may not be applicable without further theorems to take the drift into account. However, according to Leonard [23]:

> "...we assume dynamics are secondary to kinematics. This can be justified in the case of a symmetric vehicle or in the limit of low Reynolds number. However, even for the more general vehicle control problem, our investigation of the nonlinear coupling in the vehicle kinematics provides an important first step."

Appendix B provides a summary of the background theory in differential geometry and geometric control. A more detailed account and further treatment of the subject is provided by a recent text by Jurdjevic [20]. For those who are unfamiliar with differential geometry, a good starting point is the text by Curtis [6]. For mathematical details of how Leonard uses geometric control to develop algorithms for direct and synthesized controls, see her thesis [21]. In the next section we will present a non-mathematical description of the control methodology.

4.2 Control Concept

The control model used to develop the control algorithms is based on a kinematic model. We apply the control algorithms to a fully dynamic model. We have followed

Leonard's approach and used her algorithms which divide the control generation into two routines: control for motion in directions that have actuators available, and control for synthesis of motion in directions that do not have actuators available.

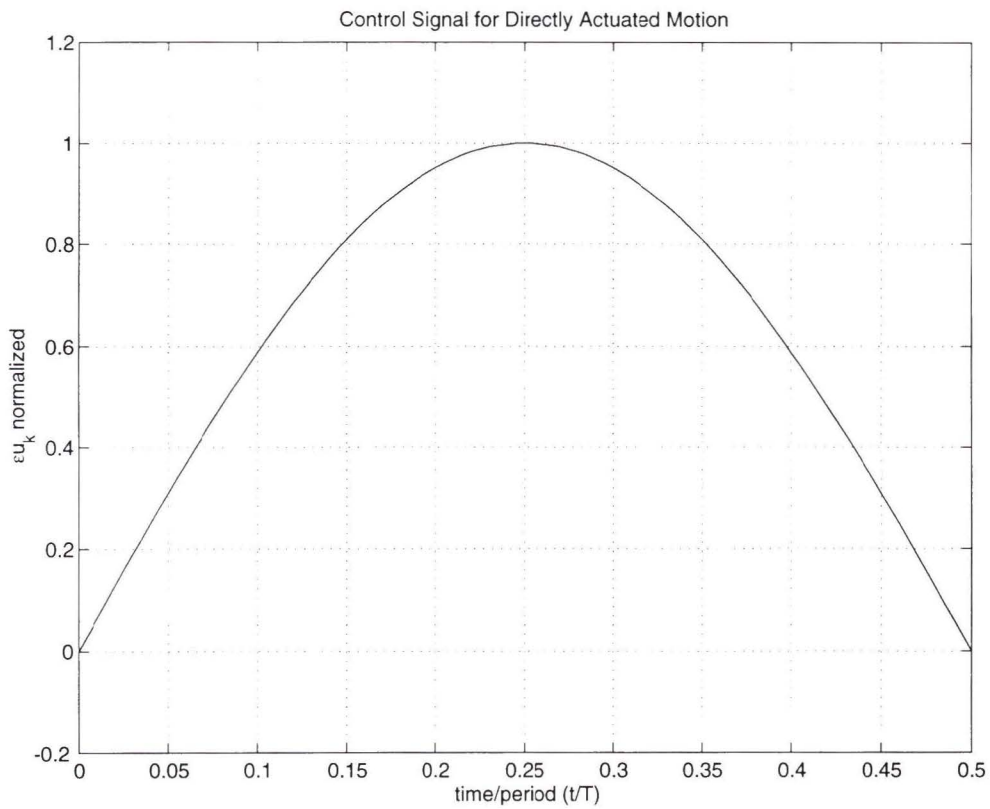

Figure 4.1: Control Input Signal for Motion in DOF Directly Actuated

For motions in DOF's that have direct actuation available, we use a half sine wave to reorient the vehicle (see Figure 4.1). The half sine wave is applied to the desired control plane. As long as the control plane is at a non-zero angle of attack, the vehicle will change orientation with respect to the inertial frame. The angular velocity of the vehicle follows the sine wave, so that the velocity is zero at the start and the end of the control signal, but the orientation of the vehicle has changed by an

amount proportional to the area under the half sine wave. From this it is clear that the magnitude of the reorientation is a function of the magnitude and the period of the sine wave. Also, the period of the sinusoidal signal must be long enough to allow the vehicle to follow the command input. Direct control is achieved by a $\frac{1}{2}$ sine wave of amplitude $\frac{1}{2}c_k\omega$:

$$\epsilon\, u_k = \frac{1}{2}c_k\omega \sin\left(\omega\left(t - t_0\right)\right) \tag{4.3}$$

where ω is determined by the choice of the period, T, of the control signal.

$$\omega = \frac{2\pi}{T}$$

With $t_0 = 0$, and $t_f = \frac{\pi}{\omega}$ (a half of the period), since the angle of reorientation, k, is the integral of the angular rate over the duration of the signal,

$$k = \int_{t_0}^{t_f} \epsilon\, u_k\left(t\right) dt$$

$$\begin{aligned} k &= \int_{t_0}^{t_f} \frac{1}{2}c_k\omega \sin\left(\omega t\right) dt \\ &= -\frac{1}{2}c_k\omega \left[\cos\left(\omega t\right)\right]_{t_0}^{t_f} \\ &= -\frac{1}{2}c_k\omega \left[-1 - 1\right] \\ &= c_k \end{aligned}$$

So c_k represents the controllable portion of the magnitude of the sinusoidal signal sent to the control planes, while k represents the desired change in angle of orientation. We shall denote the desired response in the direct case as k_d to differentiate it from the synthesized case, k_s.

Synthesis of motion for DOF's that do not have direct actuation available is based on non-commutativity of two successive rotations. This can be illustrated be a series

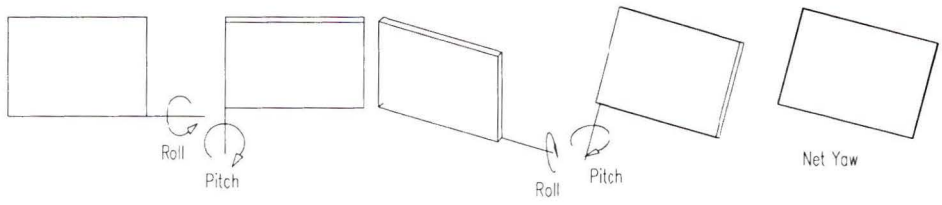

Figure 4.2: Example of Non-Commutativity of Rotations

of rotations of a book (see Figure 4.2). Roll a book through some finite angle, then pitch it through a similar angle. Follow this by rolling it back through an angle equivalent to the original roll angle, but in the opposite direction; do the same for the pitch angle. What you are left with is no net roll or pitch, but a net yaw angle. The continuous time analog of the discrete rotations is a set of two sine waves with a phase difference of 90° (see Figure 4.3). Naturally, the period of the two sine waves must be the same.

The synthesized motions are accomplished by two sine waves $(\epsilon u_i, \epsilon u_j)$which are generated from an orientation command, c_{ij}. Because the motion in this DOF is not directly controllable, $k_s = c_{ij}$ (as opposed to $k_d = c_k$), but the actual signals used require different coefficients. The generation follows the path [21]

$$c_{ij} \rightarrow (\alpha_i, \alpha_j) \rightarrow (\epsilon u_i, \epsilon u_j) \rightarrow \text{control planes} \rightarrow k_s$$

Again the signals start and end at zero. In addition they have a zero average since we ensure that they complete M cycles for the lagging signal, and $M + 1$ cycles for the leading signal (the average value for a complete cycle of a sine wave is zero). The time interval is split into three sections: the lead signal alone, the lead signal and the

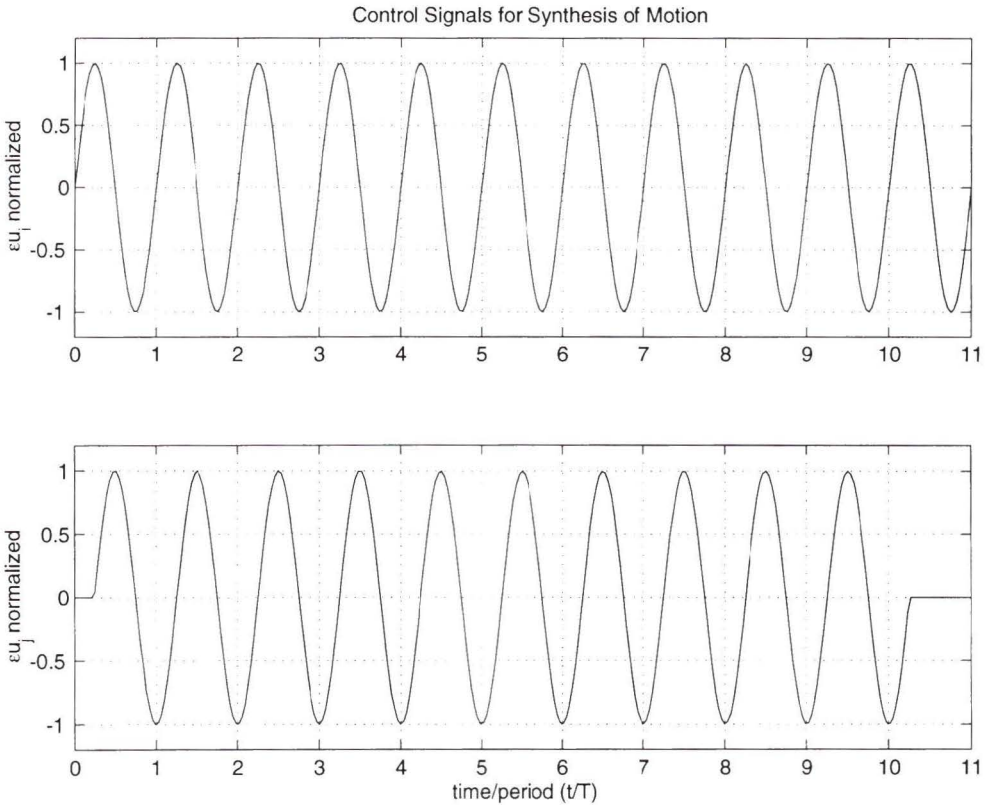

Figure 4.3: Control Input Signals to Synthesize Motion in DOF Not Directly Actuated

lag signal 90° behind, and finally the lead signal through another 270° to finish with a complete cycle.

$$
\left.\begin{aligned} \epsilon\, u_i &= \alpha_i \omega \sin\left(\omega\left(t - t_0\right)\right) \\ \epsilon\, u_j &= 0 \end{aligned}\right\} \quad t \in [0, s1]
$$

$$
\left.\begin{aligned} \epsilon\, u_i &= \alpha_i \omega \cos\left(\omega\left(t - s1\right)\right) \\ \epsilon\, u_j &= \alpha_j \omega \sin\left(\omega\left(t - s1\right)\right) \end{aligned}\right\} \quad t \in [s1, s2] \tag{4.4a}
$$

$$
\left.\begin{aligned} \epsilon\, u_i &= \alpha_i \omega \cos\left(\omega\left(t - s2\right)\right) \\ \epsilon\, u_j &= 0 \end{aligned}\right\} \quad t \in [s2, s3]
$$

where

$$\begin{aligned} s1 &= t_0 + \frac{T}{4} \\ s2 &= s1 + MT \\ s3 &= s2 + \frac{3T}{4} \end{aligned}$$

4.3 Limiting Relationships

As stated previously, the period of the control signals must be greater than the vehicle response time, so that the vehicle is able to follow the command. In addition, Leonard chooses M, the number of cycles necessary, such that M is an integer greater than or equal to $\frac{1}{\pi c}$ where c is the magnitude of the motion commanded. This M is the number of complete cycles required to achieve the magnitude of motion.

$$M \geq \frac{1}{\pi c} \quad M \in \mathbb{I}$$

Chapter 5

Determination of Control Parameters

Before we can effectively control the vehicle, we need to look at the typical response parameters. First we will look at the period, T, required for the sinusoidal signals we are using. Then we will analyze the vehicle's response to commands for motion that can be achieved by direct control, and motion that must be synthesized. We will use the resulting parameters to develop a compensator for the vehicle. The control commands are input to the vehicle as signals to drive the control planes, but it is the vehicle orientation we are aiming to affect. The compensator accounts for the mapping of control plane deflections to changes in the vehicle's orientation.

5.1 Step Input Response

For the SYMARCS model, the response time for motions in different DOF cannot be assumed to be relatively equal, e.g. the response time in roll is significantly different

than the response time in yaw. Care must be taken to ensure the vehicle has enough time to respond, so that it can follow the control inputs, and still maintain their phase difference. In order to determine the values of the response times involved, we performed a series of step inputs to the SYMARCS model. (It is to be noted that the actuators are not fully modelled in either vehicle model, that is, the delay times induced by actuator response are not taken into account, so a step input command will be seen as an instantaneous change in control plane angle of attack.)

5.1.1 Roll

The SYMARCS model gave ideal response to a roll command (see Figure 5.1).

The step input of 0.1 radians gives a step change in the (differential) angle of the foreplanes, causing a change in the roll rate, and the vehicle becomes similar to a bullet spinning through the water without drifting off course (see Figure 5.2).

5.1.2 Pitch

Again the SYMARCS model provides what we would expect as an ideal response. The step input command of 0.1 radians to the (horizontal) tailplanes effects a step change to the pitch velocity and the vehicle goes into a loop in the vertical plane (Figure 5.3).

5.1.3 Yaw

The ideal response to a 0.1 radians step input yaw command to the rudders (vertical tailplanes) is provided by the SYMARCS model (Figure 5.4) - a step change in yaw rate and a looping trajectory in the horizontal plane.

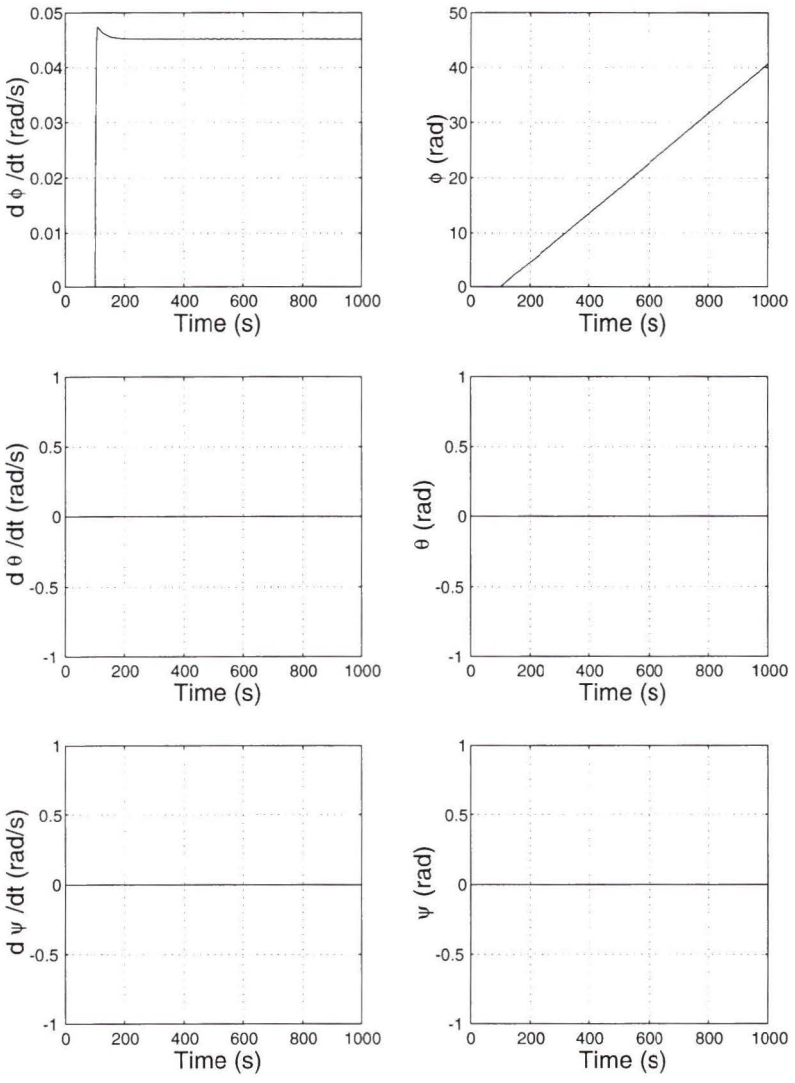

Figure 5.1: Rotational Position and Velocity for SYMARCS Model at 0.5 m/s - 0.1 radian Step Input to Foreplanes (Roll)

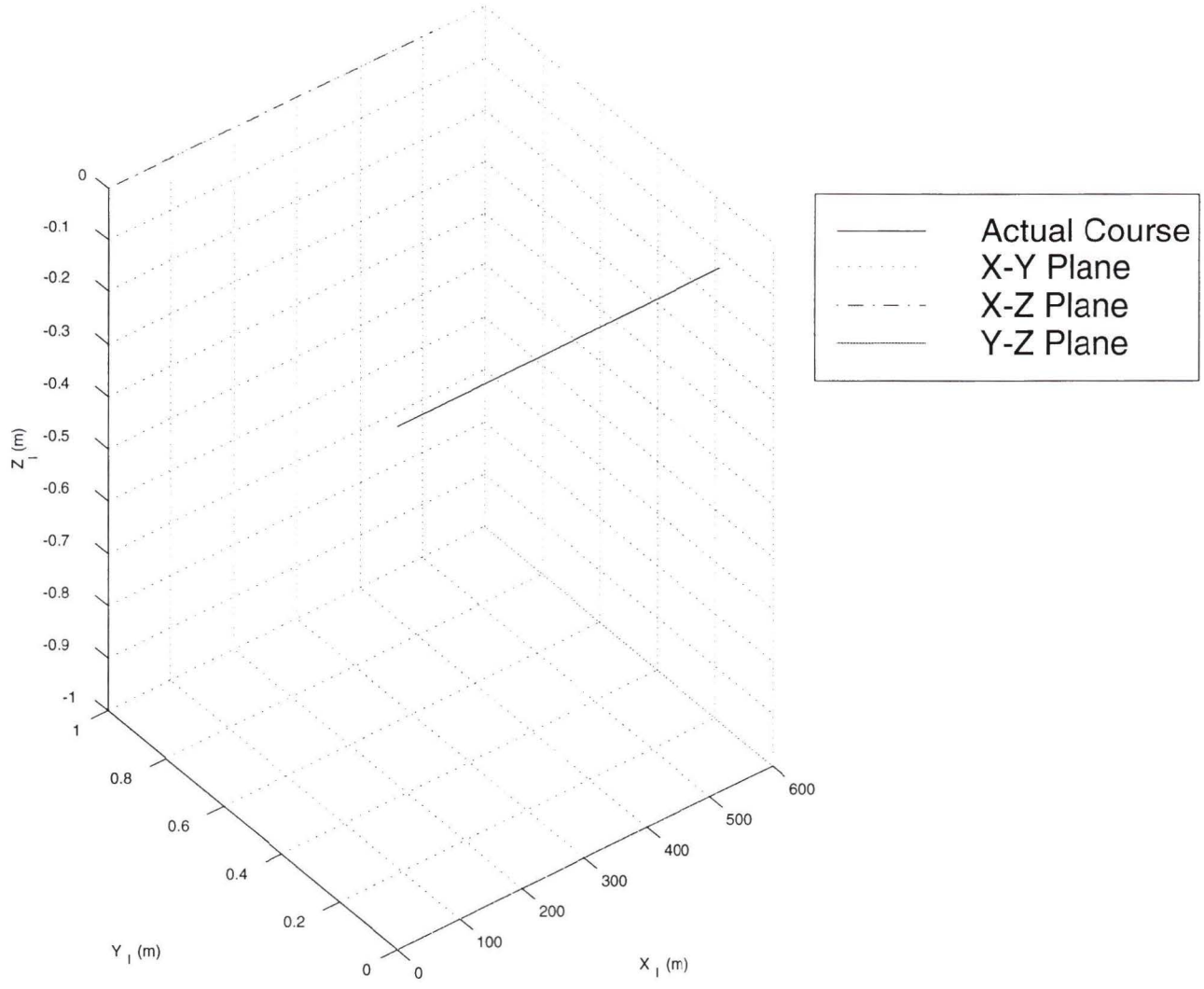

Figure 5.2: Trajectory of SYMARCS Model at 0.5 m/s - 0.1 radian Step Input to Foreplanes (Roll)

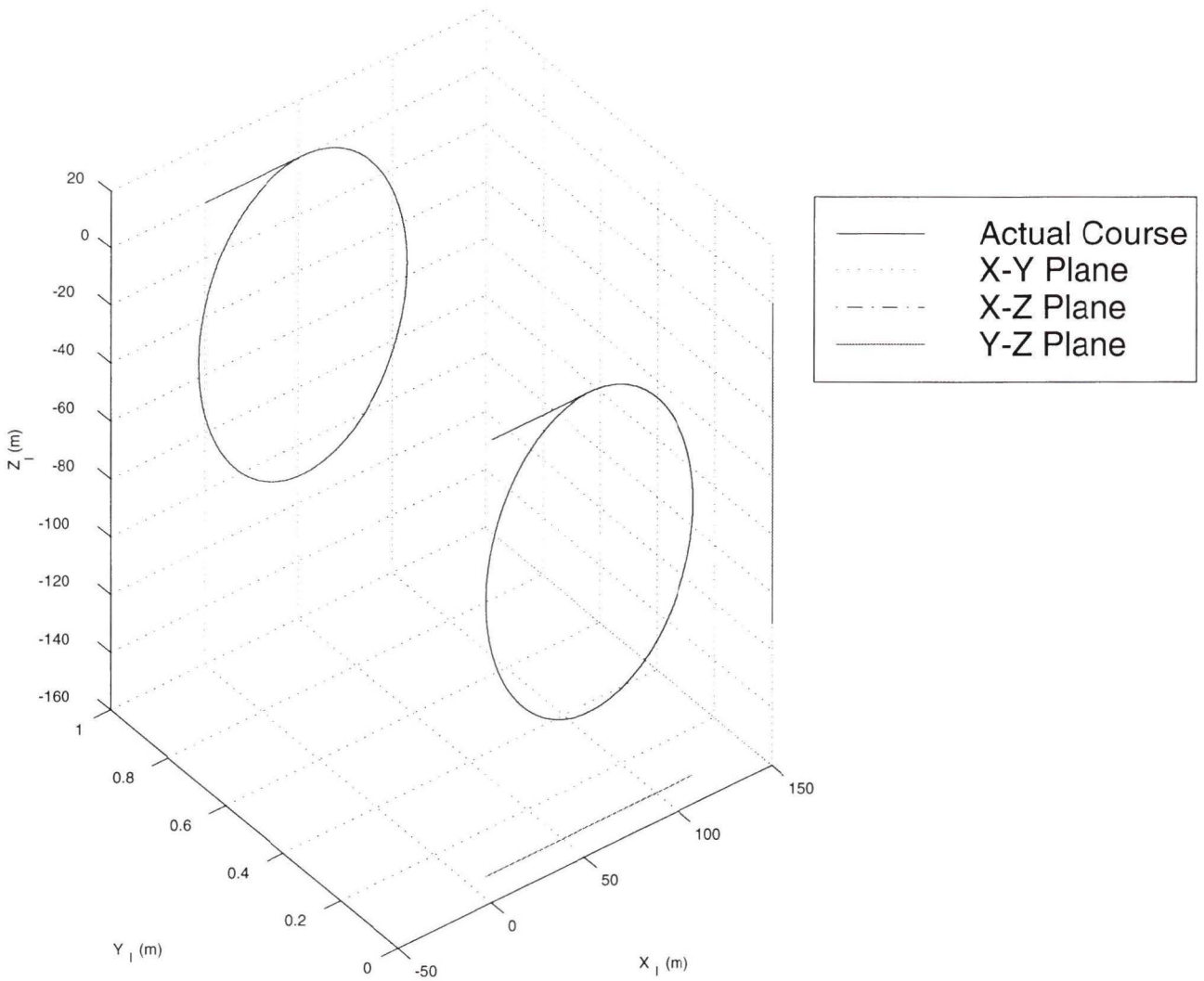

Figure 5.3: Trajectory of SYMARCS Model at 0.5 m/s - 0.1 radian Step Input to Horizontal Tailplanes (Pitch)

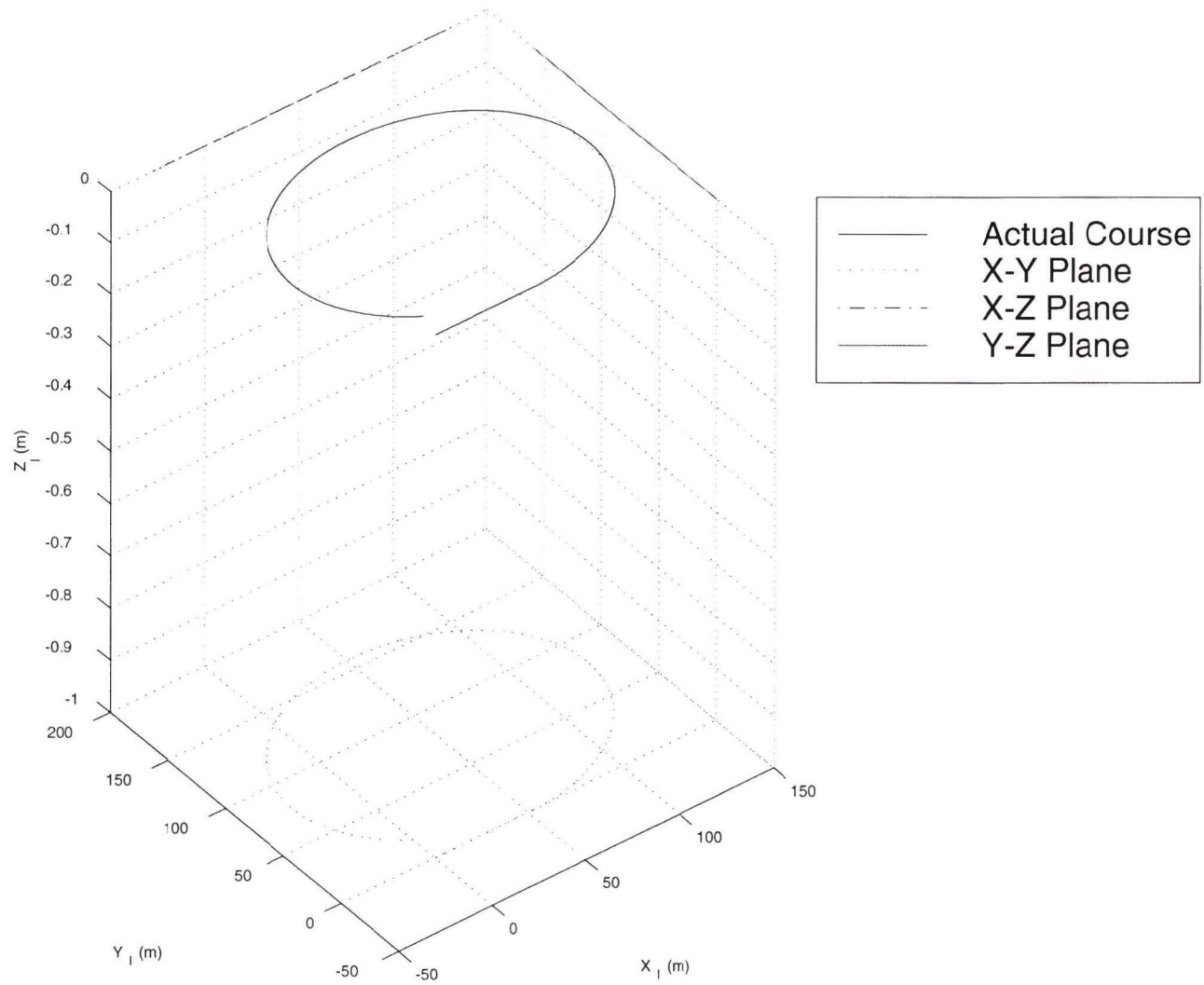

Figure 5.4: Trajectory of SYMARCS Model at 0.5 m/s - 0.1 radian Step Input to Vertical Tailplanes (Yaw)

5.1.4 Settling Times

As can be seen in Figure 5.1, the response to a step input has the characteristics of a 2^{nd} order system. We chose to use the settling time as our measure of the transient response time. We will define the settling time as the time to reach and stay within 5% of the steady state value, i.e. the response is 95% complete. Table 5.1 gives the settling times in relation to the surge velocities for each commanded motion. Based

$U\,(m/s)$	$t_{s,\phi}\,(s)$	$t_{s,\theta}\,(s)$	$t_{s,\psi}\,(s)$
0.5	9.3	3.7	25.7
1.0	1.9	1.7	12.6
1.5	1.2	1.3	8.5
2.0	0.8	0.9	6.6
2.5	0.8	0.6	5.1
3.0	0.6	0.5	4.3
3.5	0.5	0.4	3.6
4.0	0.4	0.5	3.2

Table 5.1: SYMARCS Settling Times

on this data, we chose to use a period of $T = 25s$. This one value allows the vehicle to follow the control inputs in all three orientations and at all speeds.

5.2 Direct Control

In this section we will examine the vehicle response to a half sine wave input, and determine the compensation necessary such that the vehicle response, k_d, to a control

input for a DOF that is directly controllable is equivalent to the command given, $k_{d,desired}$.

5.2.1 Vehicle Response

The SYMARCS model again provides ideal responses when we apply direct controls to the control planes. The half-sine wave causes a step change in the angle for the DOF being controlled (see Figures 5.5 and 5.6).

The maximum magnitude of the sine wave used as a control input (see (4.3)) is

$$\epsilon\, u_k = \frac{1}{2} c_k \omega \qquad k \in \left\{ \begin{array}{ccc} \phi & \theta & \psi \end{array} \right\}$$

where ω is the angular frequency of the sine wave ($\omega = \frac{2\pi}{T}$), and c_k is the commanded magnitude of vehicle rotation.

By setting c_k to 0.05 radians, and for a period of $T = 2s$[1], the SYMARCS model gave the magnitudes of response as detailed in Table 5.2.

Setting c_k to 0.05 radians, and for a period of $T = 25s$, the SYMARCS model gave the magnitudes of response in Table 5.3. The values in Table 5.3 are almost exactly the same as those in Table 5.2. This indicates the response is not significantly affected by changes in period, so we can use the data at $T = 2s$ for our control signals at $T = 25s$. This apparent invariance with period, T, is due to the dependence of the magnitude of the control input signal on its angular frequency. As T increases, ω decreases, and the magnitude of the signal is decreased, but it is active over a proportionally longer time, so that the area under the sine curve is constant.

[1]A period of $T = 2s$ was used before the step input response was performed. After the step input responses were analyzed and the period was chosen to be $25s$, we performed a spot check of responses for the new period and found them to be roughly the same as those for $T = 2s$.

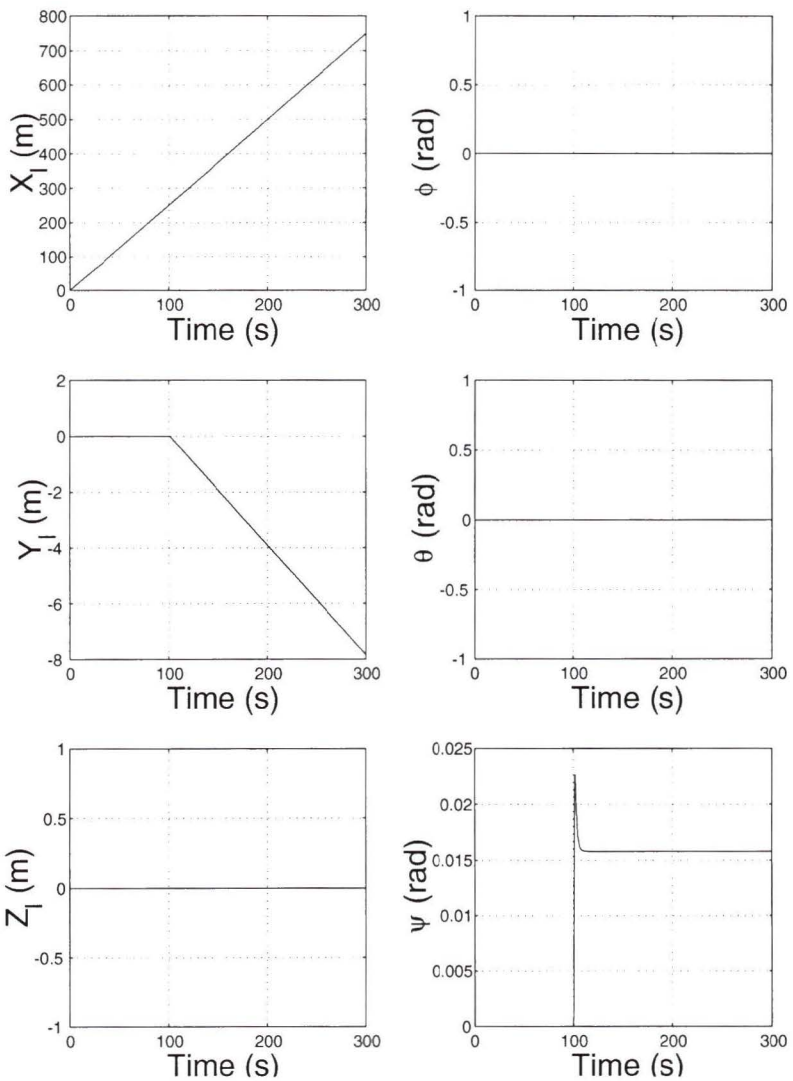

Figure 5.5: Position and Orientation for SYMARCS Model at 2.5 m/s - Direct Yaw Motion of 0.02 radians Commanded

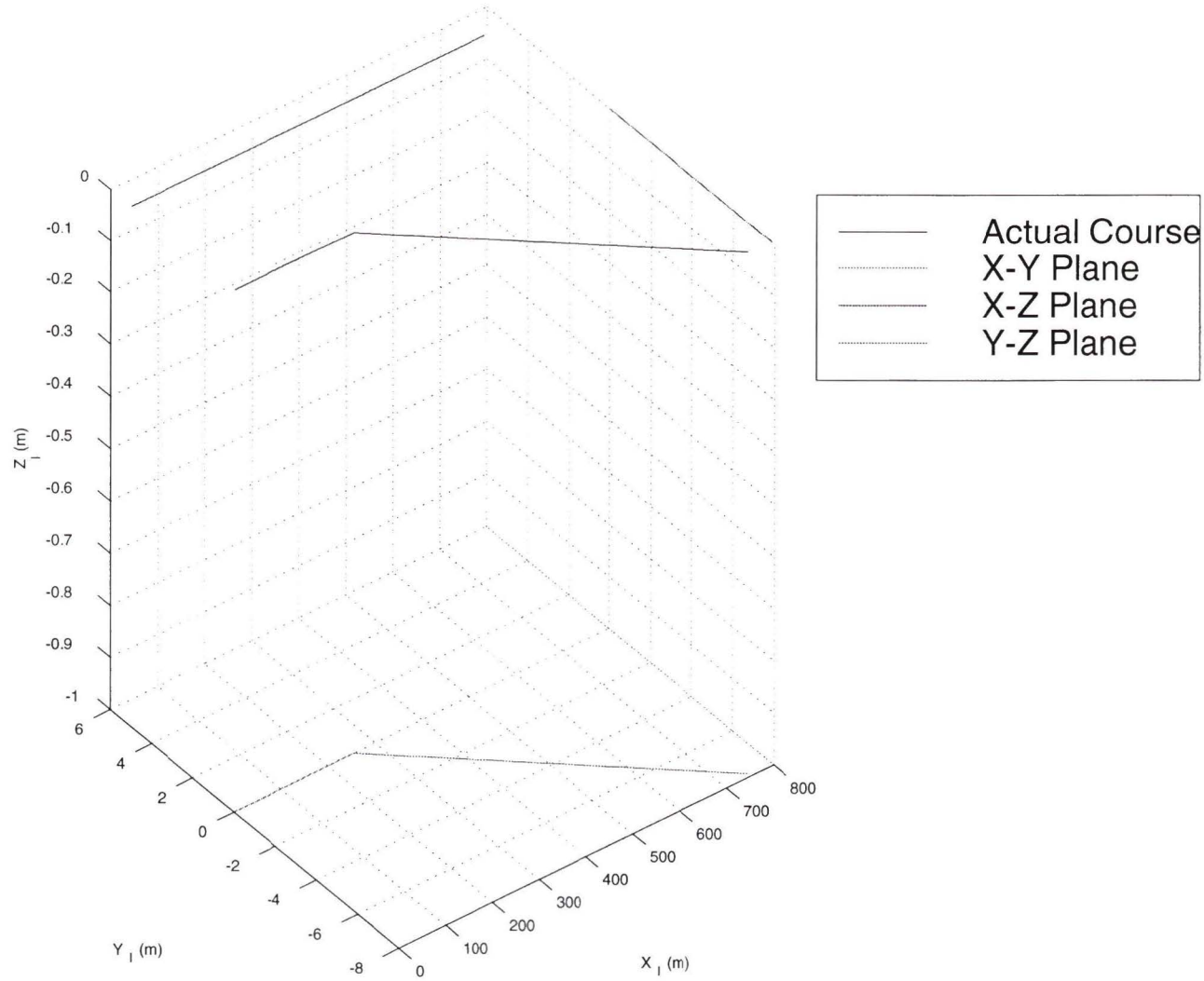

Figure 5.6: Trajectory for SYMARCS Model at 2.5 m/s - Direct Yaw Motion of 0.02 radians Commanded

$U\,(m/s)$	$\phi\,(rad)$	$\Delta\phi\,(rad)$	$\theta\,(rad)$	$\Delta\theta\,(rad)$	$\psi\,(rad)$	$\Delta\psi\,(rad)$
0.5	0.02310	–	0.00455	–	0.00319	–
1.0	0.04614	0.02303	0.00894	0.00440	0.00630	0.00312
1.5	0.06918	0.02304	0.01365	0.00471	0.00946	0.00316
2.0	0.09168	0.02250	0.01805	0.00440	0.01258	0.00312
2.5	0.11575	0.02402	0.02252	0.00448	0.01576	0.00319
3.0	0.13850	0.02275	0.02704	0.00452	0.01893	0.00317
3.5	0.16206	0.02356	0.03151	0.00447	0.02214	0.00321
4.0	0.18488	0.02282	0.03609	0.00458	0.02530	0.00315

Table 5.2: SYMARCS Magnitude of Response to Direct Control (T=2s).

$U\,(m/s)$	$\phi\,(rad)$	$\theta\,(rad)$	$\psi\,(rad)$
0.5	0.02309	0.00450	0.00316
2.5	0.11560	0.02254	0.01578
4.0	0.18496	0.03609	0.02524

Table 5.3: SYMARCS Magnitude of Response to Direct Control (T=25s).

We performed further analysis to determine if there are other relationships that will simplify the task of system compensation. Specifically, we would like to know the relationships between the vehicle response to orientation commands and the vehicle forward speed, and between the response and the magnitude of the command. If we let

$$a_k = \frac{k_d}{c_k U}$$

we find that each a_k is roughly constant over the range of vehicle speeds studied (see Table 5.4). By varying c_k at a constant vehicle speed of $U = 0.5m/s$, we find that

$U\,(m/s)$	$a_\phi\,(s/m)$	$a_\theta\,(s/m)$	$a_\psi\,(s/m)$
0.5	0.924	0.180	0.126
2.5	0.925	0.180	0.126
4.0	0.925	0.180	0.126

Table 5.4: SYMARCS Normalized Magnitude of Response to Direct Control.

a_k is also roughly constant even with changes in the magnitude of the command (see Table 5.5).

$c_\psi\,(rad)$	$\psi\,(rad)$	$a_k\,(s/m)$
0.050	0.003185	0.1274
0.025	0.001589	0.1271
0.010	0.000627	0.1254

Table 5.5: SYMARCS Dependence of Magnitude of Response (Direct Control) on the Magnitude of the Command.

Considering the approximately constant values of a_k, the vehicle angular response to direct control, $k_d \in \{\phi, \theta, \psi\}$, can be defined as follows

$$k_d = g_k\,(U)\,c_k \tag{5.1}$$

where

$$g_k\,(U) = a_k U \tag{5.2}$$

and

$$a_\phi = 0.925\,(s/m) \tag{5.3a}$$

$$a_\theta = 0.180\,(s/m) \tag{5.3b}$$

$$a_\psi = 0.126\,(s/m) \tag{5.3c}$$

5.2.2 System Compensation

To get a response equivalent to our command, a pre-gain equivalent to the reciprocal of the gains in (5.3) to the control input signals is used, i.e.,

$$c_k = \frac{1}{g_k(U)} k_{d,desired}$$

The system will respond to give the commanded input

$$k_d = g_k(U)\left(\frac{1}{g_k(U)} k_{d,desired}\right) = k_{d,desired}$$

where k_d is the actual angle of orientation of the vehicle.

After the compensation was added, the vehicle response was within about 1% of the command. Figure 5.5 shows the step change in yaw angle and the corresponding rate of change of sway (motion in the y-direction). Figure 5.6 shows the trajectory of the SYMARCS for a directly actuated yaw motion.

5.3 Synthesized Control

In this section we will examine the vehicle response to the sinusoidal control inputs required to synthesize a motion. Again, we will determine the compensation necessary such that the vehicle response, k_s, to a control input for a DOF that is not directly controllable is equivalent to the command given, $k_{s,desired}$.

5.3.1 Vehicle Response

The response to synthesized controls is also dependent on the speed of the vehicle as we would expect, since the control is effected by lift and drag forces induced by varying the control plane angles. This response, however, is not linear with respect

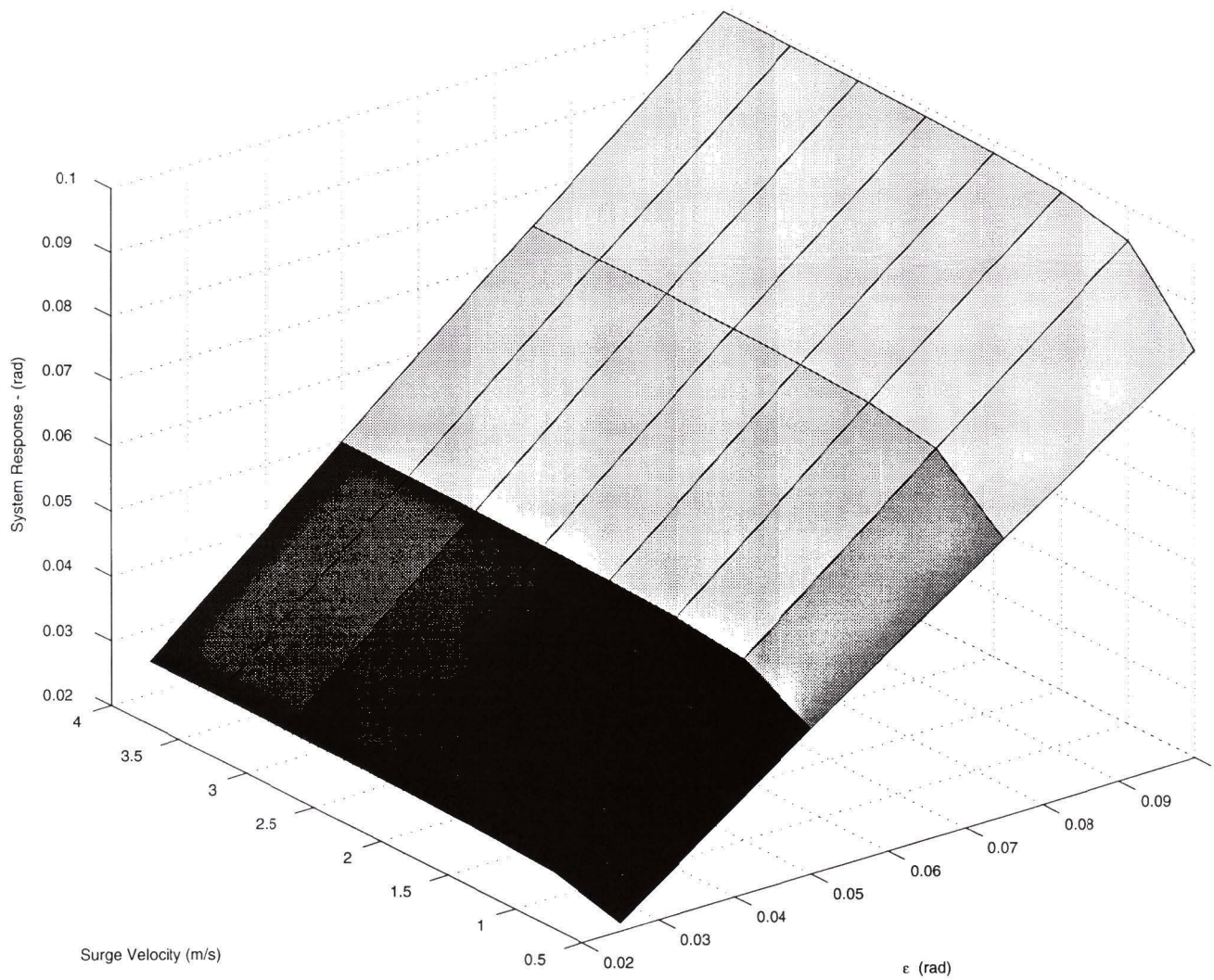

Figure 5.7: Response of Vehicle to Variation in Forward Velocity and Magnitude of Motion Commanded

to the forward velocity as in the case of direct control. The relationship was determined by plotting a surface of steady state magnitude of response over a grid of surge velocities and command magnitudes (for example see Figure 5.7). In order to construct this surface, we first compensated for the system response to direct commands as detailed above, so that any difference between the command and the response is due to the synthesis and not caused by the vehicle response to a command for direct motion. A typical set of response magnitudes is given in Table 5.6. These values

$\psi_{s,desired} =$	$0.025\,(rad)$	$0.050\,(rad)$	$0.075\,(rad)$	$0.100\,(rad)$
$U\,(m/s)$	$\psi_s\,(rad)$	$\psi_s\,(rad)$	$\psi_s\,(rad)$	$\psi_s\,(rad)$
0.5	0.021240	0.042210	0.062754	0.082791
1.0	0.023974	0.047817	0.071441	0.094772
1.5	0.024562	0.049010	0.073253	0.097234
2.0	0.024777	0.049444	0.073914	0.098124
2.5	0.024881	0.049652	0.074228	0.098549
3.0	0.024939	0.049769	0.074407	0.098786
3.5	0.024975	0.049842	0.074517	0.098932
4.0	0.024999	0.049891	0.074591	0.099034

Table 5.6: SYMARCS Magnitude of Response to Controls for a Synthesized Yaw Motion.

are put in matrix form where each row represents a vehicle forward speed and each column represents a magnitude of command.

We again performed further analysis to see if we could get a vehicle angular response relationship like that in (5.1). This time we looked at the relationship

between the vehicle response and the command magnitude first. When the matrix of response values is divided by $\psi_{s,desired}$ we get values like those in Table 5.7. The

$\psi_{s,desired} =$	$0.025\,(rad)$	$0.050\,(rad)$	$0.075\,(rad)$	$0.100\,(rad)$
$U\,(m/s)$	$\frac{\psi_s}{\psi_{s,desired}}$	$\frac{\psi_s}{\psi_{s,desired}}$	$\frac{\psi_s}{\psi_{s,desired}}$	$\frac{\psi_s}{\psi_{s,desired}}$
0.5	0.84959	0.84420	0.83671	0.82791
1.0	0.95897	0.95634	0.95255	0.94772
1.5	0.98248	0.98020	0.97671	0.97234
2.0	0.99109	0.98889	0.98552	0.98124
2.5	0.99523	0.99304	0.98971	0.98549
3.0	0.99754	0.99538	0.99209	0.98786
3.5	0.99900	0.99684	0.99355	0.98932
4.0	0.99998	0.99782	0.99455	0.99034

Table 5.7: SYMARCS Dependence of Magnitude of Response (Synthesized Control) on Epsilon.

average of each of the rows of Table 5.7 is given in Table 5.8. From these average values we find the dependence of the vehicle response on the forward velocity. These values fit the curve given by the following equation:

$$\frac{s_\psi}{s_{\psi,des}} = h_\psi\,(U) = 0.0155U^3 - 0.1288U^2 + 0.3398U + 0.7085$$

The synthesis of roll and pitch commands were analyzed in a similar manner. The resulting set of system response functions are:

$$\frac{s_\phi}{s_{\phi,des}} = -0.035U^5 + 0.476U^4 - 2.502U^3 + 6.517U^2 - 8.649U + 6.056 \quad (5.4a)$$

$$\frac{s_\theta}{s_{\theta,des}} = -0.001U^3 + 0.046U^2 - 0.293U + 1.563 \quad (5.4b)$$

$U\,(m/s)$	$\frac{\psi_s}{\psi_{s,desired}}_{avg}$
0.5	0.83960
1.0	0.95389
1.5	0.97793
2.0	0.98668
2.5	0.99087
3.0	0.99322
3.5	0.99468
4.0	0.99567

Table 5.8: SYMARCS Average Dependence of Magnitude of Response (Synthesized Control) on Epsilon.

$$\frac{s_\psi}{s_{\psi,des}} = 0.016U^3 - 0.129U^2 + 0.340U + 0.709 \tag{5.4c}$$

From these, we can write

$$k_s = h_k\,(U)\,c_{ij} \tag{5.5}$$

where c_{ij} is the command.

5.3.2 System Compensation

We can compensate for the system response by applying the reciprocal of the gains in 5.4. First the compensation for the motion to be synthesized is applied:

$$c_{ij} = \frac{1}{h_k\,(U)} k_{s,desired}$$

where c_{ij} is the value used to generate the commands to the directly actuated control planes that will synthesize the desired motion. (The i and j indices indicate that

the commanded motion must be synthesized rather than actuated directly, as with the index k.) Then the coefficients, $\alpha_i^{'}$ and $\alpha_j^{'}$, for the directly controlled signals are determined via Leonard's algorithms [21] and compensation is applied to them

$$\begin{aligned} \alpha_i &= \frac{1}{g_i(U)}\alpha_i^{'} \\ \alpha_j &= \frac{1}{g_j(U)}\alpha_j^{'} \end{aligned}$$

With this compensation the system will respond to give the commanded input such that

$$k_{s,actual} = k_{s,desired}$$

With compensation the vehicle response was within approximately 5% of the command for a synthesized yaw motion. Figure 5.8 shows the state of the vehicle orientation over time and the effect on vehicle position. Figure 5.9 shows the vehicle trajectory for a synthesized yaw motion. It can be seen from these two plots that at the end of a synthesized yaw there are unwanted non-zero values of pitch angle, roll angle, and heave displacement. We will address these parasitic motions in Chapter 6.

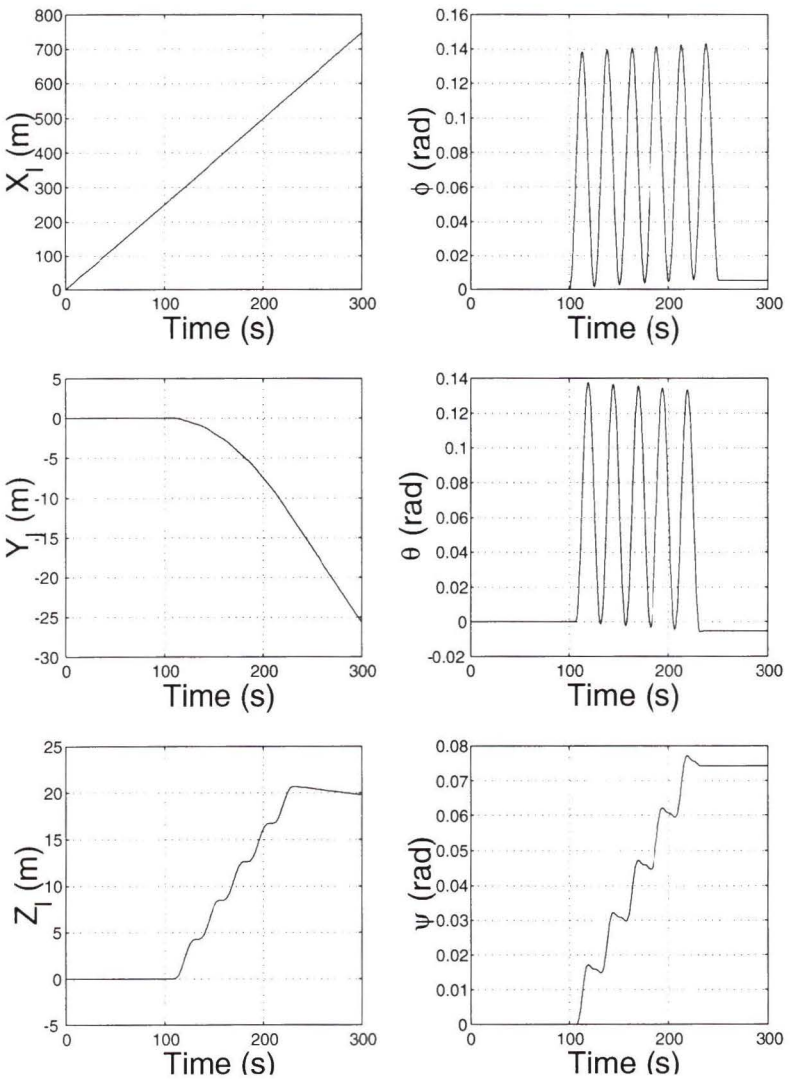

Figure 5.8: Position and Orientation for SYMARCS Model at 2.5 m/s - Synthesized Yaw Motion of 0.07 radians Commanded

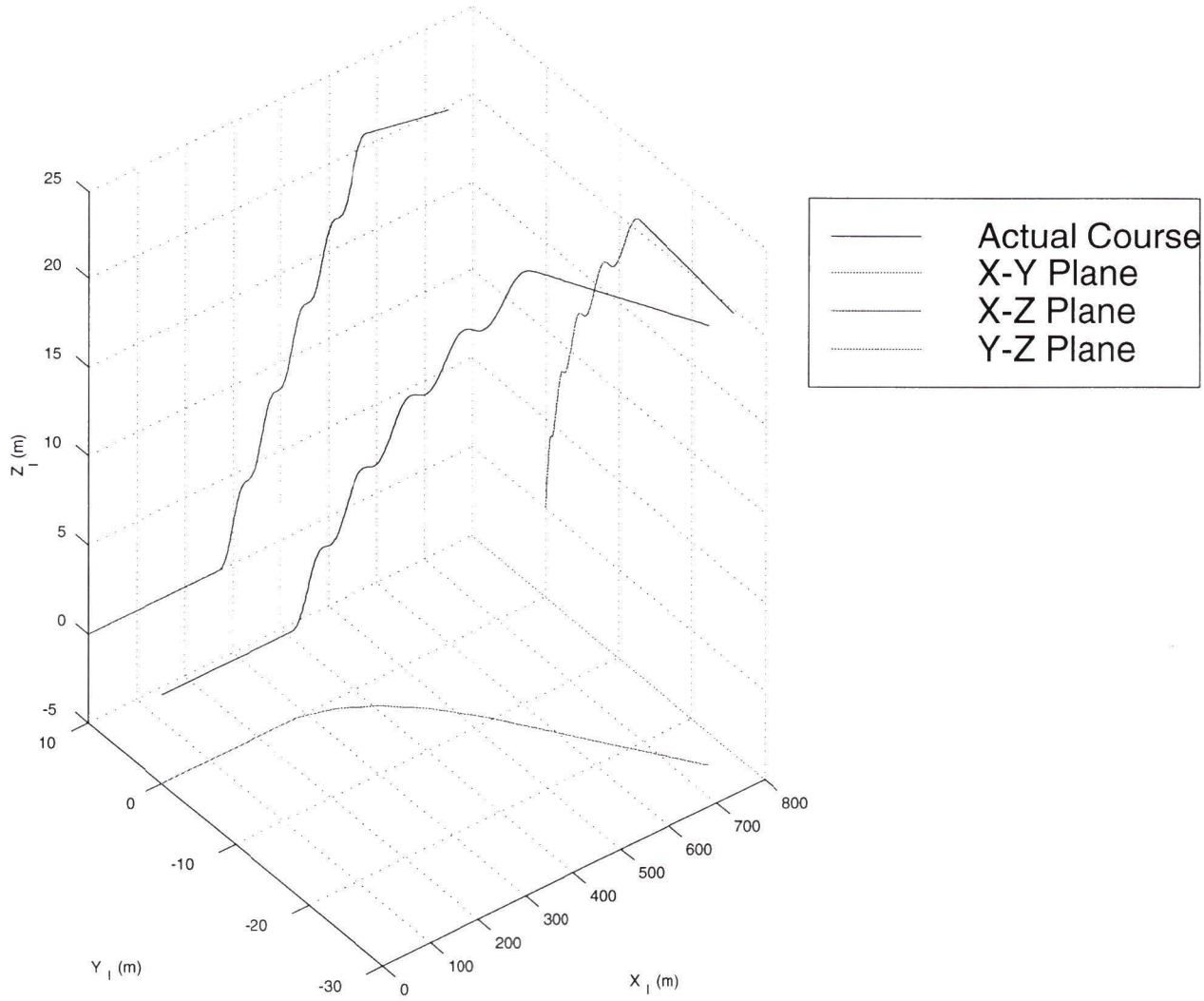

Figure 5.9: Trajectory for SYMARCS Model at 2.5 m/s - Synthesized Yaw Motion of 0.07 radians Commanded

Chapter 6

The Controller

The control signals generated by this application of geometric control methods are nominally open-loop. For some small desired motion, we use a direct or a synthesized signal to achieve that motion from a starting position which is assumed to be correctly known. If there is an error in our knowledge of the starting position, it will affect the end result of the control action and any subsequent motions.

The control algorithms result from theory based on a kinematic model, but we are testing them on a dynamic model. As can be seen from Figures 5.8 and 5.9, the dynamics of the SYMARCS model may result in unwanted values of orientation angles and positional displacements. These unwanted motions must be corrected for in order to allow subsequent use of the open-loop controller. In order to determine the amount of correction required, we must either use some form of feedback, or know the vehicle very well in order to accurately predict the outcome of our control actions. In order to reduce our dependency on our limited knowledge of the vehicle parameters and to simplify the controller, we add intermittent feedback to our nominal open-loop controller.

In addition we must take into account the physical limitations of the control actuators; specifically, the maximum deflection of the control planes. Our controller must be able to deal with larger motions than are possible with a single open-loop command.

This chapter will address these issues and present a review of the controller we developed. We will end the chapter with an example of the controller action.

6.1 Parasitic Motions

When the motions of the SYMARCS are directly controlled, there are no unwanted motions in the other DOF. At the end of a synthesized motion, however, there are net motions in the other orientations, and there is a net motion in y- and z-directions. The magnitude of these unwanted motions is dependent on the surge speed of the vehicle, the magnitude of the commanded motion, and the DOF commanded. Depending on which DOF is commanded, the motion in y- and z-directions is either a natural result of the commanded motion (e.g. if yaw is commanded, one would expect the vehicle to move in the y-direction), or it is an undesirable "parasitic" motion (as motion in the z-direction is in the case of a yaw manoeuver). These parasitic motions are the result of vehicle dynamics involving the inertia of the vehicle, and the rigid body coupling of the vehicle orientation and the forward velocity. To ensure we start from a reliably known position in any subsequent steps or control motion demands, it is necessary to correct for these parasitic motions. The magnitudes of these parasitic motions could be mapped as we did for the synthesized motions. However, the dependencies are more complicated and it is more difficult to fit a surface to them. In addition, the maps assume we know the vehicle very well. In reality there may be variations

in the parameters that limit the applicability of the maps. In this kind of scenario, it becomes much more realistic to incorporate some form of feedback to account for these errors. We use intermittent feedback to determine the values of the parasitic motions. Intermittent feedback was chosen rather than continuous feedback, so that the resulting corrective actions would not interfere with the open-loop control action. At the end of each open-loop command we sense the parasitic motions and then issue commands to drive the vehicle back to the initial values so that the net motion of the vehicle corresponds only to the demanded control action.

The parasitic motions are of two types: orientation and position. The parasitic angular motions can be correct by direct control, since the only motion not desired must be in the two DOF's that were used to synthesize the desired motion. It turns out that the positions can also be corrected using the direct motions. The parasitic translation for a synthesized yaw motion (rudders unavailable) is heave, which can be corrected using pitch via the horizontal tailplanes. Similarly, the parasitic translation for a synthesized pitch motion (horizontal tailplanes unavailable) is sway, which can be corrected using yaw via the rudders. For a synthesized roll motion any sway or heave is a parasitic motion, but each of these can be corrected by commanding yaw and pitch motions respectively.

A typical synthesized motion, complete with parasitic motion correction, is shown in Figures 6.1 and 6.2. The magnitude of parasitic motion in the orientation DOF's was small and easily corrected within one time period of the sinusoidal signal. The parasitic motions in the position DOF were larger and required several periods to correct.

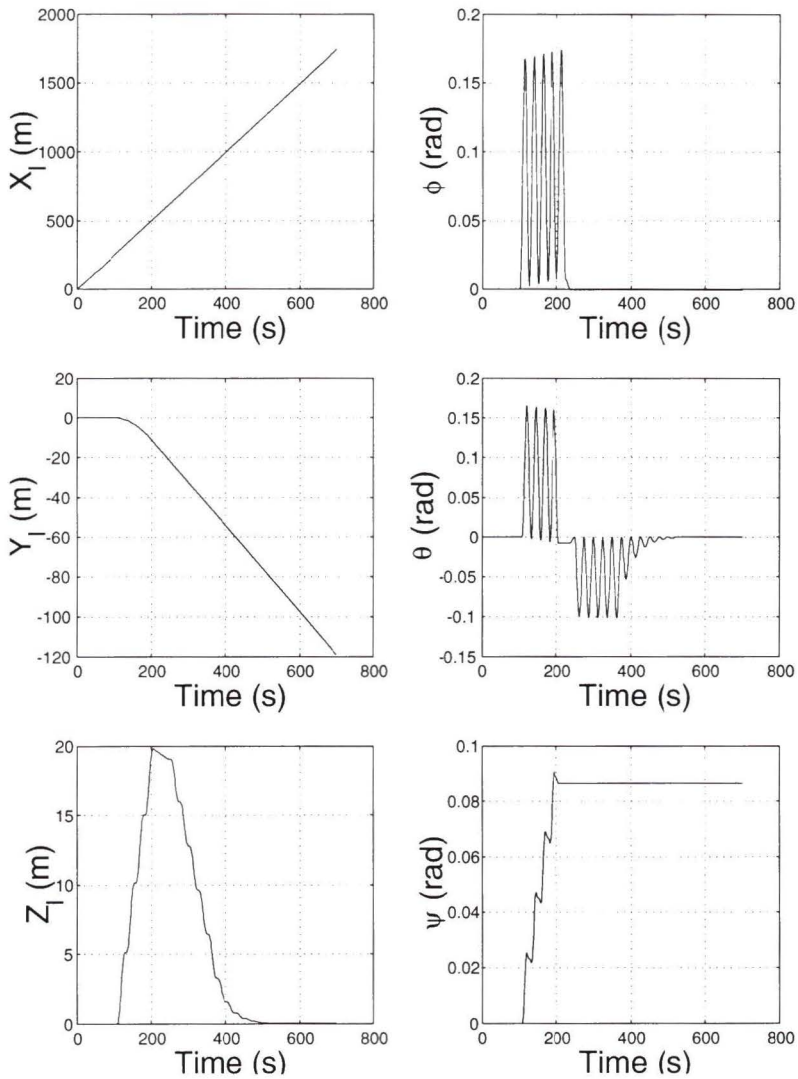

Figure 6.1: Position and Orientation for SYMARCS Model at 2.5 m/s - Synthesized Yaw Motion of 5 Degrees (˜0.87 rad)

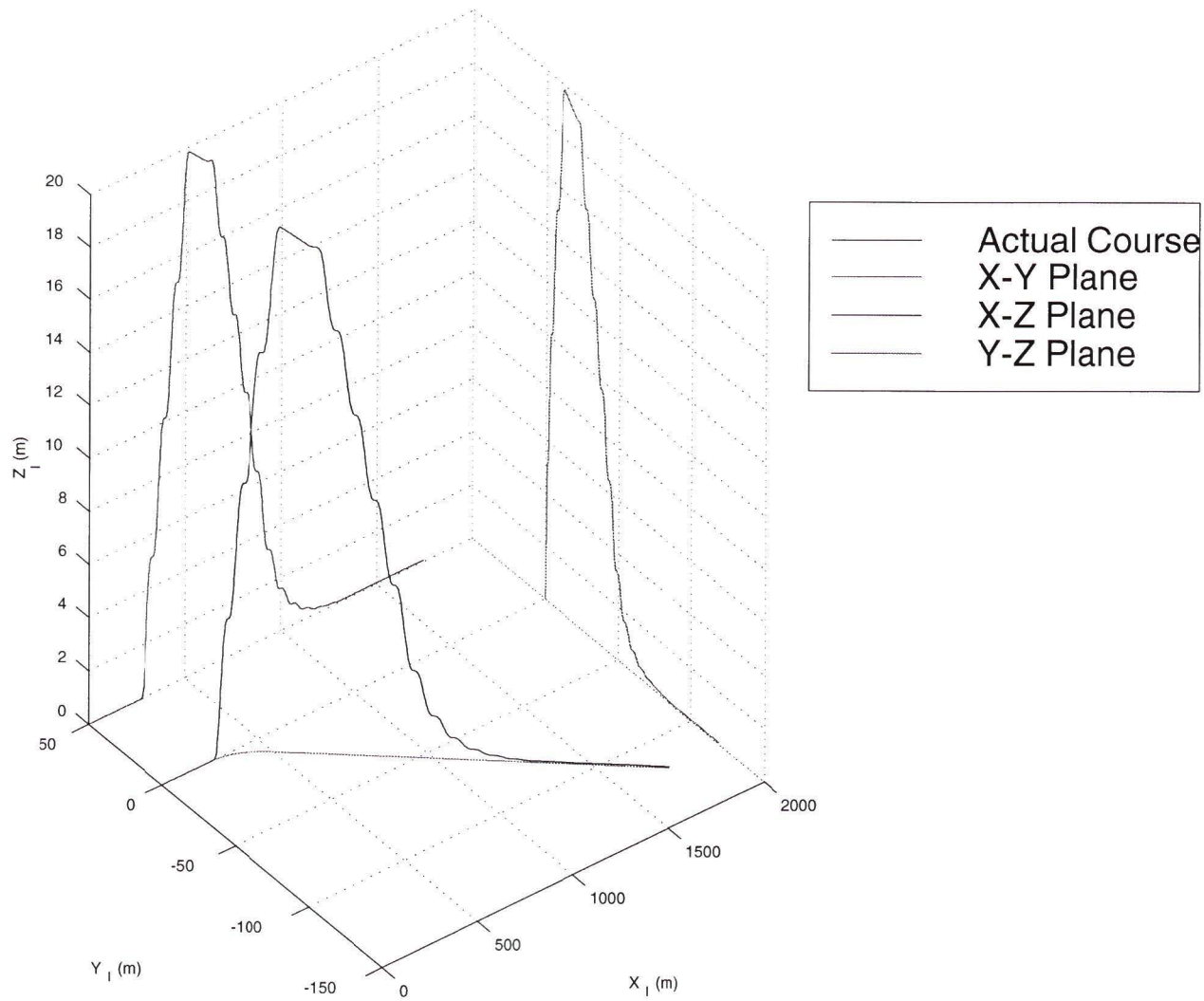

Figure 6.2: Trajectory for SYMARCS Model at 2.5 m/s – Synthesized Yaw Motion 0f 5 Degrees (˜0.87 rad)

6.2 Maximum Magnitude of Command

The system attenuations, $g_k(U)$, relate the actual orientation angle for the k^{th} DOF to the desired angle by way of control plane deflection, which has a limit. One of the things that must be avoided is control plane saturation. If one or more of the planes saturate, the sinusoidal signal is truncated. As a result we will get less of one of the required motions and may not be able to synthesize the desired motion properly. This limits the size of motion we can command.

The maximum control plane deflection is 25° or 0.43633 radians. For directly controlled motions (4.3) allows us to determine the maximum command magnitude.

$$\epsilon\, u_{k,\max} = 0.43633 = \frac{1}{2} c_{k,\max}\omega = \frac{1}{2}\frac{1}{g_k(U)} k_{d,\max}\frac{2\pi}{T}$$

Rearranging this equation in terms of $k_{d,\max}$ gives

$$k_{d,\max} = \frac{g_k(U)\,T}{\pi}(0.43633)$$

Typical values for $T = 25s$ are given in table 6.1.

$U\,(m/s)$	$\phi_d\,(rad)$	$\theta_d\,(rad)$	$\psi_d\,(rad)$
0.5	1.6	0.3	0.2
4.0	12.8	2.5	1.7

Table 6.1: SYMARCS Maximum Command Magnitudes for T=25 s

For synthesized motions the task is more complicated due to the method of generating the two α coefficients from the c_{ij} command. We can work back through the control generating algorithm to find the maximum command magnitude that will avoid control plane saturation. By doing this in an iterative manner, we determined

that $k_{s,\max} = 0.1$ for ψ_s at $U = 0.5m/s$. We chose to use this value for all DOF and vehicle speeds because it is the minimum maximum (i.e. the worst case maximum).

6.2.1 Larger Motions

A input command of 0.1 radians corresponds to a 5.7° change in orientation. We looked at how to achieve motions greater than 5.7°.

What didn't work.

Our first attempt to get larger motions involved amplifying the control signal after it was generated and just before it was applied to the control plane. Before applying the signal to the SYMARCS model, we multiplied it by a constant, the value of which was different for each DOF. What we were really doing was modifying the area under the input curve to the control planes so that proper synthesis was inhibited. As a result we were unable to achieve the desired motion. Any change to the amplitude of the input signals - especially to compensate for differing response times in different DOF - must be done when the control signals are generated.

We also attempted to get larger motions by increasing the number of cycles, M, for each open-loop command. There was no change in the size of the motion, because the α coefficients are functions of $\frac{1}{M}$, so the amplitude of motion is, by definition, independent of M.

$$M\left(\frac{amp}{M}\right) = amp \quad \forall M$$

What did work.

Another option is to command multiple small changes in orientation rather than a single large change. For a given input command, we limit the magnitude to 0.1 rad and keep track of the residual desired motion.

$$k_{res} = k_{desired} - k_{\max} \tag{6.1}$$

In the case where $k_{desired} > k_{\max}$, $k_{\max}$ is used as a control input demand for the first step. Once the step has been completed, including correction for parasitic motions, the residual desired motion is acted upon in a similar manner. If $k_{res} > k_{\max}$, we apply (6.1) again and keep the new residual desired motion value to be acted on in the next step. If $k_{res} < k_{\max}$, then k_{res} is used as the control input demand.

6.3 Structure

The controller is structured as three time intervals (see Figure 6.3): an open-loop step ($t \in [r2, s]$) and two corrective intervals ($t \in [s, r1]$ and $t \in [r1, r2]$) that are activated based on intermittent feedback. The length of each of the time intervals is determined dynamically according to how much time is needed to perform the necessary control action. During the first pass through each interval the coefficients c_k for direct motions, and α_i and α_j for synthesized motions are determined along with the endpoint of the time interval (which will be the starting point of the next interval if another interval is required).

When a new orientation command is given, the controller determines whether the motion can be accomplished in one step. If not, a maximum step of 0.1 radian is performed and the residual motion required is stored for further action after this

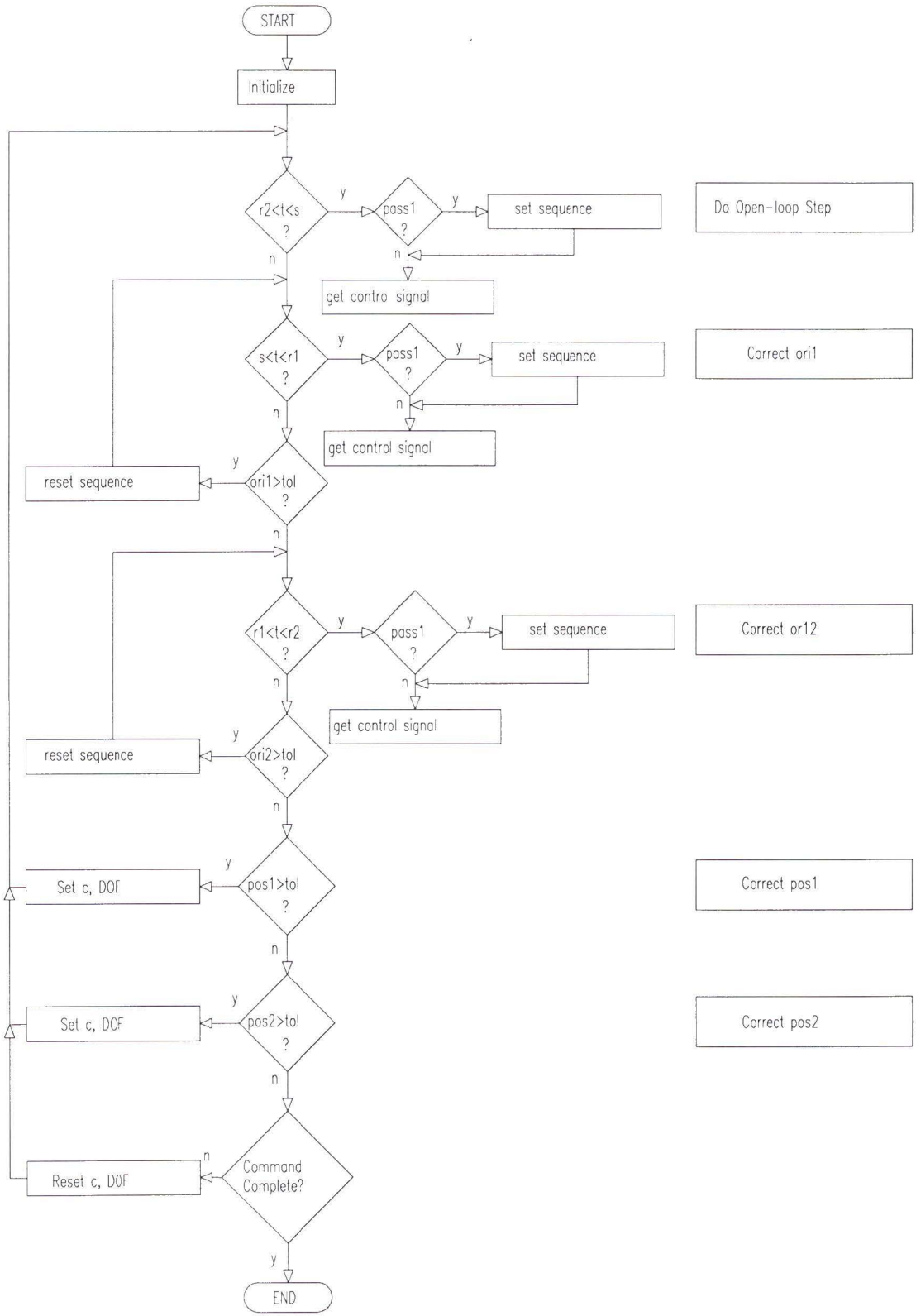

Figure 6.3: Controller Structure

maximum step is performed. The open-loop control is performed. Then the value of the first non-commanded orientation DOF is sensed and a direct control is used to bring the it within a specified tolerance. The controller will loop through this interval until the orientation is within the tolerance. A similar procedure is followed for the second non-commanded orientation DOF. Correcting a position DOF is handled in a different manner. After the open-loop command has been effected and the orientations corrected as required, the value of the first position DOF is sensed. If it is not within a predetermined tolerance, it is acted on as if it were an open-loop command in itself. The second position DOF is handled in this way also. Once all the non-commanded orientation and position DOF are within the tolerances, the controller will act on the residual command. This process will be repeated until there is no further residual command to act on.

6.4 Control Example

We start with the vehicle traveling forward at $2.5m/s$ on a straight and level course. We desire to adjust the vehicle's heading by $10°$ to starboard (make a right turn), but remain at the same depth. The vehicle's rudders are both inoperative, so the controller must synthesize the motion. At the end of the motion we want less than $10^{-3}rad$ of pitch or roll angle, and we want the depth of the vehicle to be within $1m$ of the starting depth. Figure 6.4 shows the control plane deflections commanded by the controller, while Figure 6.5 shows the resulting motions of the vehicle. The synthesis of yaw begins at point 1, where the sinusoidal signals are carried out by the foreplanes effecting roll and the tailplanes effecting pitch. The synthesis continues until point 2, where correction of the parasitic roll and pitch angles takes place. At point 3 the

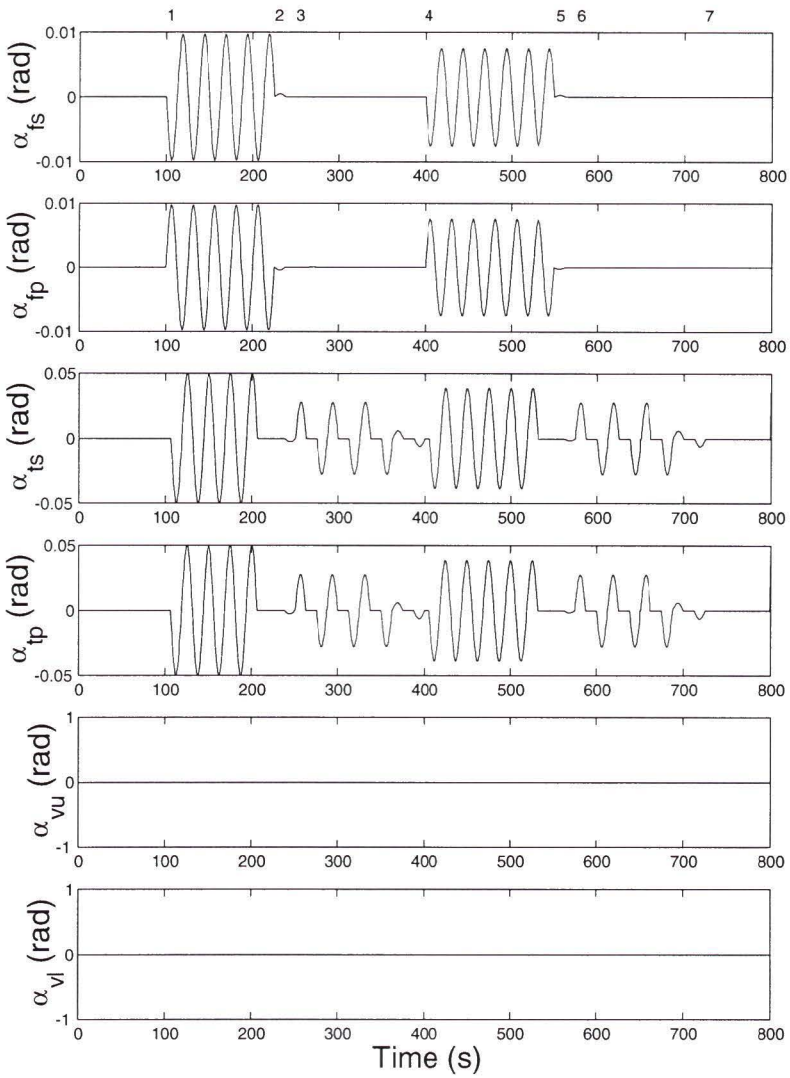

Figure 6.4: Control Plane Deflections for a Synthesized Yaw Motion of 10 Degrees at 2.5 m/s

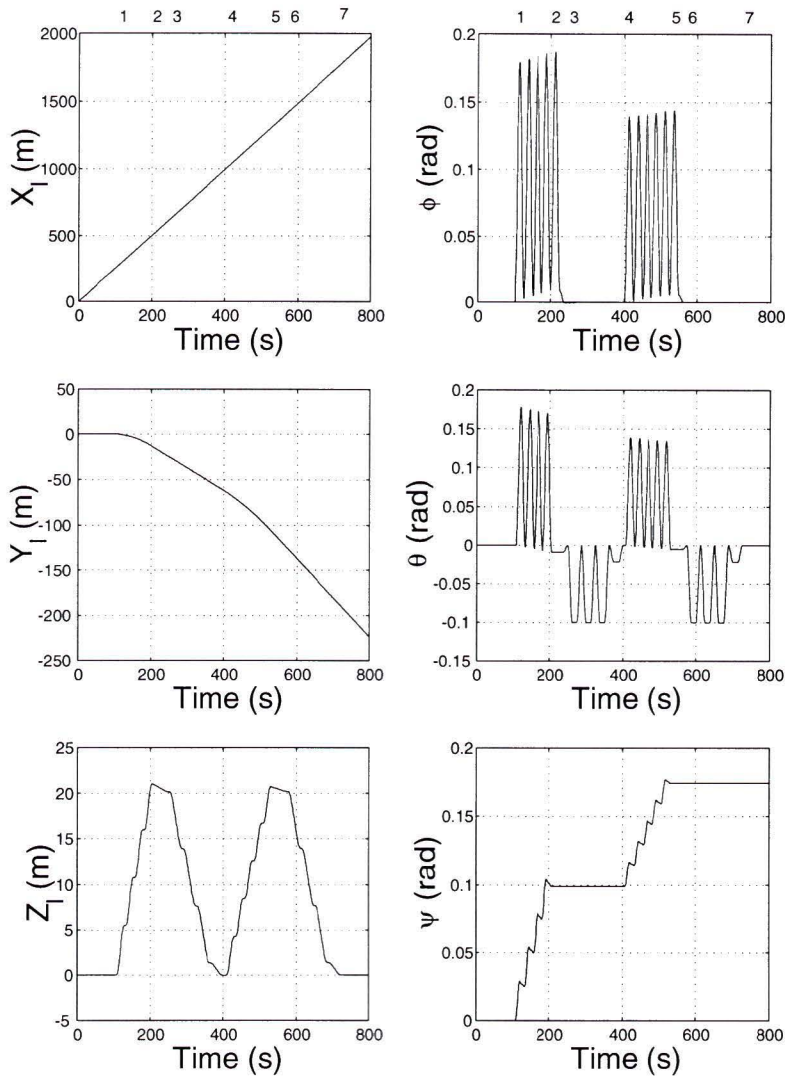

Figure 6.5: Position and Orientation for a Synthesized Yaw Motion of 10 Degrees at 2.5 m/s

orientation corrections are completed and the correction of the heave motion begins. At point 4, the vehicle has completed a yaw of 5.7° and the whole process is repeated in points 4 through 7 so that the complete motion is a yaw of 10° with motions in other DOF's within acceptable limits. The trajectory is shown in Figure 6.6. We have achieved the 10° yaw and ended the control action with approximately zero pitch and roll angles and with an acceptable amount of change in depth of the vehicle.

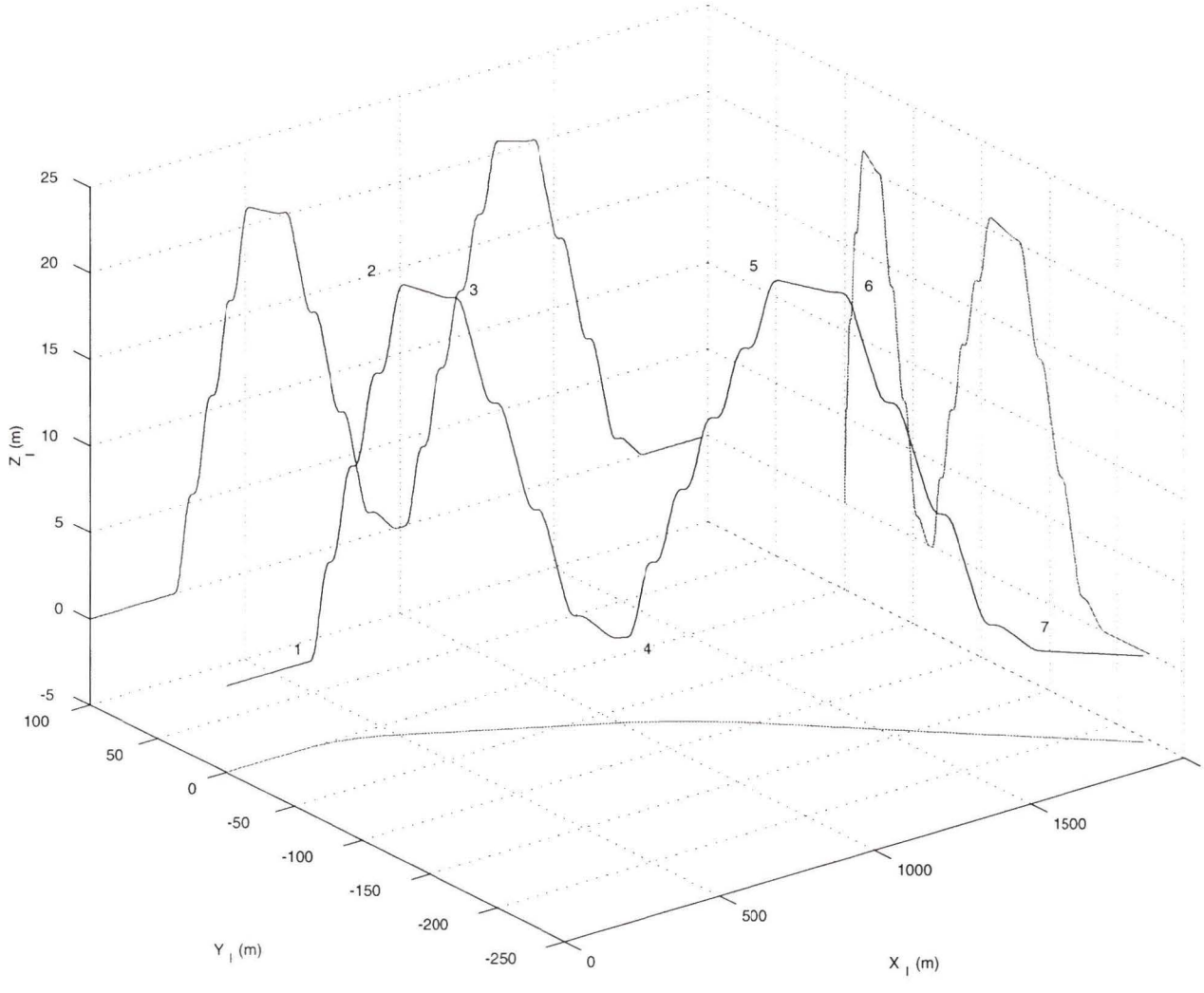

Figure 6.6: Synthesized 10 Degree Yaw Motion at 2.5 m/s

Chapter 7

Conclusions/Future work

7.1 Conclusions

In the present work we have adapted the theory developed by Leonard [21] to allow implementation on a typical, streamlined vehicle (the ARCS). We have found that such implementation is not directly viable because of the righting moment inherent in the design of the vehicle. We modified the model to make the centers of buoyancy and mass coincident, negating the righting moment, and found that the control methods are directly applicable to the modified model (SYMARCS).

This modified model responds well to commands for motions in DOF that are directly actuated. We were able to design compensation for the vehicle response. The resulting motion is within 1% of the command, with no undesired motion in DOF's other than that which was commanded. Compensation for synthesized motions was also accomplished resulting in motions within approximately 5% of the command. There were, however, motions in DOF not commanded. These parasitic motions were sensed via intermittent feedback, and commands were generated to drive the vehicle

back to the desired orientation and position. The magnitude of parasitic motion in the orientation DOF's was small and easily corrected within one time period of the sinusoidal signal. The parasitic motions in the position DOF were larger and required several periods to correct.

Applying the control method to the ARCS requires more detailed theory to take into account the righting moment. This indicates that a kinematic control model may be insufficient for the real world vehicle. An alternative is to devise a method of physically redistributing mass within the vehicle to cause the center of mass to coincide with the center of buoyancy.

7.2 Future Work

1. In this work we have assumed that the control planes that cannot be actuated get jammed at 0° angle of attack. Further work could be done to determine what the effects are of the planes getting jammed at a non-zero angle of attack. There could also be an investigation of the case where the control planes are not jammed at all, but align themselves with the flow of water.

2. We also chose two parameters, the period and the maximum magnitude of the commanded motion, as constant values. By determining these values dynamically at the time of control signal generation, the controller would be more efficient. The period, T, is based on the 5% settling time of the vehicle response to a step input to the control planes. We chose $T = 25s$ so that the vehicle would be able to follow the command at all vehicle speeds and for any DOF, but the settling time varies widely with the forward speed of the vehicle and the

DOF commanded. The maximum magnitude of the command also varies with speed and DOF. We chose 0.01 rad as the maximum command magnitude based on a synthesized yaw motion at 0.5 m/s, but this value changes significantly with vehicle speed and for other DOF.

3. We have not developed the surge speed controller since we assume that a simple PID controller would suffice (as is used in the real vehicle). Future work could determine the effects of this PID control, or some other controller, on the compensation we used here.

4. It may be worthwhile to investigate the possibility of compensating for the effects of the righting moment within a kinematic model.

5. To make the control system reliable, intermittent feedback is to be used to ensure that the desired position and orientation are achieved with no undesired motions in directions other than that commanded. Feedback must also be used to deal with disturbances to the system. These disturbances may be from environmental influences such as currents, or they may result from vehicle problems such as control planes that are jammed at some non-zero angle of attack. This feedback must also be intermittent in nature so that it allows the open loop algorithms to complete the required motion synthesis.

6. As part of the control system there also needs to be a supervisory feedback which determines the state of the actuators and determines the control authority required. The open-loop input signals will be based on this control authority.

References

[1] Yu K. Alekseev, V. V. Kosenko, and A. Ye Shumsky. Use of identification and fault diagnostic methods for underwater robotics. In *Proceedings of OCEANS '94. Vol. 2*, pages 489–494, New York, 1994. IEEE.

[2] D.M. Barnett, S.R. McClaran, E.L. Nelson, M. McDermott, and G.N. Williams. Architecture of the Texas A & M autonomous underwater vehicle controller. In *Proceedings of the 1996 Symposium on Autonomous Underwater Vehicle Vehicle Technology. AUV '96*, pages 34–43, New York, 1996. IEEE.

[3] Abdelkader Chellabi and Meyer Nahon. Feedback linearization control of undersea vehicles. In *Proceedings of OCEANS '93. Vol. 1*, pages 410–415, Victoria, B. C., 1993. IEEE.

[4] John J. Craig. *Introduction to Robotics - Mechanics and Control 2nd Edition.* Addison Wesley, 1989.

[5] Roberto Cristi, Fotis A. Papoulias, and Anthony J. Healey. Adaptive sliding mode control of autonomous underwater vehicles in the dive plane. *IEEE Journal of Oceanic Engineering*, 15(3):152–160, July 1990.

[6] Morton L. Curtis. *Matrix Groups.* Springer-Verlag, 1984.

[7] Frank Dougherty, Tom Sherman, Gary Woolweaver, and Gib Lovell. An autonomous underwater vehicle (AUV) flight control system using sliding mode control. In *Proceedings of OCEANS '88. Vol. 4*, pages 1265–1270, New York, 1988. IEEE.

[8] Ola-Erik Fjellstad and Thor I. Fossen. Singularity-free tracking of unmanned underwater vehicles in 6 DOF. In *Proceedings of the 33rd IEEE Conference on Decision and Control*, Orlando, FL, 1994. IEEE.

[9] Thor I. Fossen. *Guidance and Control of Ocean Vehicles.* John Wiley & Sons, 1994.

[10] Thor I. Fossen and Ola-Erik Fjellstad. Robust adaptive control of underwater vehicles: A comparative study. In *Proceedings of the 3rd IFAC Workshop on Control Applications in Marine Systems CAMS'95*, pages 362–369, Trondheim, Norway, 1995.

[11] Thor I. Fossen and Bjarne A. Foss. Sliding control of MIMO nonlinear systems. In *Proceedings of the European Control Conference*, pages 1855–1860, Grenoble, FRA, 1991.

[12] Thor I. Fossen and Svein I. Sagatun. Adaptive control of nonlinear underwater robotic systems. In *Proceedings of the IEEE Conference on Robotics and Automation*, pages 1687–1695, Sacramento, CA, 1991. IEEE.

[13] Kevin R. Goheen and E. Richard Jefferys. Multivariable self-tuning autopilots for autonomous and remotely operated underwater vehicles. *IEEE Journal of Oceanic Engineering*, 15(3):144–151, July 1990.

[14] Anthony J. Healy. Model-based maneuvering controls for autonomous underwater vehicles. *Transactions of the ASME: Journal of Dynamic Systems, Measurement, and Control*, 114:614–622, December 1992.

[15] Anthony J. Healy. A neural network approach to failure diagnostics for underwater vehicles. In *Proceedings of the 1992 Symposium on Autonomous Underwater Vehicle Technology. AUV '92*, pages 131–134, New York, 1992. IEEE.

[16] Anthony J. Healy. Towards an automatic health monitor for autonomous underwater vehicles using parameter identification. In *Proceedings of the 1993 American Control Conference*, pages 585–589, Piscatawy, NJ, 1993. IEEE.

[17] R. C. Hibbeler. *Engineering Mechanics Dynamics.* Prentice Hall, 7th edition, 1995.

[18] Bjorn Jalving and Nils Storkersen. The control system of an autonomous underwater vehicle. In *Proceedings of the 1994 IEEE Conference on Control Applications. Part 2*, pages 851–856, Glasgow, UK, 1994. IEEE.

[19] Velimir Jurdjevic. *The Lie Bracket and Control*, chapter 55.1, pages 861–872. CRC Press, 1996.

[20] Velimir Jurdjevic. *Geometric Control Theory.* Cambridge University Press, 1997.

[21] Naomi Ehrich Leonard. *Averaging and Motion Control of Systems on Lie Groups.* PhD thesis, University of Maryland, 1994.

[22] Naomi Ehrich Leonard. Compensating for actuator failures: Dynamics and control of underactuated underwater vehicles. In *Proceedings of the 9th International Symposium on Unmanned Untethered Submersible Technology*, Durham, NH, 1995. University of New Hampshire.

[23] Naomi Ehrich Leonard. Control synthesis and adaptation for an underactuated autonomous underwater vehicle. *IEEE Journal of Oceanic Engineering*, 20(3):211–220, July 1995.

[24] Naomi Ehrich Leonard and P. S. Krishnaprasad. Motion control of drift-free, left-invariant systems on lie groups. *IEEE Transactions on Automatic Control*, 40(9):1539–1554, September 1995.

[25] International Submarine Engineering Research Ltd. ARCS new control system fault-tolerant control strategies. Technical report, I. S. E. Research Ltd., 1992.

[26] W. Magnus. On the exponential solution of differential equations for a linear operator. *Communications on Pure and Applied Mathematics*, VII:649–673, 1954.

[27] Meyer Nahon. A simplified dynamics model for autonomous underwater vehicles. In *Proceedings of the 1996 IEEE Symposium on Autonomous Undersea Vehicles*, pages 373–379, Monterey, CA, June 1996.

[28] Yoshihiko Nakamura and Shrikant Savant. Nonholonomic motion control of an autonomous underwater vehicle. In *Proceedings IEEE/RSJ International Workshop on Intelligent Robots and Systems '91 IROS '91*, pages 1254–1258, New York, 1991. IEEE.

[29] Yoshihiko Nakamura and Shrikant Savant. Nonlinear tracking control of autonomous underwater vehicles. In *Proceedings 1992 IEEE International Conference on Robotics and Automation*, pages A4–A9, Los Alimitos, CA, May 1992. IEEE.

[30] David W. Payton, David Keirsey, Dan M. Kimble, Jimmy Krozel, and J. Kenneth Rosenblatt. Do whatever works: A robust approach to fault-tolerant autonomous control. *Applied Intelligence: The International Journal of Artificial Intelligence, Neural Networks, and Complex Problem-Solving Technologies*, 2(3):225–250, September 1992.

[31] Rafel R. Rodriguez and Gerald J. Dobeck. Guidance and control system of the large scale vehicle. In *Proceedings of the 6th International Symposium on Unmanned Untethered Submersible Technology*, pages 434–451, Durham, NH, 1989.

[32] O. J. Sordalen, M. Dalsmo, and O. Egeland. An exponentially convergent control law for a nonholonomic undeerwater vehicle. In *Proceedings of the IEEE International Conference on Robotics and Automation*, pages 790–795, New York, 1993. IEEE.

[33] Gilbert Strang. *Linear Algebra and its Applications.* Academic Press, 1976.

[34] G. Tacconi and A. Tiano. Reconfigurable control of an autonomous underwater vehicle. In *Proceedings of the 6th International Symposium on Unmanned Untethered Submersible Technology.*, pages 486–493, Durham, NH, 1989. University of New Hampshire.

[35] J. Wei and E. Norman. On global representations of the solution of linear differential equations as a product of exponentials. *Proceedings of the American Mathematical Society*, pages 327–334, 1964.

[36] Dana R. Yoerger and Jean-Jacques E. Slotine. Robust trajectory control of underwater vehicles. *IEEE Journal of Oceanic Engineering*, OE-10(4):462–470, October 1985.

[37] Junku Yuh. Modeling and control of underwater robotic vehicles. *IEEE Transactions on Systems, Man, and Cybernetics*, 20(6):1475–1483, December 1990.

[38] Junku Yuh. A neural net controller for underwater robotic vehicles. *IEEE Journal of Oceanic Engineering*, 15(3):161–166, July 1990.

[39] Junku Yuh. Control of underwater robotic vehicles. In *Proceedings of 1993 IEEE/RSJ International Conference on Intelligent Robots and Systems. IROS '93*, pages 517–521, Yokohama, Japan, 1993. IEEE.

[40] Junku Yuh, Joel S. Fox, and R. Lakshmi. Control and optical sensing in underwater robotic vehicles (URVs). In *Proceedings of OCEANS '90*, pages 88–93, Washington, D. C., 1990. IEEE.

Appendix A

ARCS Response

In the ARCS model the center of buoyancy lies above the center of mass, resulting in a stabilizing moment when the vehicle is not upright and level. However, this righting moment interferes with the control method being used. The ARCS model was modified to make the two centers coincident and in line with the horizontal planes. This modified model, SYMARCS, has no righting moment. When the vertical distance between the center of mass and the center of buoyancy is present in the model, the response to the control inputs is significantly different than when the center of mass is coincident with the center of buoyancy. This appendix will discuss the differences.

A.1 Baseline Vehicle Response

We start by looking at the steady state at various speeds with no command input.

As can be seen in Figure A.1, the ARCS model has a non-zero pitch angle even though there is no control input. This pitch offset is not present in the SYMARCS

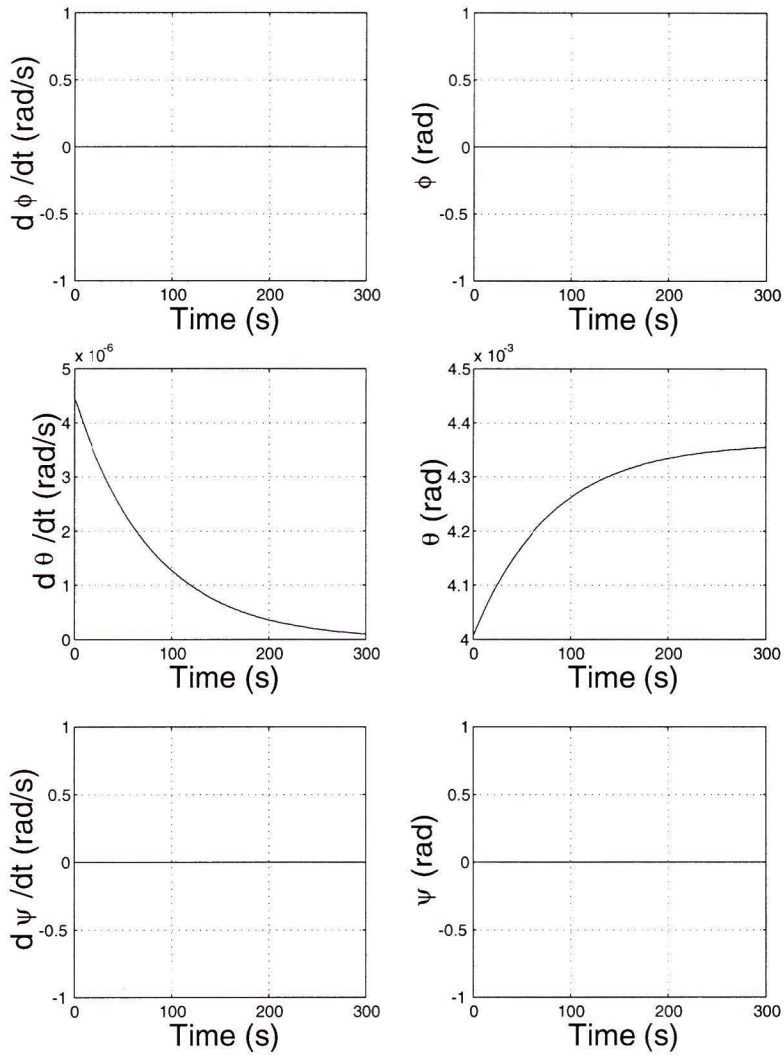

Figure A.1: Rotational Position and Velocity for ARCS Model at 4.0 m/s

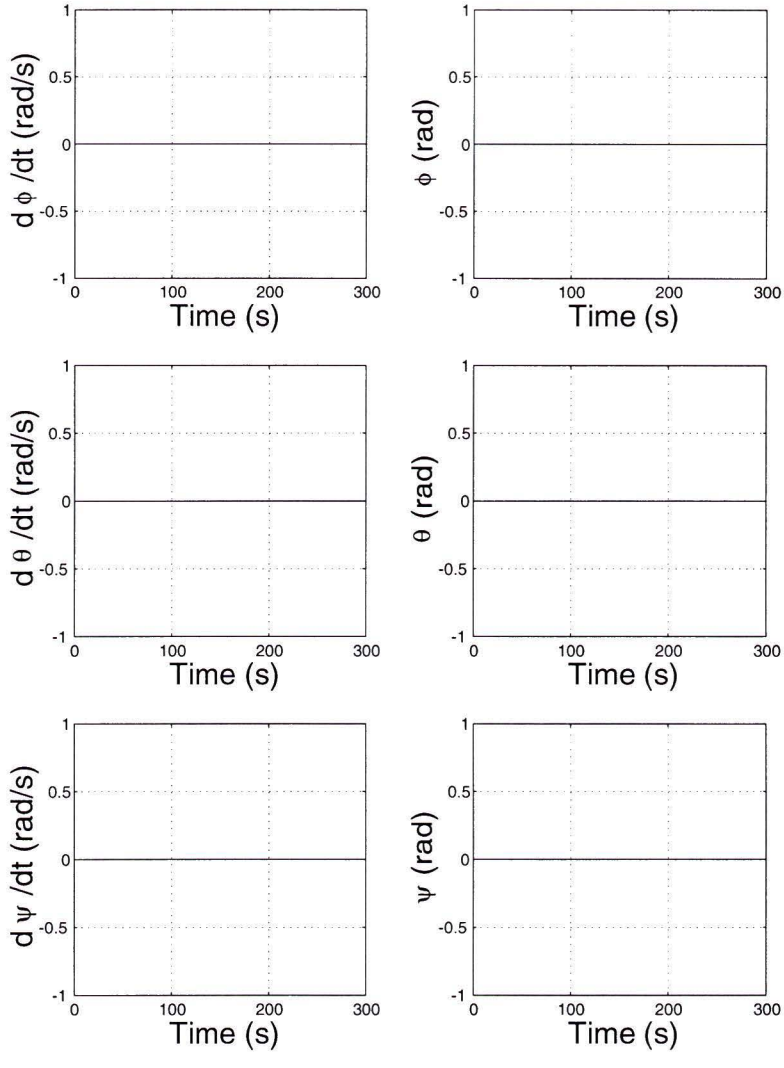

Figure A.2: Rotational Position and Velocity for SYMARCS Model at 4.0 m/s

model (Figure A.2). The non-zero pitch angle results in a slight rise in position as the vehicle moves forward (approximately 5 m rise over 1200 m of forward displacement). The pitch offset in the ARCS model is due to the drag on the foreplanes and tailplanes. The magnitude of the drag force is a function of the vehicle surge speed. Because the center of mass is below the foreplanes and tailplanes, the drag on the planes induces a moment about the center of mass. For a given surge speed, the righting moment will dynamically balance the drag induced moment at some particular pitch angle.

A.2 Vehicle Response

A.2.1 Step Input Response

For the ARCS model, as with the SYMARCS model, the response time for motions in different DOF cannot be assumed to be relatively equal. Again, we did a series of step inputs to the ARCS model to examine the transient response.

Roll

The ARCS model has two different types of response depending on the surge velocity. At and below 2.5 m/s (see Figure A.3), the righting moment is able to dynamically balance the roll moment caused by the step change in control surface deflection, resulting in a step change of roll angle. This response is very different from SYMARCS where, it is recalled, a step change in control surface deflection produced a step change in roll rate. At vehicle speeds of 3.0 m/s (Figure A.4) and above, the righting moment is unable to balance the roll command, and the vehicle does "spin" about the surge axis (as SYMARCS did), but in an oscillation fashion. The oscillation is like a

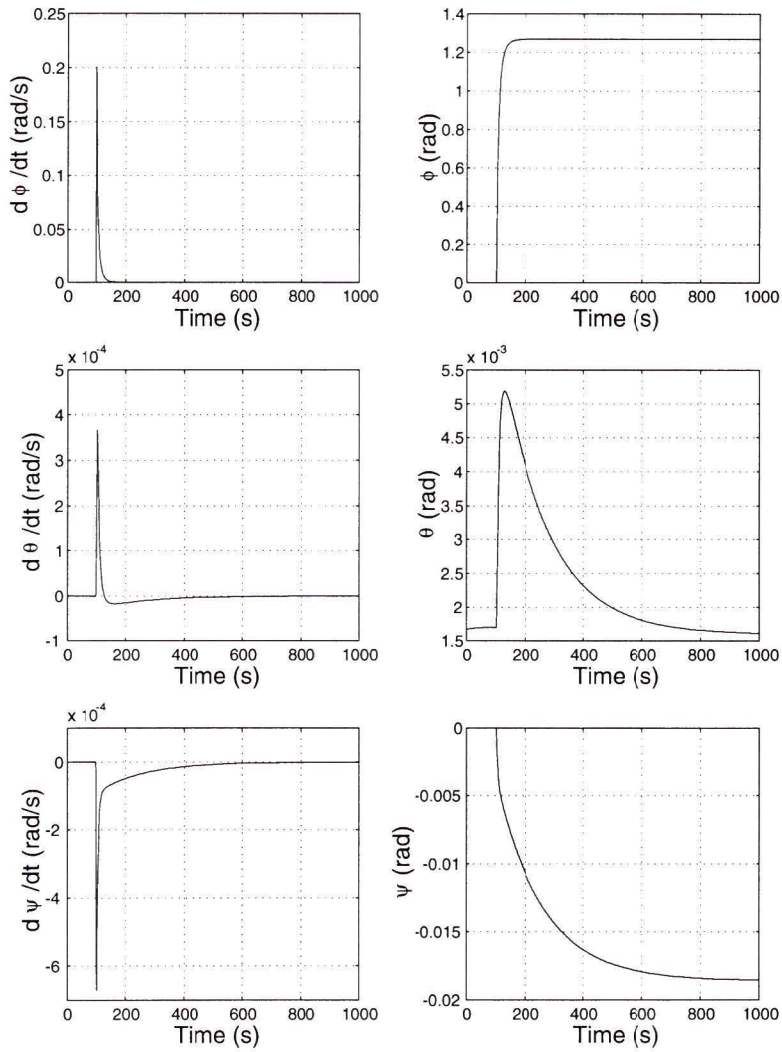

Figure A.3: Rotational Position and Velocity for ARCS Model at 2.5 m/s: Step Roll Command of 0.1 radian.

pendulum swinging around, gaining energy as the bob on the end swings downward and losing energy as it swings upward. For half of the vehicle roll, the righting moment is working with the roll, and for the other half it is working against the roll, resulting in an oscillating roll rate as opposed to a nice step response.

It is also important to note in both Figures A.3 and A.4 (i.e. at all speeds), that the pitch and yaw are affected by the roll. This is because of the offset in the pitch and rigid body coupling. As a result the ARCS does not really spin at higher speeds, but it wobbles about the surge axis and drifts off course in the sway and heave directions. Figure A.5 shows the vehicle at 2.5 m/s. It takes a new heading due to the changes in pitch and roll. In Figure A.6, the vehicle continues to change its course because the roll angle continues to change, so the pitch and yaw angles are constantly changing due to rigid body coupling.

Pitch

The ARCS model again has two types of response to a step input pitch command. For surge speed of 1.5 m/s or less, the righting moment dynamically balances the pitch command, resulting in a step change to the pitch angle. The roll and yaw DOF are not affected, confirming that the offset in pitch causes the coupling of motions previously seen in the roll and, as will be seen later, in the yaw responses. Figure A.7 shows the vehicle starting from (0,0,0), entering a steep descent with no lateral drift. For speeds at and above 2.0 m/s (see Figure A.8), the righting moment is insufficient to balance the control input, and the vehicle does loops with an average downward trajectory mainly due to the pendulum-like effect of the righting moment.

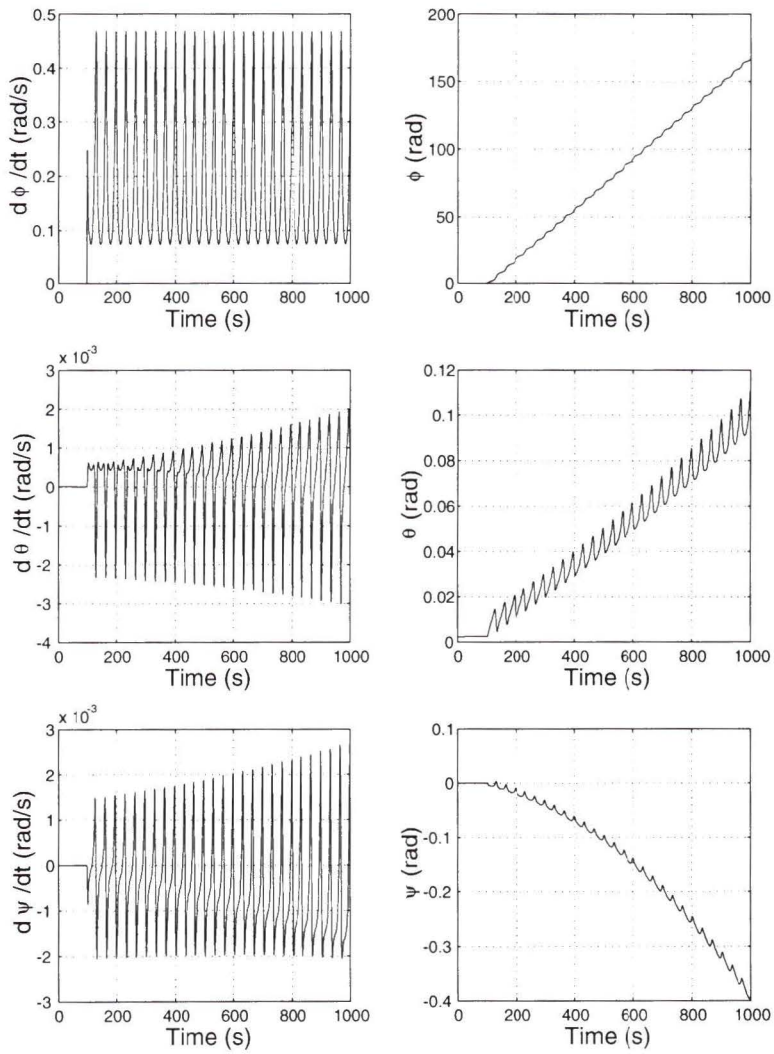

Figure A.4: Rotational Position and Velocity for ARCS Model at 3.0 m/s: Step Roll Command of 0.1 radian.

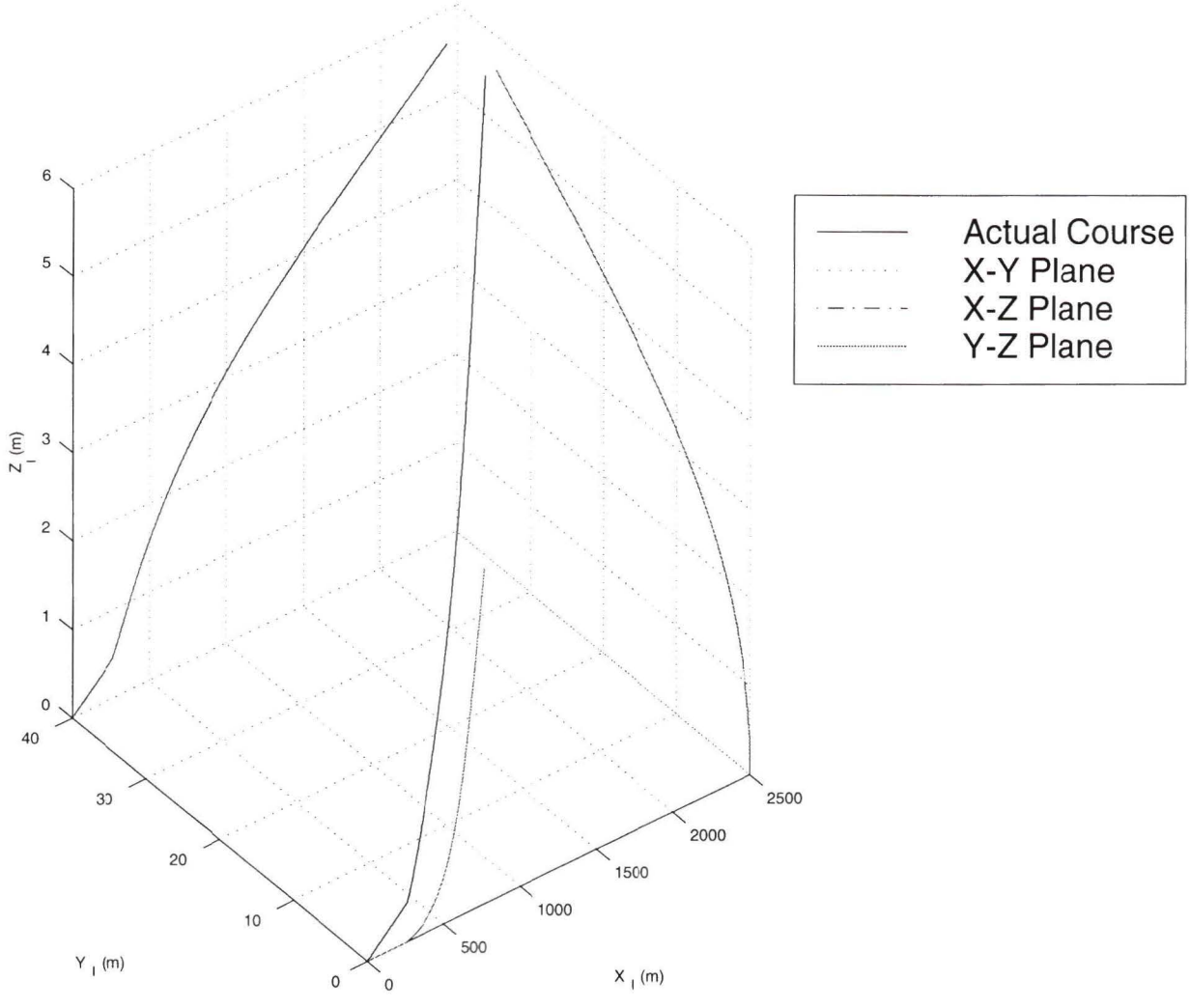

Figure A.5: Trajectory of ARCS Model at 2.5 m/s: Step Roll Command of 0.1 radian.

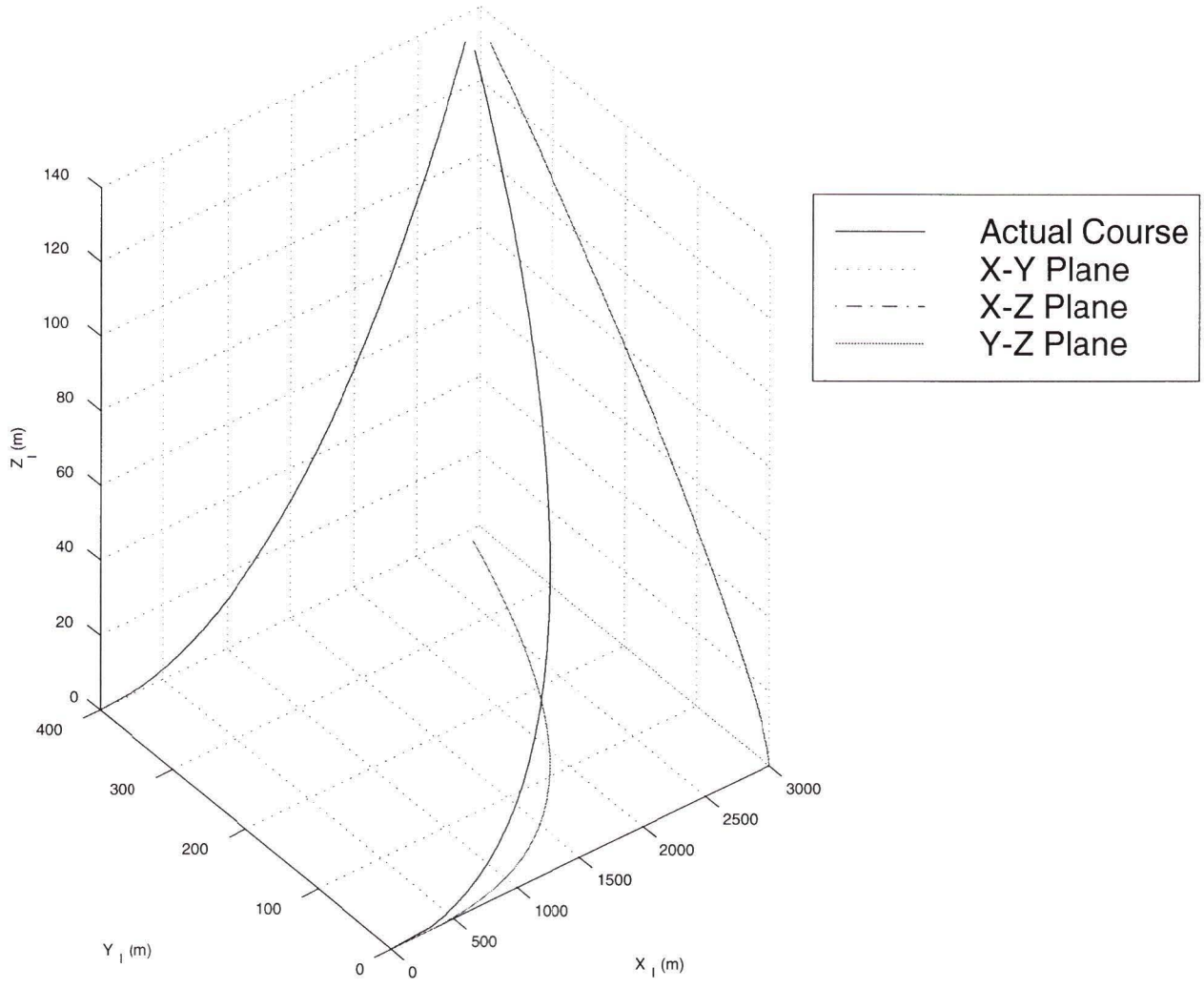

Figure A.6: Trajectory of ARCS Model at 3.0 m/s: Step Roll Command of 0.1 radian.

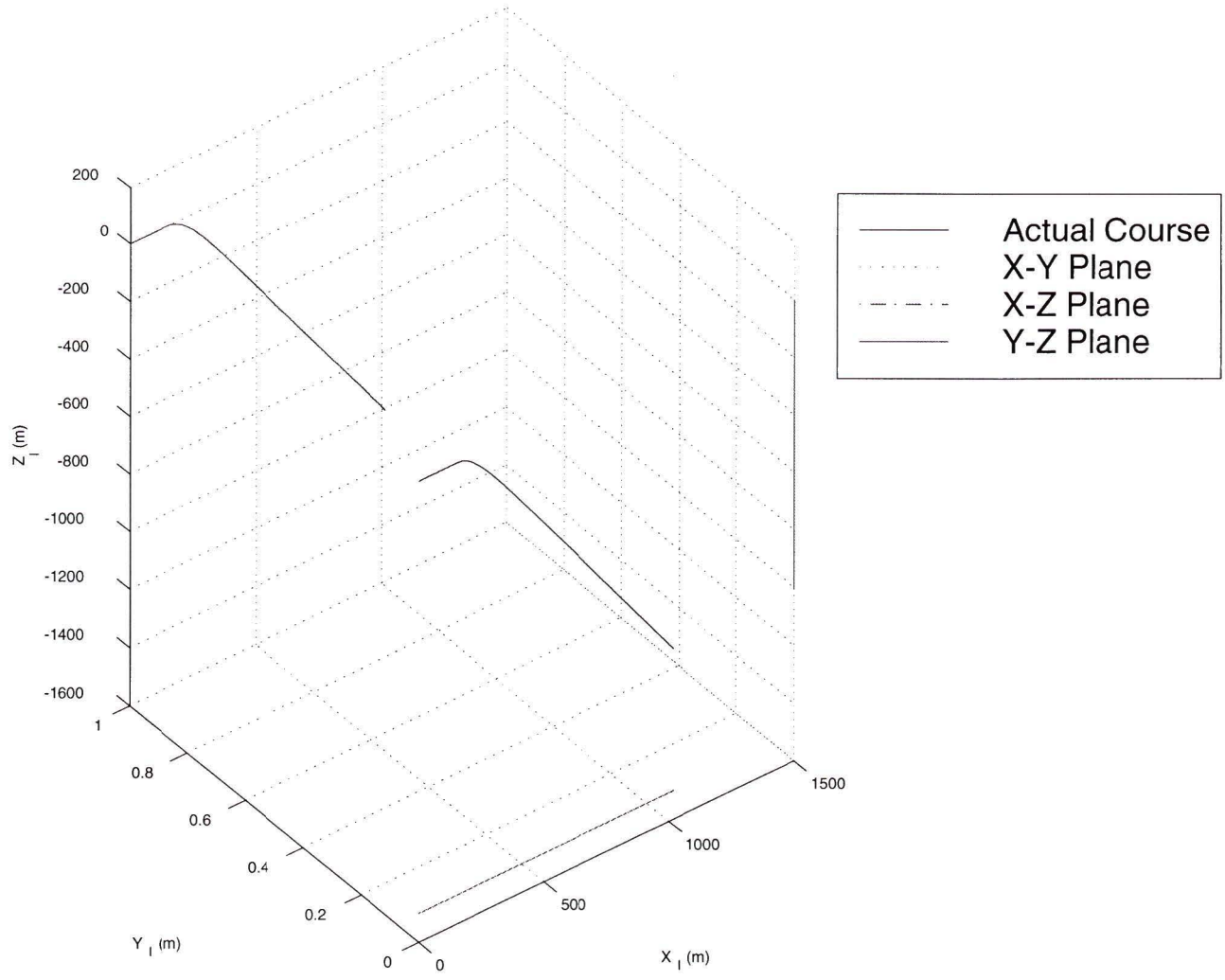

Figure A.7: Trajectory of ARCS Model at 1.5 m/s: Step Pitch Command of 0.1 radian.

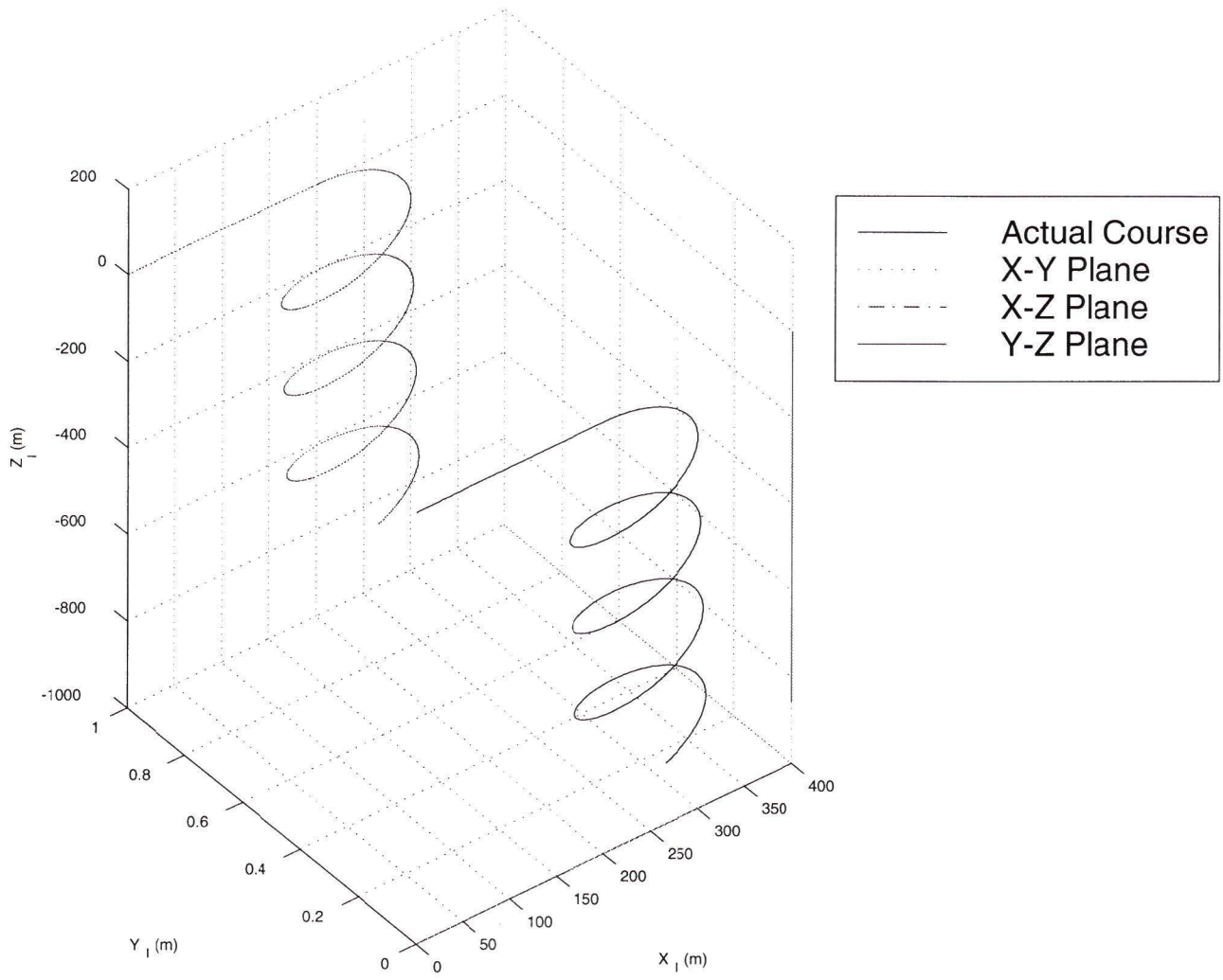

Figure A.8: Trajectory of ARCS Model at 2.0 m/s: Step Pitch Command of 0.1 radian.

Yaw

The ARCS model response to a step input yaw command is similar for all speeds: a step change in yaw rate with resulting transitory deviations to the roll and pitch rates (see Figure A.9) due to the offset in pitch and the righting moment acting longitudinally and laterally. The righting moment has no effect on the yaw motion itself because there is no horizontal distance (when the vehicle is level) between the center of mass and the center of buoyancy. The vehicle does loops in the horizontal plane but there is a net rise or descent of the vehicle, depending on the surge speed, so the loops become a spiral up or down (see Figures A.10 and A.11). This is caused by the offset in the pitch.

Settling Times

Because of the oscillating nature of the responses, there are no settling times for roll and pitch rates. The settling times for a yaw command (see Table A.1) were similar to those found for the SYMARCS model.

A.2.2 Response to Direct Control

With the SYMARCS model, the response in any DOF to a half sine wave was a step change in the angle of orientation of the vehicle. The half sine wave was input to the applicable control planes, which directly affected the angular velocity of the vehicle in the chosen DOF so that the change in angle for that DOF corresponded to the area under the half sine wave. The ARCS model gives impulse like responses in roll and pitch rates as the righting moment immediately returns the roll angle to zero and the pitch angle to one consistent with the pitch offset. Only the yaw has a lasting

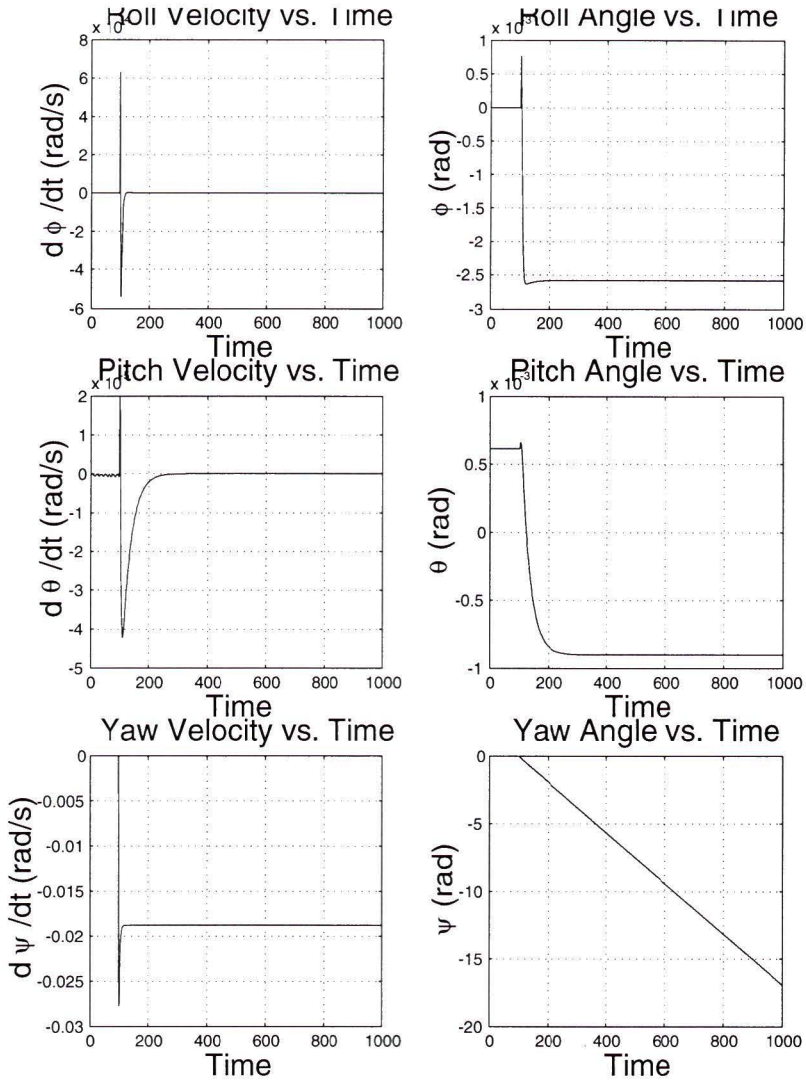

Figure A.9: Orientation and Angular Velocity of ARCS Model: Step Yaw Command.

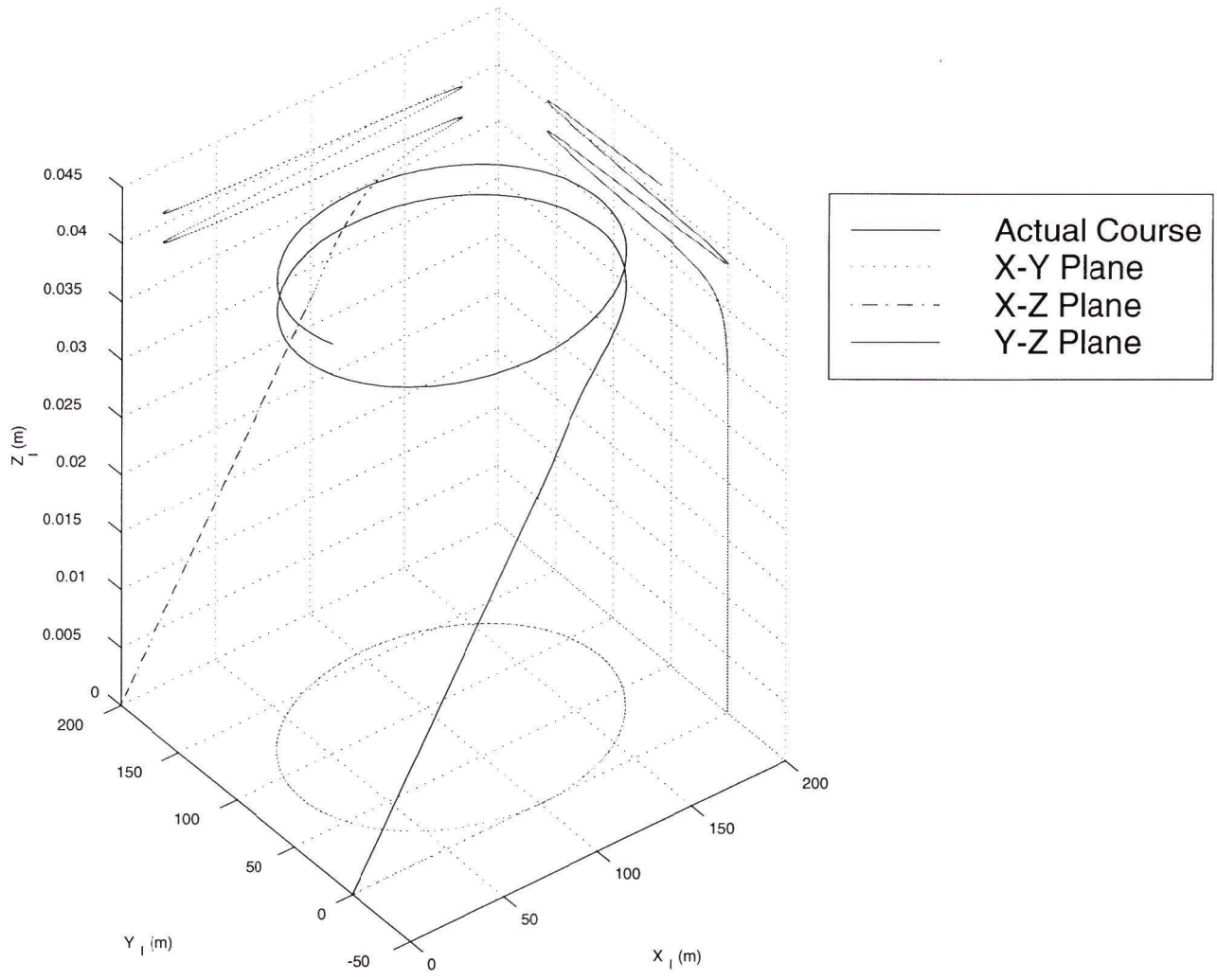

Figure A.10: Trajectory of ARCS Model at 1.0 m/s: Step Yaw Command of 0.1 radian.

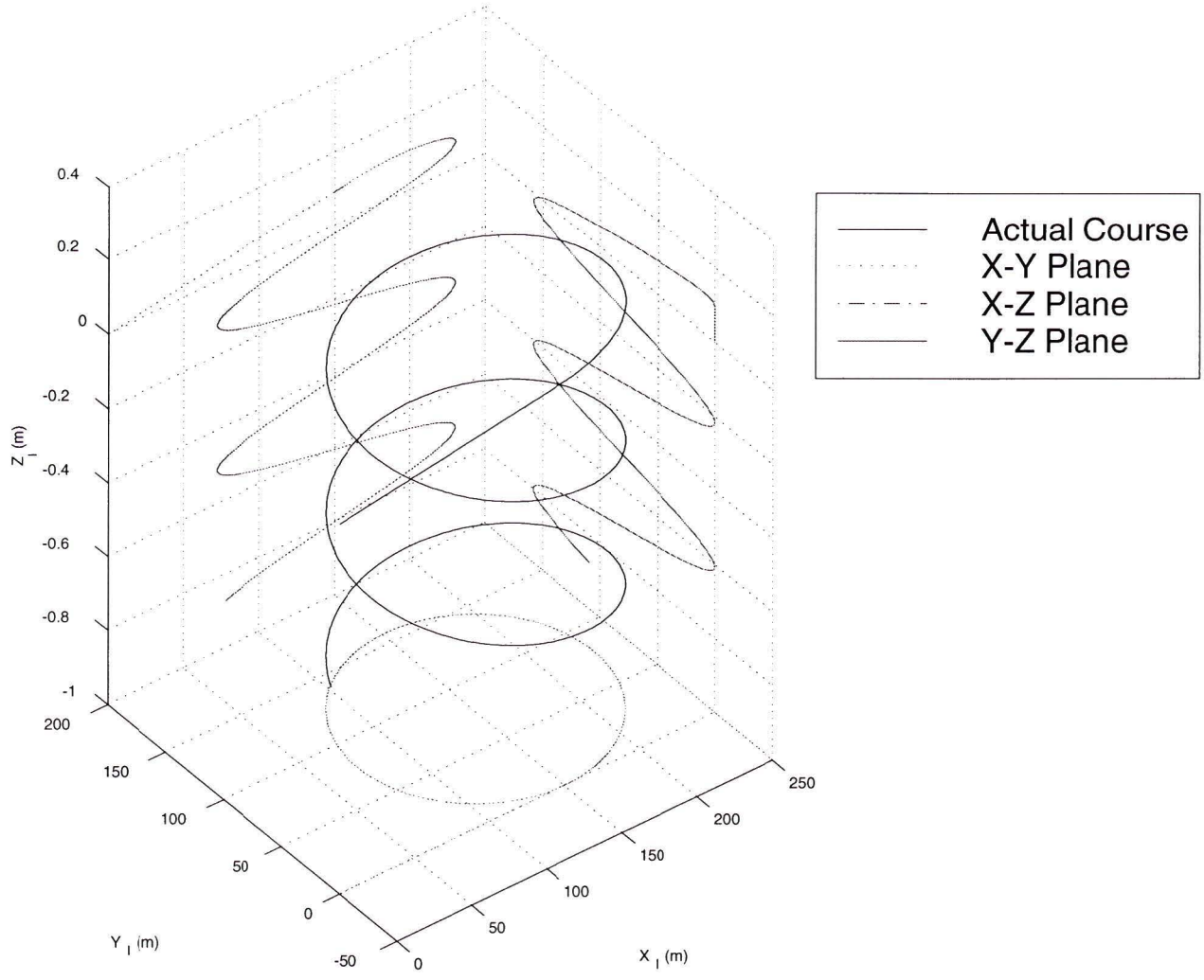

Figure A.11: Trajectory of ARCS Model at 1.5 m/s: Step Yaw Command of 0.1 radian.

$U\,(m/s)$	$t_{s,\psi}\,(s)$
0.5	24.4
1.0	13.1
1.5	8.1
2.0	5.8
2.5	4.7
3.0	3.9
3.5	3.6
4.0	2.6

Table A.1: ARCS Settling Times

change in the angle (see Figures A.12 through A.14). In both the roll and yaw cases the offset in pitch couples the commanded motion to motion in the other two DOF. As can be seen in Figures A.15 through A.17, the roll command results in a tiny sway offset; the pitch command results in a small heave displacement; and the yaw command only causes the vehicle to turn as it should.

A.2.3 Response to Synthesized Control

It appears that synthesizing controls for the ARCS is not possible using the present methods. This is due to two differences that separate the ARCS from the SYMARCS:

1. the offset in pitch, and

2. the righting moment

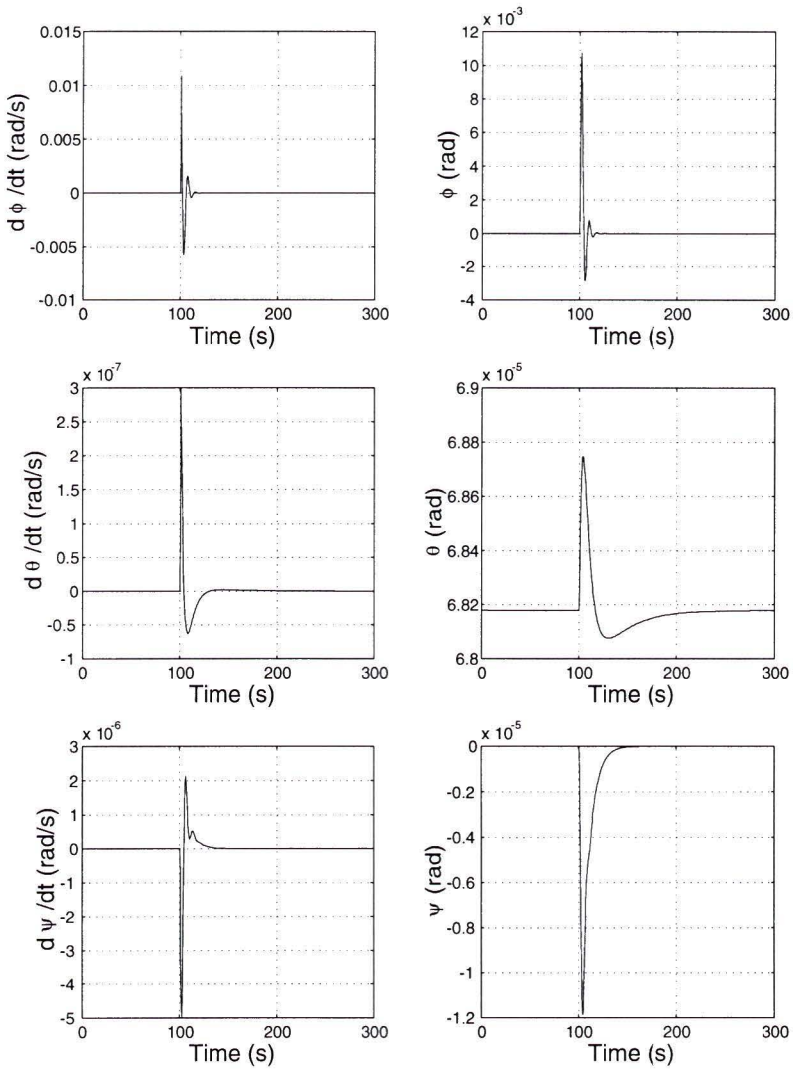

Figure A.12: Rotational Position and Velocity for SYMARCS Model at 0.5 m/s – Roll Commanded

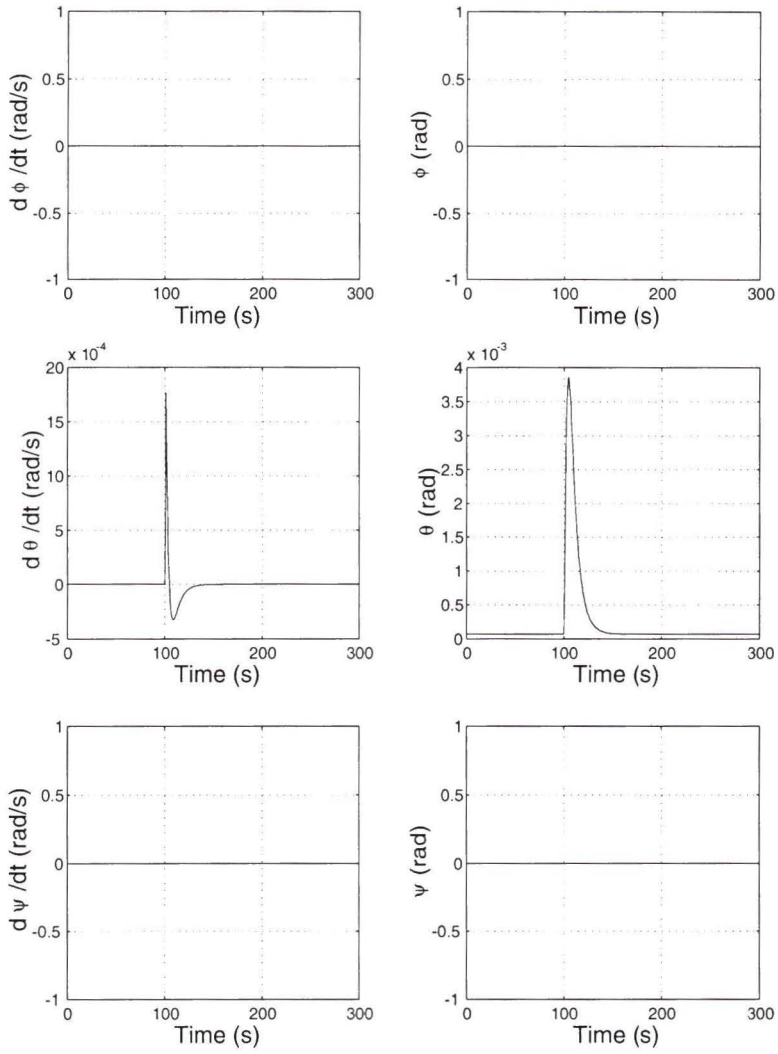

Figure A.13: Rotational Position and Velocity for SYMARCS Model at 0.5 m/s – Pitch Commanded

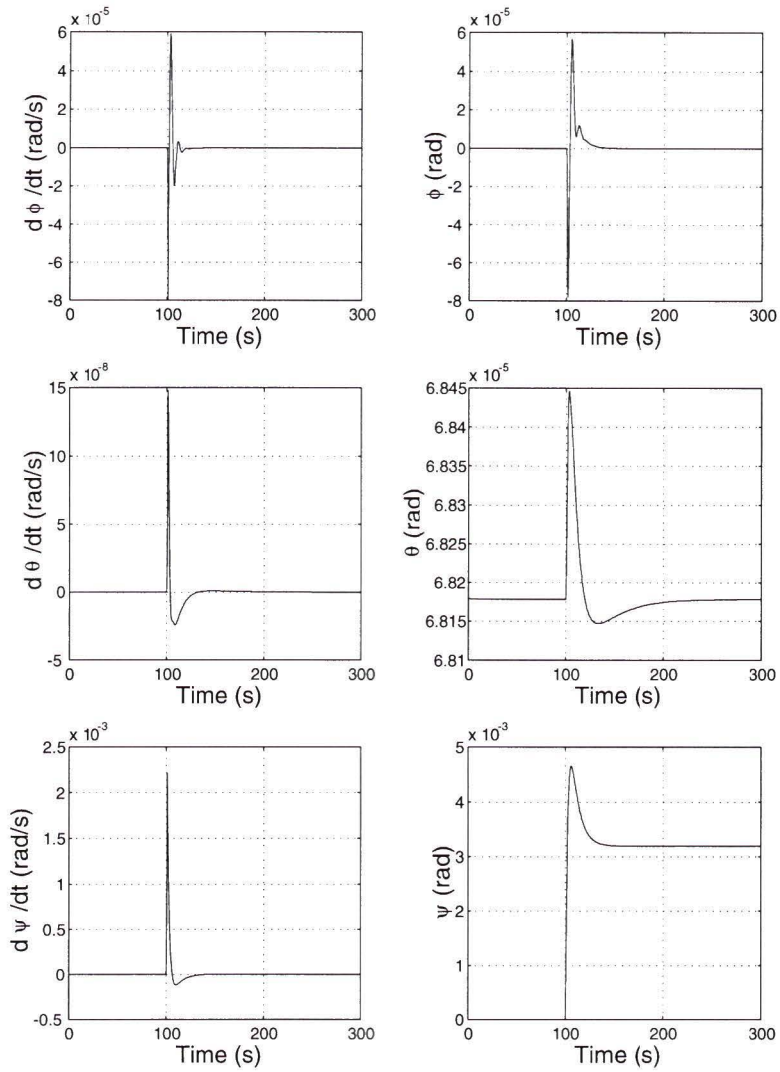

Figure A.14: Rotational Position and Velocity for SYMARCS Model at 0.5 m/s – Yaw Commanded

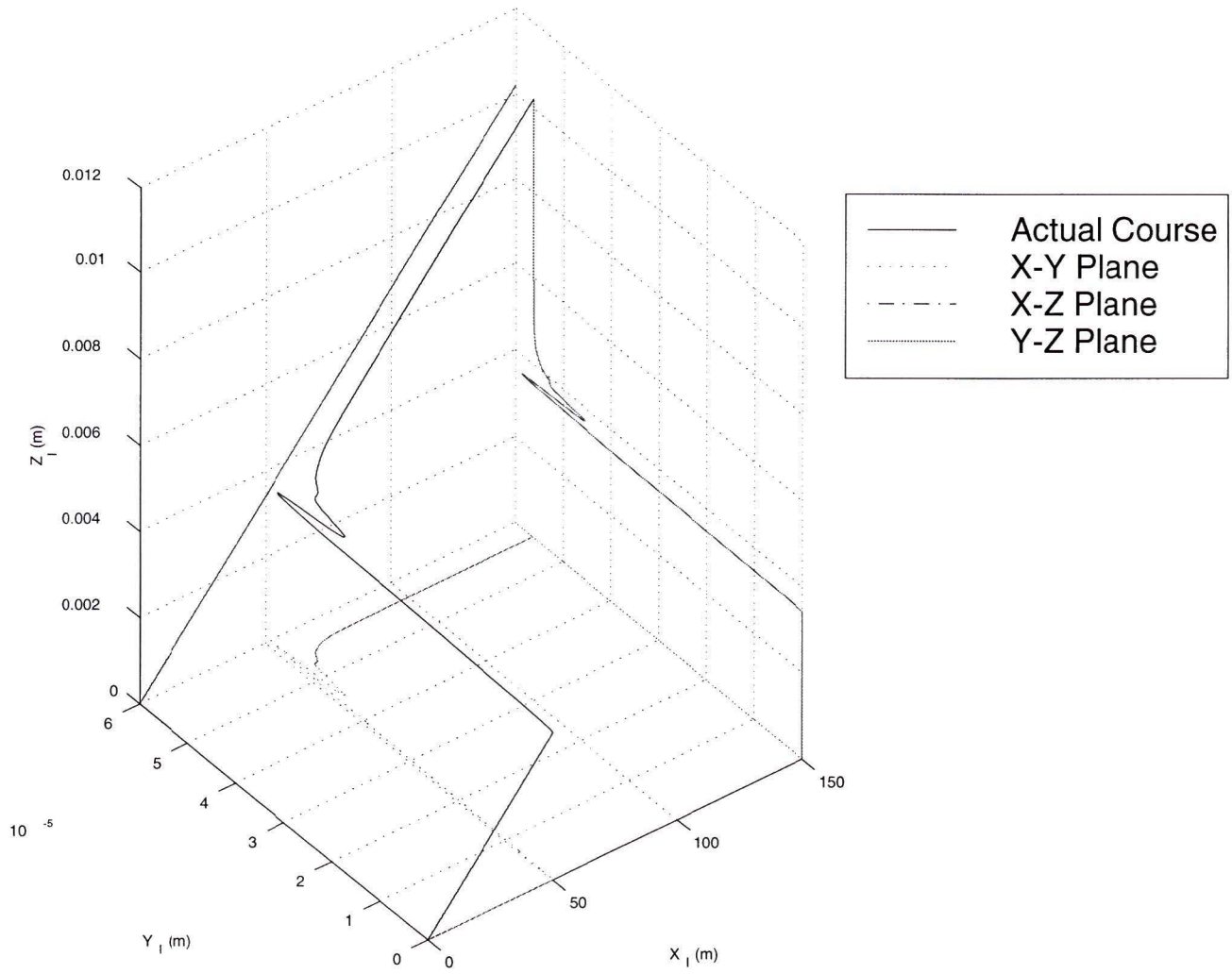

Figure A.15: Trajectory of ARCS Model at 0.5 m/s – Roll Commanded

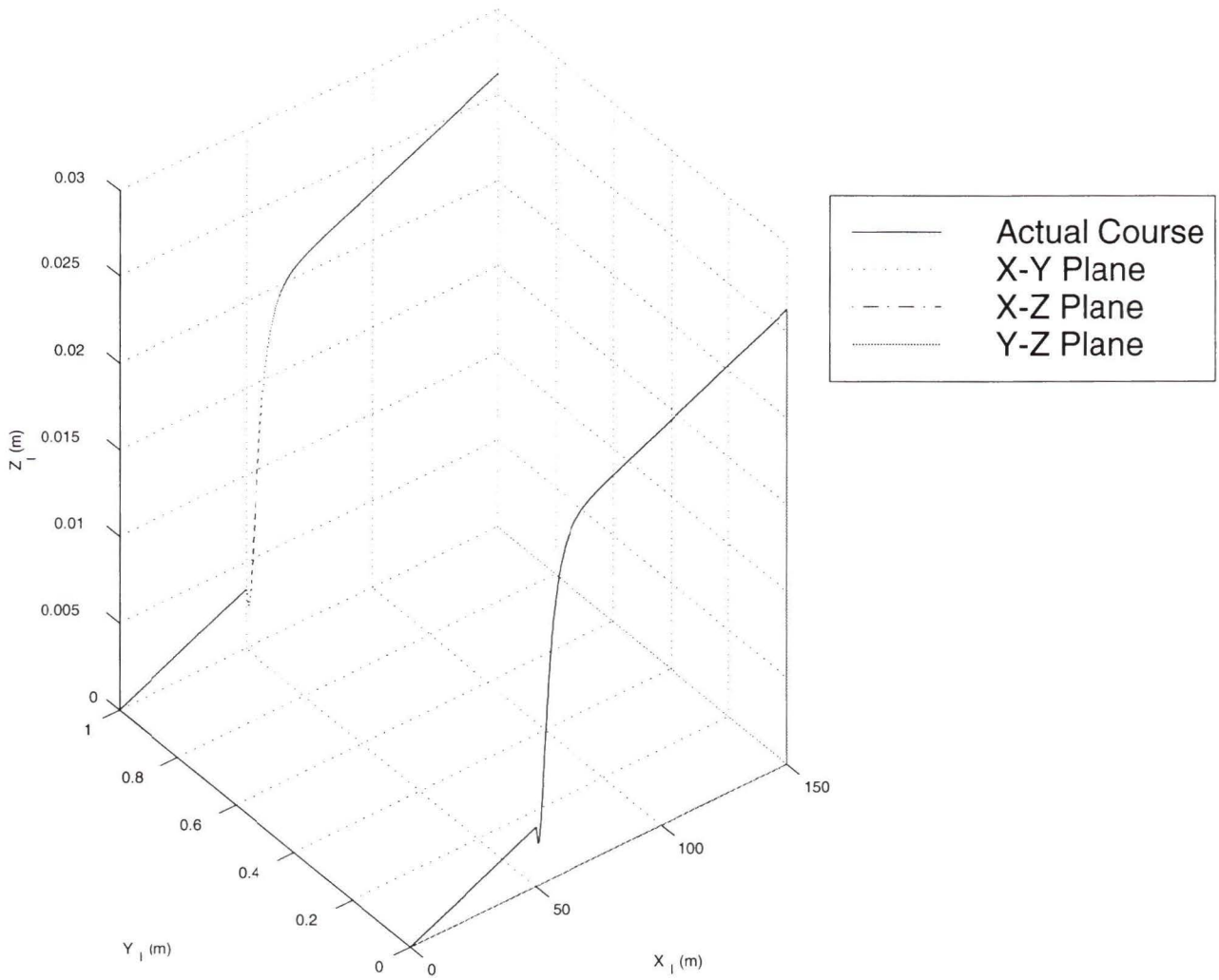

Figure A.16: Trajectory of ARCS Model at 0.5 m/s – Pitch Commanded

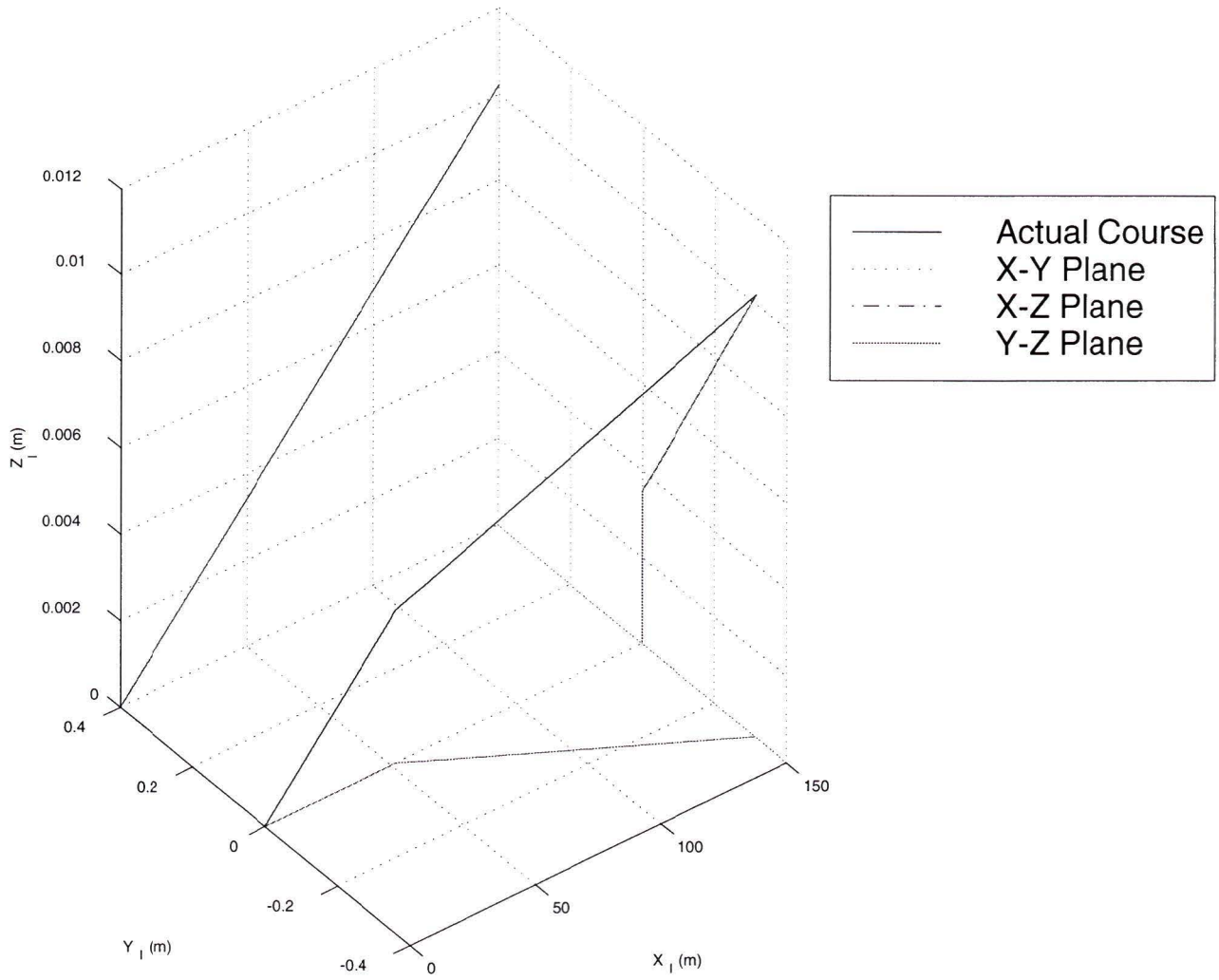

Figure A.17: Trajectory of ARCS Model at 0.5 m/s – Yaw Commanded

Offset in Pitch

At 0.5 m/s, the steady state offset in pitch angle is of the order 10^{-5} radians, while at 4.0 m/s the pitch offset increases to 5×10^{-3} radians, so that the maximum value of the pitch offset is in the order of 0.25 degrees. This may be acceptable, and if it is then the offset in pitch becomes a non-issue in terms of controlling the vehicle, since we will actively correct the parasitic motions.

Righting Moment

The different responses from the ARCS (as opposed to those of SYMARCS) are caused by the effects of the righting moment which reduces the effect of the control signals, inhibiting the proper synthesis of motions.

It still may be possible to use the control synthesis method with a vehicle like the ARCS if the vehicle design is modified. In an emergency situation it may be possible to redistribute the weight in the vehicle to cause the center of mass to be coincident with the center of buoyancy. The control synthesis would then be achievable. Therefore, the methods used to control the SYMARCS model used in Chapters 4 through 6 could still have some value for controlling the ARCS.

Appendix B

Review of Differential Geometry and Geometric Control Theory

> From a geometric point of view, a control system is a family of vector fields parameterized by controls. Each control value determines a vector field, and the corresponding trajectory is a solution curve of this field.
>
> V. Jurdjevic [19]

Differential geometry deals with curves in n-dimensional space, the functions that define them, and change of co-ordinate mappings. From the study of these functions and mappings, general properties are determined so that the methods of characterization or operation can be carried over from one situation to another. For example, we may be able to use methods and operations defined in one dimensional space, in higher order dimensions. Geometric control theory uses differential geometry to achieve the control of a system. For details of geometric control theory the reader is referred to the recently published text by Jurdjevic [20].

B.1 Differential Geometry

A control system can be thought of as a dynamical system where we can adjust some or all of the variable parameters to bring about a particular system response. It is possible to view the state space of a system as an *n-dimensional manifold*, M. The control problem then becomes one of directing the system from one "point" on the manifold, to another "point" along a desired locus of "points", i.e. a desired trajectory. What is also natural, though less obvious, is that the system dynamics can be described by vector fields which depend on the control parameters. A vector field, F, is a mapping from the manifold to the *tangent space*, T_pM, of the manifold at a given point, p

$$F : M \times U \rightarrow T_pM$$

where U represents the set of control parameters, such that for each control input, $u \in U$,

$$F_u : M \rightarrow T_pM$$

$$v = F_u(p); \quad p \in M,\ v \in T_pM$$

For example, if we define the state of our system as the position of a point on the exterior of a sphere, then the entire surface of the sphere defines the state space. Surfaces in three dimensional space are easy to visualize as manifolds, but the concept can be carried over into higher dimensions. Just as the tangent of a curve represents the rate of change of the curve at that point, so a tangent space to a manifold represents the possible rates of change of the manifold at that point (i.e. it is the space of all directional derivatives). For example, the tangent space to a point on the sphere is a plane of vectors tangent to the sphere. Each of these vectors is a directional derivative of some curve passing through that point on the sphere. By choosing the

directional derivative at each point, we control the trajectory of positions along the surface of the sphere.

Differential geometry and geometric control theory are not limited to $SE(3)$ (Appendix C) or $SO(3)$ (Chapters 3 and 4) and their associated derivatives $se(3)$ or $so(3)$, nor even just to matrices, but for the purposes of this work we will limit our discussion to these sets of matrices. In addition to being expedient, it will allow us to ground some fairly abstract ideas to familiar concepts. To further simplify things, we will limit our discussion to $SO(3)$ and $so(3)$, since these are sufficient for application of the theory to the type of vehicle we are considering (see Chapter 2). However, all of the arguments apply equally well for $SE(3)$ and $se(3)$.

B.1.1 Lie Groups

A *Lie group* is a group that is also a differentiable manifold (see Curtis [6] for mathematical definitions of a group and a differential manifold). A group of matrices, such as $SO(3)$, that is also a differentiable manifold is a *matrix* Lie group. We let G denote the matrix Lie group, $G = SO(3)$.

We will look at the tangent space to the manifold shortly, but first we need to define an important mathematical procedure.

B.1.2 Lie Bracket Operation

The group $so(3)$ is not closed under matrix multiplication, i.e.

$$\mathbf{S}(\boldsymbol{\alpha})\,\mathbf{S}(\boldsymbol{\beta}) = \begin{bmatrix} -(\alpha_y\beta_y + \alpha_z\beta_z) & \alpha_y\beta_x & \alpha_z\beta_x \\ \alpha_x\beta_y & -(\alpha_x\beta_x + \alpha_z\beta_z) & \alpha_z\beta_y \\ \alpha_x\beta_z & \alpha_y\beta_z & -(\alpha_y\beta_y + \alpha_y\beta_y) \end{bmatrix} \notin so(3)$$

However, it is closed under an operation called the Lie bracket multiplication (or *Lie bracket* for short):

$$[\mathbf{A},\mathbf{B}] = \mathbf{AB} - \mathbf{BA} \tag{B.1}$$

Proof:

$$\begin{aligned}
\mathbf{S}(\boldsymbol{\alpha})\mathbf{S}(\boldsymbol{\beta}) - \mathbf{S}(\boldsymbol{\beta})\mathbf{S}(\boldsymbol{\alpha}) &= \begin{bmatrix} -(\alpha_y\beta_y + \alpha_z\beta_z) & \alpha_y\beta_x & \alpha_z\beta_x \\ \alpha_x\beta_y & -(\alpha_x\beta_x + \alpha_z\beta_z) & \alpha_z\beta_y \\ \alpha_x\beta_z & \alpha_y\beta_z & -(\alpha_y\beta_y + \alpha_y\beta_y) \end{bmatrix} \\
&\quad - \begin{bmatrix} -(\alpha_y\beta_y + \alpha_z\beta_z) & \alpha_x\beta_y & \alpha_x\beta_z \\ \alpha_y\beta_x & -(\alpha_x\beta_x + \alpha_z\beta_z) & \alpha_y\beta_z \\ \alpha_z\beta_x & \alpha_z\beta_y & -(\alpha_y\beta_y + \alpha_y\beta_y) \end{bmatrix} \\
&= \begin{bmatrix} 0 & -(\alpha_x\beta_y - \alpha_y\beta_x) & \alpha_z\beta_x - \alpha_x\beta_z \\ \alpha_x\beta_y - \alpha_y\beta_x & 0 & -(\alpha_y\beta_z - \alpha_z\beta_y) \\ -(\alpha_z\beta_x - \alpha_x\beta_z) & \alpha_y\beta_z - \alpha_z\beta_y & 0 \end{bmatrix} \\
\therefore \mathbf{S}(\boldsymbol{\alpha})\mathbf{S}(\boldsymbol{\beta}) - \mathbf{S}(\boldsymbol{\beta})\mathbf{S}(\boldsymbol{\alpha}) &\in so(3)
\end{aligned}$$

The Lie bracket operation has the following properties:

$$[\mathbf{A},\mathbf{B}] = -[\mathbf{B},\mathbf{A}];$$

$$\begin{aligned}
[\mathbf{A},\mathbf{B}+\mathbf{C}] &= [\mathbf{A},\mathbf{B}] + [\mathbf{A},\mathbf{C}], \\
[\mathbf{A}+\mathbf{B},\mathbf{C}] &= [\mathbf{A},\mathbf{C}] + [\mathbf{B},\mathbf{C}];
\end{aligned}$$

$$c[\mathbf{A},\mathbf{B}] = [c\mathbf{A},\mathbf{B}] = [\mathbf{A},c\mathbf{B}] \quad c \in \mathbb{R};$$

and

$$[\mathbf{A},[\mathbf{B},\mathbf{C}]] + [\mathbf{B},[\mathbf{C},\mathbf{A}]] + [\mathbf{C},[\mathbf{A},\mathbf{B}]] = \mathbf{0}.$$

B.1.3 Lie Algebras

A real vector space with a product that satisfies the above properties is called a *Lie algebra*, $\mathcal{G}$. A Lie algebra is a vector field [20]. The group $so(3)$ is a real vector space, since $\boldsymbol{\alpha}, \boldsymbol{\beta} \in \mathbb{R}^3$. It satisfies the properties of the Lie Bracket, making it a Lie algebra. Now the significance of the Lie algebra will be explained.

To map the matrix group to its associated tangent space, we can use $\mathbf{f} = \exp$ and, therefore, $\mathbf{f}^{-1} = \ln$ is the inverse mapping. These mappings are valid within limits. Just as e^x is defined $\forall\, x$ and $\ln x$ is defined only for $x > 0$, the exponent of real matrices is defined for all real matrices

$$e^{\mathbf{X}t} = \mathbf{I} + t\mathbf{X} + \frac{(t\mathbf{X})^2}{2!} + \ldots$$

and the natural logarithm of a matrix will be defined only for matrices near the identity matrix $\mathbf{I}$.

$$\ln \mathbf{X} = (\mathbf{X} - \mathbf{I}) - \frac{(\mathbf{X} - \mathbf{I})^2}{2} + \frac{(\mathbf{X} - \mathbf{I})^3}{3} - \frac{(\mathbf{X} - \mathbf{I})^4}{4} + \cdots$$

The mapping, exp, is one-to-one and continuous, and its inverse, *ln*, is continuous in the neighbourhood of the identity matrix. It is, therefore, a *homeomorphism.* For our application (i.e. matrix Lie groups)

$$\exp : T_{\mathbf{I}}G \rightarrow G$$

and

$$\ln : G \rightarrow GT_{\mathbf{I}}$$

$\mathbf{I}$ is a "point" on the manifold, G. We are, therefore, particularly interested in the tangent space to the identity matrix, $\mathbf{I} \in G$, since we have so convenient a homeomorphism.

For $G = SO(3)$, $\mathbf{R}(t)$ is a locus of states (a curve) on the manifold, G. Mathematically, t could represent any parameter, but in reality the orientation of the vehicle is a function of time. Let the arbitrary curve $\mathbf{R}(t)$ which passes through the identity element of $G = SO(3)$ at $t = 0$, be expressed as:

$$\mathbf{R}(t) = e^{\mathbf{A}t} = \mathbf{I} + t\mathbf{A} + \frac{(t\mathbf{A})^2}{2!} + \dots$$

then

$$\mathbf{R}(0) = \mathbf{I} \text{ and } \frac{d\mathbf{R}(t)}{dt} \mid_{t=0} = \mathbf{A}$$

so

$$T_{\mathbf{I}}G = \left\{ \mathbf{A} \mid e^{\mathbf{A}t} \in SO(3) \right\} \tag{B.2}$$

And we can rearrange $\mathbf{R}^T\mathbf{R} = \mathbf{I}$ to get

$$\mathbf{R}^{-1} = \mathbf{R}^T$$

meaning

$$e^{-\mathbf{A}t} = \left(e^{\mathbf{A}t}\right)^T = e^{\mathbf{A}^T t}$$

so

$$-\mathbf{A} = \mathbf{A}^T$$

i.e., $\mathbf{A}$ is skew symmetric and is an element of $so(3)$. The Lie algebra, $\mathcal{G} = so(3)$, is the tangent space to the Lie group at the identity element of the Lie group.

$$T_{\mathbf{I}}G = \mathcal{G} = so(3)$$

$\mathcal{G}$ is a vector field and by choosing an appropriate element of $\mathcal{G}$, we control the trajectory of the vehicle; the curve of orientations in time, $\mathbf{R}(t)$. Since each element of $\mathcal{G}$ is a skew-symmetric matrix representative of some angular velocity, the appropriate choice of angular velocity will effect the desired change of orientation of the vehicle.

B.1.4 Left Translation and Left Invariance

Up to this point we have confined ourselves to talking about the tangent space at the identity of G. We will now turn our attention to arbitrary points on the manifold not at the identity element. At some arbitrary point, $\mathbf{R} \in G$ on the manifold, the tangent space, $T_{\mathbf{R}}G$, is:

$$T_{\mathbf{R}}G = \left\{ \frac{d}{dt}\mathbf{R}(t) \mid_{t=0} \forall\, \mathbf{R}(t) \in G \text{ which satisfy } \mathbf{R}(0) = \mathbf{R} \right\}$$

that is, the space containing all the tangent curves that pass through $\mathbf{R}$. For the arbitrary point $\mathbf{R}$, we can define two loci of states in $SO(3)$, $\mathbf{R}_1$ and $\mathbf{R}_2$, such that

$$\begin{aligned} \mathbf{R}_1 &= \mathbf{R}e^{\mathbf{A}t} \\ \mathbf{R}_2 &= e^{\mathbf{A}t}\mathbf{R} \end{aligned}$$

where $\mathbf{A}$ is a matrix element of the tangent space at $\mathbf{I}$ (see equation (B.2)). These curves both pass through $\mathbf{R}$ at $t = 0$ (i.e. $\mathbf{R}_1(0) = \mathbf{R}e^{\mathbf{0}} = \mathbf{R}$ and $\mathbf{R}_2(0) = e^{\mathbf{0}}\mathbf{R} = \mathbf{R}$), and their tangent vectors at $\mathbf{R}$ are

$$\left(\frac{d\mathbf{R}_1}{dt}\right)_{t=0} = \mathbf{RA} \tag{B.3}$$

$$\left(\frac{d\mathbf{R}_2}{dt}\right)_{t=0} = \mathbf{AR} \tag{B.4}$$

equation (B.3) is the *left translation* of $\mathbf{A}$ by $\mathbf{R}$ and equation (B.4) is the right translation of $\mathbf{A}$ by $\mathbf{R}$. In this manner, the tangent space of G at a point $\mathbf{R}$ on the curve $\mathbf{R}(t)$ can be described by either left- or right-translations of $so(3)$, the tangent space of G at $\mathbf{I}_3$.

A vector field, $\mathbf{F}$, assigns a point, $\mathbf{A} \in T_{\mathbf{R}}G$, in the tangent space to each $\mathbf{R} \in G$.

$$\mathbf{F} : G \rightarrow T_{\mathbf{I}}G$$

$\mathbf{A}$ being a directional derivative. Therefore, the choice of a particular skew symmetric matrix, $\mathbf{A}$, induces the associated vector field on $G = SO(3)$, i.e. the choice of $\mathbf{A}$ defines the vector field used. With left-translation,

$$T_{\mathbf{R}}G = \mathbf{R}T_{\mathbf{I}}G$$

and with right-translation,

$$T_{\mathbf{R}}G = T_{\mathbf{I}}G\mathbf{R}$$

so

$$\begin{aligned} \mathbf{A}_l &= \mathbf{R}\mathbf{A} \\ \mathbf{A}_r &= \mathbf{A}\mathbf{R} \end{aligned}$$

Just as a vector field at the identity of the Lie group corresponds to the $\mathbf{A}$ matrix, the vector field at an arbitrary point corresponds to the left- or right-translation of the $\mathbf{A}$ matrix.

$$\mathbf{F}\tilde{}\mathbf{A}$$

$$\mathbf{F}_l\tilde{}\mathbf{R}\mathbf{A} \tag{B.5}$$

$$\mathbf{F}_r\tilde{}\mathbf{A}\mathbf{R} \tag{B.6}$$

$\mathbf{F}_l$ is called a *left-invariant* vector field induced by $\mathbf{A}$ because the tangent matrix at $\mathbf{R}$ is the left translation by $\mathbf{R}$ of the tangent matrix at $\mathbf{I}$. This invariance means that any point on the curve on the manifold can be treated as if it were the identity matrix of the matrix Lie group; essentially making the solution of the trajectory control problem independent of the initial position. Similarly $\mathbf{F}_r$ is a right-invariant vector field induced by $\mathbf{A}$.

The tangent space at the Lie group identity element has special properties that make it nice to work with, mostly it is easy to define mathematically. Right- and left-invariance allow us to right- or left-translate the representation of a desired velocity matrix to the Lie algebra at the identity of G to facilitate the use of the simple mathematical properties.

A similar development can be followed for $G = SE(3)$ leading to $\mathcal{G} = se(3)$ which is the tangent space to $G = SE(3)$ at its identity element.

B.2 Geometric Control

B.2.1 Basis Matrices

If all the vectors in a vector space, such as $\mathcal{G}$, can be expressed as linear combinations of a particular set of vectors, the particular set said to *span* the vector space. A *basis* for a vector space is a set of spanning vectors that are linearly independent [33]. For example, the tangent space of a sphere at a point is a plane and can be spanned by two orthogonal unit vectors, $\hat{x}$ and $\hat{y}$ in the plane, i.e., every other vector in the plane can be written in terms of $\hat{x}$ and $\hat{y}$. This relates the tangent plane to the Cartesian plane we are familiar with from basic geometry. In three dimensions we can use the orthogonal unit vectors $\hat{x}$, $\hat{y}$, and $\hat{z}$, the Cartesian coordinate system. For a tangent space made up of angular velocity vectors, the natural basis vectors are those unit vectors corresponding to the roll, pitch, yaw velocities, i.e., the axes about which the rotations take place, where $\hat{x}$ is the roll axis, $\hat{y}$ is the pitch axis, and $\hat{z}$ is the yaw axis

$$\left\{ \begin{array}{ccc} \mathbf{b}_1 & \mathbf{b}_2 & \mathbf{b}_3 \end{array} \right\}$$

where

$$\begin{aligned} \mathbf{b}_1 &= \begin{bmatrix} 1 & 0 & 0 \end{bmatrix}^T \\ \mathbf{b}_2 &= \begin{bmatrix} 0 & 1 & 0 \end{bmatrix}^T \\ \mathbf{b}_3 &= \begin{bmatrix} 0 & 0 & 1 \end{bmatrix}^T \end{aligned}$$

These basis vectors can be written as elements of $so(3)$

$$\left\{ \begin{array}{ccc} \mathbf{B}_1 & \mathbf{B}_2 & \mathbf{B}_3 \end{array} \right\}$$

where

$$\begin{aligned} \mathbf{B}_1 &= \begin{bmatrix} 0 & 0 & 0 \\ 0 & 0 & -1 \\ 0 & 1 & 0 \end{bmatrix} \\ \mathbf{B}_2 &= \begin{bmatrix} 0 & 0 & 1 \\ 0 & 0 & 0 \\ -1 & 0 & 0 \end{bmatrix} \\ \mathbf{B}_3 &= \begin{bmatrix} 0 & -1 & 0 \\ 1 & 0 & 0 \\ 0 & 0 & 0 \end{bmatrix} \end{aligned}$$

Since the basis matrices themselves are elements of the Lie algebra too, they are subject to the Lie bracket operation. However as a subgroup of $\mathcal{G}$, they are not closed under the Lie bracket multiplication. When the Lie bracket applied to basis matrices does result in another basis matrix, that basis matrix is redundant in the sense that if it were missing, it could be synthesized by the basis matrices involved in the Lie bracket operation. Fundamentally this demonstrates the utility of this method for

reconfiguring control in the event of a failure: if the system is underactuated for whatever reason, full control may still be available via synthesis of the missing basis matrix.

Any differentiable curve $\mathbf{R}(t) \in SO(3)$ defines a curve of tangent vectors $\frac{d\mathbf{R}(t)}{dt}$ at $\mathbf{R}(t)$ which can be expressed by either left- or right-basis. Let

$$\frac{d\mathbf{R}(t)}{dt} = \mathbf{R}(t) \sum_{i=1}^{3} \omega_i(t) (\mathbf{B}_i)_l \tag{B.7}$$

$$\frac{d\mathbf{R}(t)}{dt} = \sum_{i=1}^{3} \Omega_i(t) (\mathbf{B}_i)_r \mathbf{R}(t) \tag{B.8}$$

where ω_i and Ω_i are magnitudes only and the directions are provided by $\mathbf{B}_i$, the basis matrices. Since each $\mathbf{B}_i$ is skew symmetric, this amounts to

$$\dot{\mathbf{R}} = \mathbf{R}\mathbf{S}(\boldsymbol{\omega}) \tag{B.9}$$

$$\dot{\mathbf{R}} = \mathbf{S}(\boldsymbol{\Omega})\mathbf{R} \tag{B.10}$$

where $\boldsymbol{\omega}$ in equations (B.7) and (B.9) corresponds to the angular velocity expressed in the body-fixed frame, and $\boldsymbol{\Omega}$ ((B.8) and (B.10)) corresponds to the angular velocity expressed in the inertial frame. We will therefore use equation (B.9) which is analogous to equation (B.5), meaning that we are using left-invariance.

B.2.2 Structure Constants

As was stated before, the set of basis matrices is a subset of $\mathcal{G}$, and this subset is not closed under the Lie bracket multiplication. This is where the vital concept of *structure constants* comes in. If the Lie bracket of two basis matrices results in a third valid basis matrix, the structure constant is set to 1. If the Lie bracket results in the negative of a valid basis matrix, the structure constant is set to -1. If the result is

neither a valid basis matrix or its negative, the structure constant is set to 0. For a *single* Lie bracket operation, also known as a *depth-one Lie bracket*:

$$\Gamma_{ij}^{k} = 1$$

means

$$\left[\mathbf{B}_i, \mathbf{B}_j\right] = \mathbf{B}_k \qquad \mathbf{B}_i, \mathbf{B}_j, \mathbf{B}_k \in \ \{\mathbf{B}_1, \cdots, \mathbf{B}_n\}$$

where $\{\mathbf{B}_1, \cdots, \mathbf{B}_n\}$ represents the set of all valid basis matrices. Similarly,

$$\Gamma_{ij}^{k} = -1$$

means

$$\left[\mathbf{B}_i, \mathbf{B}_j\right] = -\mathbf{B}_k \qquad \mathbf{B}_i, \mathbf{B}_j, \mathbf{B}_k \in \ \{\mathbf{B}_1, \cdots, \mathbf{B}_n\}$$

and, of course

$$\Gamma_{ij}^{k} = 0$$

means that neither of the above situations is true. This can be summarized by defining the Γ_{ij}^{k} as satisfying the following

$$\left[\mathbf{B}_i, \mathbf{B}_j\right] = \sum_{k=1}^{n} \Gamma_{ij}^{k} \mathbf{B}_k$$

Note that skew symmetry of the Lie bracket on $\mathcal{G}$ means $\Gamma_{ij}^{k} = -\Gamma_{ji}^{k}$.

The above can be extended for a double Lie bracket, also known as a *depth-two Lie bracket*:

$$\Theta_{ijk}^{q} = 1$$

means

$$\left[\left[\mathbf{B}_i, \mathbf{B}_j\right], \mathbf{B}_k\right] = \mathbf{B}_q \qquad \mathbf{B}_i . \mathbf{B}_j, \mathbf{B}_k, \mathbf{B}_q \in \ \{\mathbf{B}_1, \cdots, \mathbf{B}_n\}$$

etc., so that Θ_{ijk}^{q} satisfies

$$\left[\left[\mathbf{B}_i, \mathbf{B}_j\right], \mathbf{B}_k\right] = \left[\sum_{l=1}^{n} \Gamma_{ij}^{l} \mathbf{B}_l, \mathbf{B}_k\right] = \sum_{l=1}^{n} \Gamma_{ij}^{l} \left[\mathbf{B}_l, \mathbf{B}_k\right] = \sum_{q=1}^{n} \sum_{l=1}^{n} \Gamma_{ij}^{l} \Gamma_{lk}^{q} \mathbf{B}_q = \sum_{q=1}^{n} \Theta_{ijk}^{q} \mathbf{B}_q$$

Again note that skew symmetry of the Lie bracket on $\mathcal{G}$ means $\Theta_{ijk}^{q} = -\Theta_{jik}^{q}$.

For $\mathcal{G} = so(3)$, the valid $\left(\Gamma_{ij}^{k} = -1, 1\right)$depth one structure constants are:

$$\Gamma_{23}^{1} \quad \Gamma_{31}^{2} \quad \Gamma_{12}^{3} \tag{B.11}$$

Since any missing basis matrices in $so(3)$ can be synthesized by the remaining two via the appropriate depth-one structure constant, there is no need for depth-two Lie bracket unless there was the loss of two basis matrices, and for $so(3)$, this would mean inability to span the Lie algebra, $\mathcal{G}$.

For $\mathcal{G} = se(3)$, the valid $\left(\Gamma_{ij}^{k} = 1\right)$depth one structure constants are:

$$\Gamma_{23}^{1} \quad \Gamma_{31}^{2} \quad \Gamma_{12}^{3} \quad \Gamma_{26}^{4} \quad \Gamma_{53}^{4} \quad \Gamma_{34}^{5} \quad \Gamma_{61}^{5} \quad \Gamma_{15}^{6} \quad \Gamma_{42}^{6} \tag{B.12}$$

Using $\mathcal{G} = se(3)$, there is opportunity to use depth two Lie brackets, and the valid $\left(\Theta_{ijk}^{q} = 1\right)$depth two structure constants are:

$$\begin{array}{cccccccccccc}
\Theta_{212}^{1} & \Theta_{121}^{2} & \Theta_{131}^{3} & \Theta_{242}^{4} & \Theta_{215}^{4} & \Theta_{512}^{4} & \Theta_{151}^{5} & \Theta_{124}^{5} & \Theta_{421}^{5} & \Theta_{161}^{6} & \Theta_{134}^{6} & \Theta_{431}^{6} \\
\Theta_{313}^{1} & \Theta_{323}^{2} & \Theta_{232}^{3} & \Theta_{343}^{4} & \Theta_{316}^{4} & \Theta_{613}^{4} & \Theta_{353}^{5} & \Theta_{326}^{5} & \Theta_{623}^{5} & \Theta_{262}^{6} & \Theta_{235}^{6} & \Theta_{532}^{6}
\end{array}$$

Clearly, we should discount the combinations that depend on themselves as physically impossible, since it would not be possible to use a non-existent control to synthesize itself. This then leaves

$$\begin{array}{cccccc}
\Theta_{215}^{4} & \Theta_{512}^{4} & \Theta_{124}^{5} & \Theta_{421}^{5} & \Theta_{134}^{6} & \Theta_{431}^{6} \\
\Theta_{316}^{4} & \Theta_{613}^{4} & \Theta_{326}^{5} & \Theta_{623}^{5} & \Theta_{235}^{6} & \Theta_{532}^{6}
\end{array} \tag{B.13}$$

as the only truly valid depth-two structure constants.

B.2.3 Controllability

The tangent space at the identity element is the Lie algebra, $\mathcal{G}$, made up of skew symmetric matrices representing, in our application, the vehicle angular velocities. Controllability is a function of being able to span the tangent space, that is, being able to describe any velocity vector with a set of controllable basis vectors. The differential geometric approach, using Lie bracket operations on the controllable basis matrices can provide us with a means of spanning the tangent space, even when one or more of the necessary basis matrices is not directly controllable.

B.2.4 Control Authority

Control authority is the definition of which m direct controls are available out of n possible controls, n being the dimension of the Lie group and of the Lie algebra at the identity of the Lie group.

$$\{\mathbf{B}_1, \ldots, \mathbf{B}_m\} \subset \{\mathbf{B}_1, \ldots, \mathbf{B}_n\}$$

It is more convenient to arrange the basis matrices $\{\mathbf{B}_1, \ldots, \mathbf{B}_m, \mathbf{B}_{m+1}, \ldots, \mathbf{B}_n\}$. For $so(3)$, $\{\mathbf{B}_1, \mathbf{B}_2, \mathbf{B}_3\}$ is appropriate when the vehicle has full control of roll, pitch, and yaw, or if it has only roll and pitch control. However, if the vehicle has pitch and yaw control but no direct control of roll, then the order of the basis vectors should be rearranged to $\{\mathbf{B}_2, \mathbf{B}_3, \mathbf{B}_1\}$. When the vehicle is controllable in roll and yaw but not directly in pitch, we would use the order $\{\mathbf{B}_3, \mathbf{B}_1, \mathbf{B}_2\}$.

B.3 Classical Averaging

Before we proceed to the development of the control model we need to address one other point of theory which is not necessarily related to geometric control itself. Leonard [21] develops averaging on left-invariant systems based on classical averaging methods. The concept is to drive the average solution exactly, thereby achieving the actual solution approximately.

Averaging can be used for systems of the form

$$\dot{x} = \epsilon f(t, x, \epsilon) \tag{B.14}$$

where ϵ is a small positive parameter, and where $f(t, x, \epsilon)$ is periodic. When ϵ is small, the solution of equation (B.14) varies "slowly" relative to the periodic change in the excitation, therefore, the response is dominated by the average of the excitation signal.

$$\dot{x} = \epsilon f_{avg}(x) \tag{B.15}$$

where

$$f_{avg}(x) = \frac{1}{T} \int_0^T f(\tau, x, 0)\, d\tau$$

When this is true, the average solution to equation (B.15) is close to the real solution of equation (B.14)

$$x_{\text{real}} = x_{avg} + O(\epsilon)$$

for a finite time interval

$$t \in \left[0, \frac{b}{\epsilon}\right]$$

where $b > 0$ is a parameter resulting from the use of perturbation theory in classical averaging [21].

B.4 Review of Control Signal Generation

Recall the control model given in chapter 4:

$$\dot{\mathbf{R}}(t) = \epsilon \mathbf{R}(t)\,\mathbf{U}(t), \qquad \mathbf{U}(t) = \sum_{k=1}^{m} u_k(t)\,\mathbf{B}_k \qquad m \leq n \tag{B.16}$$

Given a system of the form of equation (B.16), Leonard [21] uses local solutions proposed by Wei and Norman [35], and by Magnus [26] to develop averaging theory on Lie groups, leading to the equations describing the average motion of the system for different levels of Lie bracket operation. Then working from a theorem on controllability, she derives similar equations that describe the actual equations of motion for the system evolving on matrix Lie groups.

For a depth-one bracket system:

$$z_{kf}^{(2)}(t) = \epsilon\,\tilde{u}_k(t) + \epsilon^2 \frac{t}{T} \sum_{i,j=1;\,i<j}^{m} Area_{ij}(T) + z_{k0}^{(2)} \tag{B.17}$$

where $^{(2)}$ indicates that 2^{nd} order averaging has been used. The terms on the right-hand side are

$$Area_{ij}(T) = \frac{1}{2}\int_0^T \left(\tilde{u}_i(\sigma)\,u_j(\sigma) - \tilde{u}_j(\sigma)\,u_i(\sigma)\right) d\sigma$$

the result of applying Green's theorem to the area bounded by the closed curve described by $\tilde{u}_i$ and $\tilde{u}_j$ over one period (σ is a dummy variable for time); and

$$\tilde{u}_k(t) = \int_0^t u_k(\tau)\,d\tau$$

the cumulative effect of the control input, u_k. This is the result from the averaging approach, while

$$z_{kf}(t) = c_k + \sum_{i,j=1;\,i<j}^{m} c_{ij}\Gamma_{ij}^{k} \tag{B.18}$$

results from the controllability theorem. By comparing the two equations, it is easy to see that when the initial position $z_{k0}^{(2)}$ is taken to be 0 (which follows from the property of left invariance), we can equate the coefficients of $z_{kf}^{(2)}(t)$ and $z_{kf}(t)$ to get

$$\epsilon\,\tilde{u}_k(t_f) = c_k \qquad k = 1, \cdots, m \tag{B.19}$$

corresponding to the directly actuated control input signals, and

$$\epsilon^2 \frac{t}{T} Area_{ij}(T) = c_{ij} \qquad i, j = 1, \cdots, m, \quad i < j \tag{B.20}$$

corresponding to the synthesized control input signals. We can also write equation (B.18) as follows:

$$z_{kf} = \begin{cases} c_k + \sum_{i,j=1;\, i<j}^{m} c_{ij}\Gamma_{ij}^k & k = 1, \cdots, m \\ \sum_{i,j=1;\, i<j}^{m} c_{ij}\Gamma_{ij}^k & k = m+1, \cdots, n \end{cases} \tag{B.21}$$

This form makes it easy to see that we can solve for the c_{ij} since we can easily determine the structure constants, Γ_{ij}^k, and we specify z_{kf}. We can then easily solve for c_k by subtraction.

We have followed Leonard's approach and used her algorithms which divide the control generation into two routines for depth-one control: direct control for motion in directions that have actuators available, and synthesized control for motion in directions that do not have actuators available.

Direct control is achieved by a $\frac{1}{2}$ sine wave of amplitude $\frac{1}{2}c_k\omega$ (see Figure B.1). Let

$$\epsilon\,u_k = \frac{1}{2} c_k \omega \sin(\omega(t - t_0)) \tag{B.22}$$

with $t_0 = 0$, and $t_f = \frac{\pi}{\omega}$ (a half of the period), then, since

$$\tilde{u}_k = \int_{t_0}^{t_f} u_k(t)\, dt$$

$$\begin{aligned}
\epsilon\,\tilde{u} &= \int_{t_0}^{t_f} \frac{1}{2} c_k \omega \sin(\omega t)\, dt \\
&= -\frac{1}{2} c_k \omega \left[\cos(\omega t)\right]_{t_0}^{t_f} \\
&= -\frac{1}{2} c_k \omega \left[-1 - 1\right] \\
&= c_k
\end{aligned}$$

satisfying equation (B.19). The amplitude of the control input of equation (B.22) also starts and ends at 0.

$$\epsilon\, u_k(t) = \epsilon\, u_k(t_f) = 0$$

The synthesized motions are accomplished by two sine waves $(\epsilon u_i, \epsilon u_j)$ with a phase difference of 90° (see Figure B.2). These signals have 0 average since we ensure that they complete M cycles for the lagging signal, and $M+1$ cycles for the leading signal (the average value for a complete cycle of a sine wave is zero). The time interval is split into three sections: the lead signal alone, the lead signal and the lag signal 90° behind, and finally the lead signal through another 270° to finish with a complete cycle.

$$\left.\begin{aligned}
\epsilon\, u_i &= \alpha_i \omega \sin(\omega(t - t_0)) \\
\epsilon\, u_j &= 0
\end{aligned}\right\} \quad t \in [0, s1]$$

$$\left.\begin{aligned}
\epsilon\, u_i &= \alpha_i \omega \cos(\omega(t - s1)) \\
\epsilon\, u_j &= \alpha_j \omega \sin(\omega(t - s1))
\end{aligned}\right\} \quad t \in [s1, s2] \qquad \text{(B.23a)}$$

$$\left.\begin{aligned}
\epsilon\, u_i &= \alpha_i \omega \cos(\omega(t - s2)) \\
\epsilon\, u_j &= 0
\end{aligned}\right\} \quad t \in [s2, s3]$$

where

$$s1 = t_0 + \frac{T}{4}$$

$$\begin{aligned} s2 &= s1 + MT \\ s3 &= s2 + \frac{3T}{4} \end{aligned}$$

These controls will satisfy equation (B.20) when

$$c_{ij} = \alpha_i \alpha_j \pi M$$

In addition they start and end with 0 amplitude.

$$\epsilon\, u_i\,(t) = \epsilon\, u_i\,(t_f) = \epsilon\, u_j\,(t) = \epsilon\, u_j\,(t_f) = 0$$

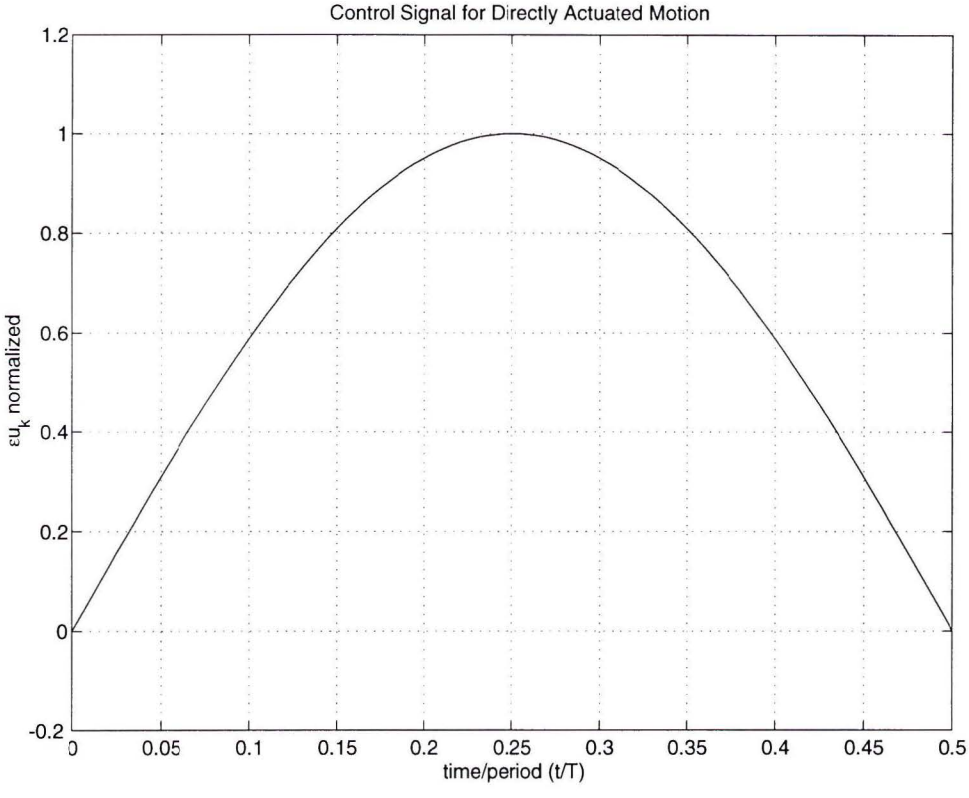

Figure B.1: Control Input Signal for Motion in DOF Directly Actuated

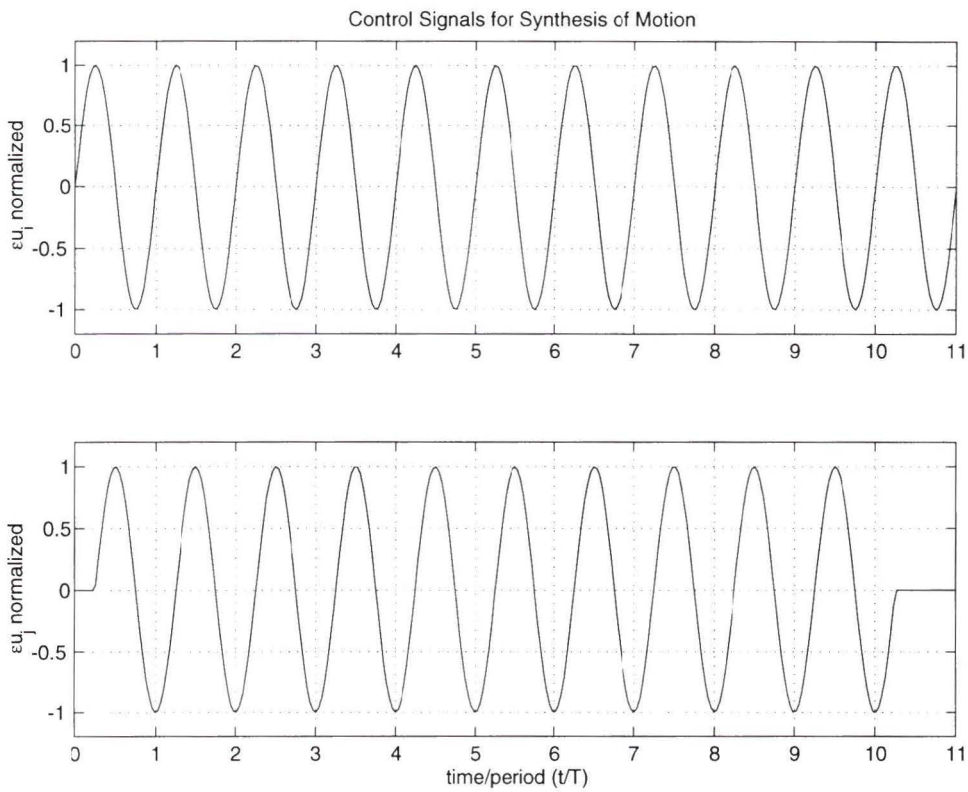

Figure B.2: Control Input Signals to Synthesize Motion in DOF Not Directly Actuated

Appendix C

Position and Orientation Kinematics

C.1 Position Kinematics

The position (see Figure C.1) of a given arbitrary point, P, in the vehicle, with respect to the origin of the inertial frame, is given by [17]

$$\left[\mathbf{r}_{P/O}\right]_I = \left[\mathbf{r}_{B/O}\right]_I + \left[\mathbf{r}_{P/B}\right]_I \tag{C.1}$$

where $\left[\mathbf{r}_{P/O}\right]_I$ is the position of the point relative to the origin of the inertial frame and described in the inertial frame; $\left[\mathbf{r}_{B/O}\right]_I$ is the position of the origin of the body frame described with respect to the origin of the inertial frame; and $\left[\mathbf{r}_{P/B}\right]_I$ is the description of the position of the point relative to the origin of the body-fixed frame, but described in the inertial frame. All the vectors must be described in the same frame in order to carry out vector addition. Most often, however, the position of P with respect to the origin of the body frame is described in the body frame (i.e.,

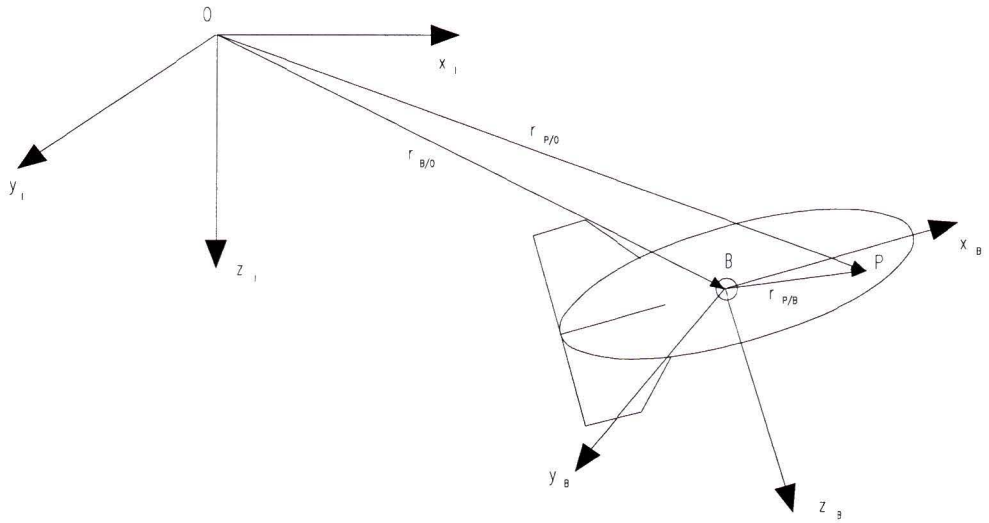

Figure C.1: Position of Arbitrary Point P

$\left[\mathbf{r}_{P/B}\right]_B$), and therefore, there is a requirement to map that description into the inertial frame.

The orientation of the vehicle can be described in the inertial frame by three Euler angles: ϕ (roll angle), θ (pitch angle), and ψ (yaw angle). At any instant of time, knowledge of the value of these three angles allows us to relate the description of any vector, in the body-fixed frame, to its description in the inertial frame via an orthogonal rotation matrix, $\mathbf{R}$:

$$\left[\mathbf{r}_{P/B}\right]_I = \mathbf{R}\left[\mathbf{r}_{P/B}\right]_B$$

Now equation (C.1) can be written

$$\left[\mathbf{r}_{P/O}\right]_I = \left[\mathbf{r}_{B/O}\right]_I + \mathbf{R}\left[\mathbf{r}_{P/B}\right]_B \tag{C.2}$$

The rotation matrix $\mathbf{R}$ contains all the relevant information about the orientation of the vehicle, while $\mathbf{r}_{B/O}$ provides the position of the origin of the body frame with respect to the inertial frame. Together they give us the complete picture of the motions of the vehicle. To include information about both the orientation and position of the vehicle in a single representation, $\mathbf{R}$ is combined with $\mathbf{r}_{B/O}$ in a *homogeneous transform*

$$\mathbf{H} = \begin{bmatrix} \mathbf{R} & \left[\mathbf{r}_{B/O}\right]_I \\ \mathbf{0} & 1 \end{bmatrix}$$

where $\mathbf{0}$ is a 1×3 zero vector. $\mathbf{H}$ accomplishes the vector addition of equation (C.2). Note that the vector resulting from the transformation is a *new* vector, different from the original, and the length of the vector is not preserved under the mapping. Again, we will define $\mathbf{H}$ as the homogeneous transform from the body-fixed reference frame to the inertial reference frame and avoid the use of frame indices except for noting other cases.

$$\begin{aligned} \left[\mathbf{r}_{P/O}\right]_I' &= \mathbf{H}\left[\mathbf{r}_{P/B}\right]_B' \\ \begin{bmatrix} \left[\mathbf{r}_{P/O}\right]_I \\ 1 \end{bmatrix} &= \mathbf{H}\begin{bmatrix} \left[\mathbf{r}_{P/B}\right]_B \\ 1 \end{bmatrix} \end{aligned} \tag{C.3}$$

This relationship corresponds to two equations; the first being equation (C.2) and the second an identity.

C.2 Velocity Kinematics

Taking the time derivative of $\mathbf{H}$ gives

$$\dot{\mathbf{H}} = \begin{bmatrix} \dot{\mathbf{R}} & \left[\dot{\mathbf{r}}_{B/O}\right]_I \\ \mathbf{0} & 0 \end{bmatrix}$$

Recall that

$$\dot{\mathbf{R}} = \mathbf{RS}$$

Using this relation and the rotation of $\left[\dot{\mathbf{r}}_{B/O}\right]$ from the body frame to the inertial frame

$$\left[\dot{\mathbf{r}}_{B/O}\right]_I = \mathbf{R}\left[\dot{\mathbf{r}}_{B/O}\right]_B$$

leads to

$$\dot{\mathbf{H}} = \begin{bmatrix} \mathbf{RS} & \mathbf{R}\left[\dot{\mathbf{r}}_{B/O}\right]_B \\ \mathbf{0} & 0 \end{bmatrix} = \begin{bmatrix} \mathbf{R} & \left[\mathbf{r}_{B/O}\right]_I \\ \mathbf{0} & 1 \end{bmatrix} \begin{bmatrix} \mathbf{S} & \left[\dot{\mathbf{r}}_{B/O}\right]_B \\ \mathbf{0} & 0 \end{bmatrix}$$

Leonard [21] defined a form somewhat like a homogeneous transform

$$\hat{\mathbf{W}} = \begin{bmatrix} \mathbf{S} & \left[\dot{\mathbf{r}}_{B/O}\right]_B \\ \mathbf{0} & 0 \end{bmatrix}$$

so that this relationship can be expressed succinctly as

$$\dot{\mathbf{H}} = \mathbf{H}\hat{\mathbf{W}} \tag{C.4}$$

C.3 Mathematical Notes

Recall that rotation matrices belong to the group of *Special Orthogonal* matrices

$$\mathbf{R} \in SO(3)$$

where

$$SO(3) \triangleq \left\{ \mathbf{R} \in \mathbb{R}^{3\times 3} \mid \mathbf{R}^T\mathbf{R} = \mathbf{I}, \det(\mathbf{R}) = 1 \right\} \tag{C.5}$$

As well, the matrix $\mathbf{S}$ belongs to the group of all 3×3 skew symmetric matrices with real elements:

$$\mathbf{S} \in so(3)$$

where

$$so(3) \triangleq \left\{ \mathbf{S}(\boldsymbol{\beta}) \in \mathbb{R}^{3\times 3} \mid \mathbf{S}^T + \mathbf{S} = \mathbf{0}; \boldsymbol{\beta} \in \mathbb{R}^3 \right\} \tag{C.6}$$

In this work, $\boldsymbol{\beta} = [\boldsymbol{\omega}]_B$.

Similarly, $\mathbf{H}$ belongs to the group of *Special Euclidean* matrices

$$\mathbf{H} \in SE(3)$$

where

$$SE(3) \triangleq \left\{ \mathbf{H} = \begin{bmatrix} \mathbf{R} & \mathbf{b} \\ \mathbf{0} & 1 \end{bmatrix} \in \mathbb{R}^{4\times 4} \mid \mathbf{R} \in SO(3), \mathbf{b} \in \mathbb{R}^3 \right\} \tag{C.7}$$

Here $\mathbf{b} = \left[\mathbf{r}_{B/O}\right]_I$. Since $\det(\mathbf{H}) = 1$, $\mathbf{H}$ is always invertible.

$\hat{\mathbf{W}}$ is also a matrix group

$$\hat{\mathbf{W}} \in se(3)$$

where

$$se(3) \triangleq \left\{ \begin{bmatrix} \mathbf{S} & \boldsymbol{\gamma} \\ \mathbf{0} & 0 \end{bmatrix} \in \mathbb{R}^{4\times 4} \mid \mathbf{S} \in so(3); \boldsymbol{\gamma} \in \mathbb{R}^3 \right\} \tag{C.8}$$

Where, in our application, $\mathbf{S}$ is a skew-symmetric matrix of $[\boldsymbol{\omega}]_B$ and $\boldsymbol{\gamma}$ is $\left[\mathbf{r}_{B/O}\right]_I$.

As we found in Chapter 3, through $\mathbf{R}$ and its derivative, $\dot{\mathbf{R}} = \mathbf{RS}$, we have all the information about the orientation and rate of change of orientation of the vehicle. $\mathbf{R}$ defines the state of the vehicle in terms of orientation. Here we have shown that

through $\mathbf{H}$ and its derivative, $\dot{\mathbf{H}} = \mathbf{H}\hat{\mathbf{W}}$, we have all the information about both the orientation and position of the vehicle and their respective rates of change (linear and angular velocities of the vehicle). $\mathbf{H}$ defines the state of the vehicle in terms of orientation and position, and allows the use of the control synthesis method on a 6 DOF system.

Vita

Surname: Perrault. **Given Names:** Douglas Edward

Place of Birth: Calgary, Alberta
Date of Birth: October 14th, 1960

Educational Institutions Attended:

St. Lawrence College at Cornwall, Ontario	1982 to 1984
Dalhousie University	1992 to 1993
Technical University of NovaScotia (TUNS)	1993 to 1996
Universtiy of Victoria	1996 to 1998

Degrees Awarded:

Diploma in Marine Engineering Technology (with Distinction)	St. Lawrence College	1984
Diploma in Mechanical Engineering Technology (with Distinction)	St. Lawrence College	1984
B. Eng. (with Distinction)	Technical University of Nova Scotia (TUNS)	1996

Honours and Awards:

Sexton Scholar	1993 to 1996
3M Canada Scholarship	1993
Weldon Scholarship	1994 & 1995
Stora Forest Industry Scholarship	1994
Dr. Alan E. Cameron Scholarship	1995
NSERC PGS A	1996
BC ASI Graduate Recruitment	1996
President's Research Scholarship	1996 & 1997
NSERC PGS B	1998

Publications:

D. Perrault, G. Hackett and M. Nahon, Simulation and Active Control of Towed Undersea Vehicles, In Proceedings of the 1997 IEEE Oceans '97, Halifax, Nova Scotia

D. Perrault and M. Nahon, Fault Tolerant Control of Autonomous Underwater Vehicles, In Proceedings of the 1998 IEEE Oceans '98, Nice, France

Partial Copyright License

I hereby grant the right to lend my thesis to users of the University of Victoria Library, and to make single copies only for such users or in response to a request from the Library of any other university, or similar institution, on its behalf or for one of its users. I further agree that permission for extensive copying of this thesis for scholarly purposes may be granted by me or a member of the University designated by me. It is understood that copying or publication of this thesis for financial gain shall not be allowed without my written permission.

Title of Dissertation:

Fault Tolerant Control of Autonomous Underwater Vehicles

Author [redacted]

Douglas Edward Perrault

August 3, 1998